8-3-2017

Analytical and Experimental Study on Coaxial Borehole Heat Exchangers

David Tyler Gordon
University of Windsor

Analytical and Experimental Study on Coaxial Borehole Heat Exchangers

By

David Gordon

A Thesis

Submitted to the Faculty of Graduate Studies

through the Department of Mechanical, Automotive, and Materials Engineering

in Partial Fulfillment of the Requirements for

the Degree of Master of Applied Science at the

University of Windsor

Windsor, Ontario, Canada

2017

Analytical and Experimental Study on Coaxial Borehole Heat Exchangers

by

David Gordon

APPROVED BY:

_____

P. Henshaw
Department of Civil and Environmental Engineering

_____

J. Defoe
Department of Mechanical, Automotive and Materials Engineering

_____

D. Ting, Co-Advisor
Department of Mechanical, Automotive and Materials Engineering

_____

T. Bolisetti, Co-Advisor
Department of Civil and Environmental Engineering

May 19, 2017

Declaration of Co-Authorship/Previous Publications

I hereby declare that this thesis incorporates material that is result of joint research, as follows:

This thesis investigates the use of coaxial borehole heat exchangers used in ground-source heat pump applications. This thesis incorporates the outcome of a joint research project undertaken in collaboration with Dr. Stanley Reitsma under the supervision of Dr. David S-K. Ting and Dr. Tirupati Bolisetti. In all cases, the key ideas, primary contributions, experimental designs, data analysis and interpretation, were performed by the author, and the contribution of co-authors was primarily through the provision of developing experimental designs and data collection.

I am aware of the University of Windsor Senate Policy on Authorship and I certify that I have properly acknowledged the contribution of other researchers to my thesis, and have obtained written permission from each of the co-author(s) to include the above material(s) in my thesis.

I certify that, with the above qualification, this thesis, and the research to which it refers, is the product of my own work.

This thesis includes three original papers that have been previously published/submitted for publication in peer reviewed journals, as follows:

Thesis Chapter	Publication title	Publication status
Chapter 2	*Gordon, D., Bolisetti, T., Ting, D.S.-K., Reitsma, S., 2017. Short-term fluid temperature variations in either a coaxial or U-tube borehole heat exchanger. Geothermics 67, 29–39.*	*Published*
Chapter 3	*"A Physical and Semi-Analytical Comparison between Coaxial BHE Designs considering Various Piping Materials," - Energy*	*Submitted*

Chapter 4	*"Experimental and Analytical Investigation on Pipe Sizes for a Coaxial Borehole Heat Exchanger," – Renewable Energy*	*Submitted*

I certify that I have obtained a written permission from the copyright owner(s) to include the above published material(s) in my thesis. I certify that the above material describes work completed during my registration as graduate student at the University of Windsor.

I declare that, to the best of my knowledge, my thesis does not infringe upon anyone's copyright nor violate any proprietary rights and that any ideas, techniques, quotations, or any other material from the work of other people included in my thesis, published or otherwise, are fully acknowledged in accordance with the standard referencing practices. Furthermore, to the extent that I have included copyrighted material that surpasses the bounds of fair dealing within the meaning of the Canada Copyright Act, I certify that I have obtained a written permission from the copyright owner(s) to include such material(s) in my thesis.

I declare that this is a true copy of my thesis, including any final revisions, as approved by my thesis committee and the Graduate Studies office, and that this thesis has not been submitted for a higher degree to any other University or Institution.

Abstract

This research focuses on methods of direct-use geothermal energy considering a coaxial borehole heat exchanger (BHE) as a major component in a ground-source heat pump (GSHP) system. A GSHP system is a sustainable energy system that transfers thermal energy between the surrounding ground and the conditioned space of a building. Various methods exist to accomplish the ground-side heat exchange for a GSHP, where the focus of this thesis remains on closed-loop systems which utilize loops of fused high-density polyethylene (HDPE) pipes buried vertically in boreholes ranging between 80 and 200 meters deep. This thesis provides an overview of the critical design considerations used in sizing a BHE where a comparison is made between a typical U-tube BHE and a thermally improved coaxial BHE where various benefits may be realized by the latter. The motivation for this research is to provide a tool to accurately compare various coaxial systems, where a semi-analytical model for heat transfer is proposed. The proposed model, referred to as the composite coaxial (CCx) model, is semi-analytical in nature being that it relies on a curve-fitted cylindrical response function, or *g-function*. The CCx model is made to produce accurate simulations for the fluid temperature measured at the outlet of a coaxial BHE over the course of a typical thermal response test (TRT). The model considers coaxial configurations where the inner and outer pipes may have differing thermal properties, diameters, and thicknesses. The model is validated using known input parameters and physical measured temperature data for three different TRTs showing root mean square errors (RMSE) as low as 0.09 °C, which is well within the uncertainty of the measurement for the given test. The general development of the model is largely empirical in nature, where various aspects were introduced keeping logical constraints in mind to produce an acceptable fit to each of the three physical tests. Further experimental analysis is performed using a lab-scale coaxial heat exchanger to verify the trends produced by the CCx model during short term operation considering laminar annular flow. The measured outlet fluid temperature is again compared to the temperature simulated by the CCx model showing an RMSE of 0.16 °C, which is again found to be within the uncertainty of the measurement. In summary, the primary contribution of this research is the CCx model itself, where this model has been developed as a tool for future use in the case-by-case optimization of coaxial systems. This model is capable of capturing the effect of various pipe materials and sizes as shown through the validation presented in this thesis.

Dedication

I dedicate this research to my family.

Acknowledgements

I would like to thank both of my advisors, Dr. David S-K Ting and Dr. Tirupati Bolisetti, for their support and crucial eyes for detail. I am greatly appreciative for the constant strive for higher quality research. I would like to thank the Turbulence and Energy Lab and all of its members and associates, both student and faculty. I thank Dr. Stanley Reitsma, Dr. Paul Henshaw, and Dr. Jeff Defoe for their support as committee members. I would like to thank Matt St. Louis for his help in setting up the experimental portion of this research. I acknowledge the support of the Ontario Centres of Excellence and GeoSource Energy, Inc. in completion of this work.

Table of Contents

List of Tables

List of Figures

Chapter 1 – Introduction

1.1 Background

Ground-source heat pump (GSHP) systems are becoming an ever more popular type of direct-use geothermal energy that is used predominately in HVAC applications (Lund and Boyd, 2016). This specific classification of geothermal energy systems have a relatively high overall coefficient of performance compared to conventional heating a cooling systems (Bernier, 2006). A GSHP system will have an associated ground-side heat exchanger, and this research focuses on coaxial borehole heat exchangers (BHE). Typically, the borehole will be filled with a "U-tube" pipe and back-filled with grout, but recent analysis has given rise to interest in the benefits realized by a concentric pipe-in-pipe heat exchanger. The concept behind the coaxial heat exchanger is to achieve a reduced outward thermal resistance to heat flow based on an increased contact area between the fluid within the annulus of the heat exchanger and its surroundings. In doing this, it is expected that a coaxial arrangement can result in a drastically reduced required length of buried heat exchanger, and in turn, a reduction in costly drilling requirements. In order to maintain performance in a coaxial configuration it would be further recommended to insulate the inner pipe to reduce any short-circuiting between the flow paths. Regardless of insulation, or the use of a thermally improved outer pipe, it is important to balance the pressure drops within a coaxial BHE in order to maintain turbulent flow within the annulus while minimizing the overall pumping power requirement. In order to optimize coaxial BHEs on a case-by-case bases, a tool is required to accurately compare the various possible configurations.

1.2 Objectives

The first major objective of the present research is to develop a semi-analytical model that is able to accurately simulate the outlet fluid temperature of a coaxial BHE during a typical thermal response test; this model is referred to as the composite coaxial model (CCx).

The second major objective of this research is to validate the CCx model using known input parameters considering a total of three full-scale thermal response tests, where further verification is provided through lab-scale experimentation.

1.3 Scope of work

This research is specific to coaxial BHEs and their various designs; however, this thesis also includes discussions on the more typical U-tube borehole configurations. The purpose of the

U-tube discussion is to introduce the concepts necessary to develop a thermal model to simulate the outlet fluid temperature of a coaxial BHE. The CCx model is validated for its intended use as a tool to investigate various optimal coaxial configurations, where preliminary insight is provided by applying the model to a modified design procedure for a single borehole application. Configurations varying in pipe size and material properties are compared while balancing the required length of heat exchanger with the system's overall coefficient of performance, remaining within the tested validity of the model.

1.4 Organization of thesis

Following this preliminary introduction, the second chapter of this thesis provides a brief overview and discussion on GSHP systems where this includes the critical design considerations used in sizing a BHE. U-tube and coaxial BHEs are compared using previously published methods, from which coaxial BHEs show a possible reduced thermal resistance and increased short-term performance.

The third chapter of this thesis uses original thermal response test data to validate a semi-analytical model for heat transfer, referred to as the composite coaxial (CCx) model, for application to a coaxial BHE. The model produces simple simulations of the outlet fluid temperature of a coaxial BHE. The model presented in this chapter considers a volumetric ratio of the inner to outer flow paths, assuming an equal ratio of inner to outer thermal resistances in order to isolate the effect of the inner pipe size.

The fourth chapter of this thesis extends the model to consider coaxial configurations where the inner and outer pipes may have differing thermal properties. This chapter introduces the remaining *design* ratios considered in the CCx model. The model is then used to compare the various material configurations while balancing the required length of a single borehole with the coefficient of performance experienced by a residential geothermal heat pump.

The fifth chapter of this thesis provides experimental findings, considering a lab-scale coaxial heat exchanger having laminar flow in the annulus tested within a small and enclosed water jacket. The results of this experiment show comparable trends between the physical test results and analytical results simulated by the CCx model, verifying the model for simulation of laminar flow within the annulus. This chapter further expands upon selecting an appropriate ratio of inner to outer pipe diameters to maximize turbulence within the annular flow path while minimizing the overall pumping requirement of the system.

Chapter 2 – Comparison of Vertical U-tube and Coaxial Borehole Heat Exchangers

2.1 Introduction

When making long-term investments on HVAC&R systems, the economic benefits and positive environmental effects of utilizing geothermal energy should be considered. *Direct-use* geothermal energy applications often use a geothermal heat pump (GHP) to transfer heat between the conditioned space of a building and the nearby subsurface, where the refrigerant loop may be modified to allow for reversible seasonal operation offering both heating and cooling capabilities. GHP systems (often referred to as ground-source heat pump, or GSHP systems, when considering HVAC&R applications) typically operate with efficiencies up to three times higher conventional methods such as coal or natural gas (Brenn et al., 2010). A GSHP operates using a typical refrigeration cycle; this cycle is driven by a compressor where the input *drive* power is to be minimized to maintain desirable efficiencies.

An assessment of the potential for global renewable energy use has been developed by the International Renewable Energy Agency (IRENA). Remap 2030, IRENA's plan for the future of renewable energy, estimates that 55% of renewable energy in the US will be in non-electricity energy uses by the year 2030 (IRENA, 2015). This initiative estimates that the US has a potential for 7 million additional GHP systems. In Canada, the number of GSHPs installed annually had previously peaked in 2009 at approximately 16 thousand units, followed by a 28% decrease in 2010 and a stabilization in 2011 at over 12 thousand units (Raymond, 2015). This trend, shown in Figure 2.1 for Canada, Germany, and Sweden, is commonly experienced in renewable technologies when there is a decrease in conventional energy costs; this reduces the economic feasibility of many environmentally friendly projects. GHP systems have had the highest impact on the geothermal market; direct-use applications make up 70.9% of total installed geothermal capacity for the year 2015.

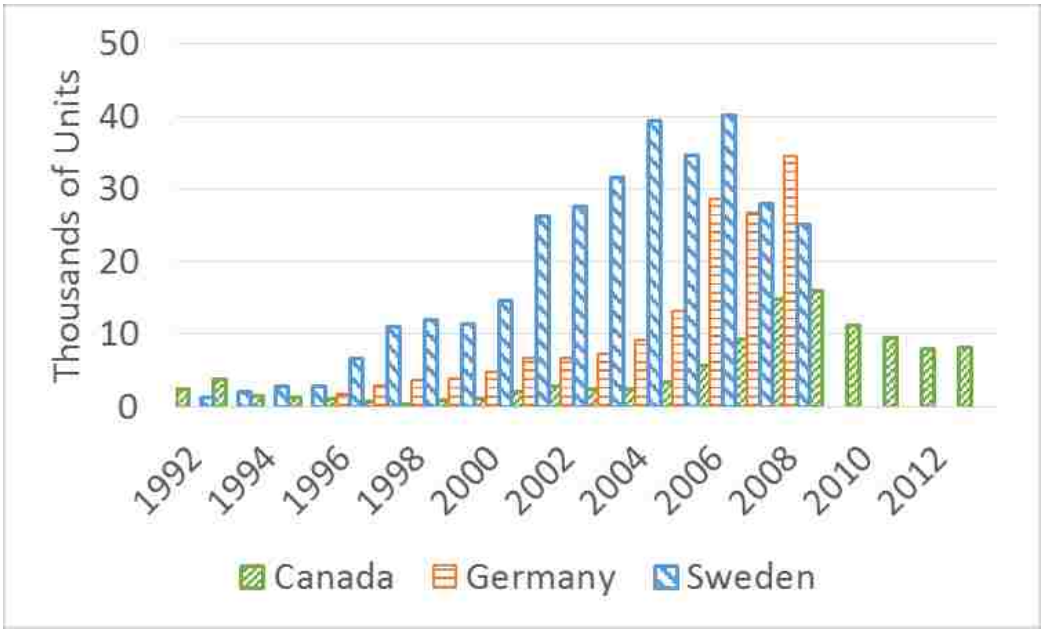

Figure 2.1: Recent number of unit installations for Canada (Raymond, 2015), Germany (Sanner, 2009), and Sweden (Lind, 2011).

A GSHP system will typically consist of three main components; a heat pump, a ground-side heat exchanger, and an interior distribution system. This research focuses on the ground-side heat exchanger and its effect on a heat pumps performance. The ground-side heat exchange may be accomplished by utilizing either open or closed ground loops. An open loop system directly utilizes groundwater from deep aquifers to act as the working-fluid entering the heat pump; these systems are subject to stricter regulations as they are prone to contaminate groundwater tables. The more popular alternative is a closed-loop system, which typically utilizes buried high-density polyethylene pipes to circulate a secondary working-fluid to exchange heat with the surrounding subsurface.

In regards to closed-loop GSHP systems, the focus of this research, the ground-loop pipes may be horizontally or vertically arranged. The vertical configuration is considered in this thesis and would consist of one or many *boreholes* with piping arrangements being either *U-tube* (a supply and return leg of HDPE piping fused together with a "U-bend" at the bottom) or *coaxial* (an inner pipe and an outer pipe, with the outer pipe capped at the bottom) style; these are referred to as borehole heat exchangers or BHEs.

A comparison is made in this chapter between coaxial and U-tube BHEs based on existing analytical solutions for heat transfer *within* and *around* the borehole. It is found that analytical

models for coaxial BHEs have been limited by how the inner pipe is considered. Conventionally, models have only considered cases where the inner pipe is assumed to have a negligible effect on overall outward heat transfer (Beier et al., 2013; Hellström, 1991). This chapter considers such a case, where a thermally improved coaxial BHE is found to have a 30% reduction in overall required length when compared to a typical U-tube BHE.

2.2 System description

Among geothermal systems, GSHPs have become a popular method to fulfill space heating and cooling demands (Lund and Boyd, 2016). This peak in interest is due to their typically high coefficient of performance (COP) (Brenn et al., 2010), where vertical systems tend to be even more effective than their horizontally arranged counterparts (Benli, 2013). The drawbacks often encountered by vertical GSHP systems include their high initial costs and, in the past, flawed design approaches (Bernier, 2006). A system can either be oversized or undersized considering the ground-side heat exchanger; in either case, performance of the heat pump will suffer. If a BHE is oversized it will have a higher than necessary initial cost. If the BHE is undersized, it will have a reduced efficiency, requiring more primary energy input (Beier et al., 2011; Bernier, 2006).

The ground-side heat exchanger can consist of one or more boreholes (or more generally, *active elements*) depending on the dominating heating/cooling demand of the project. When many boreholes are used, they are arranged in a *borefield*, spaced 3 to 5 meters apart, connected in parallel to a manifold which is then connected to a heat pump; a depiction of this arrangement is shown in Figure 2.2.

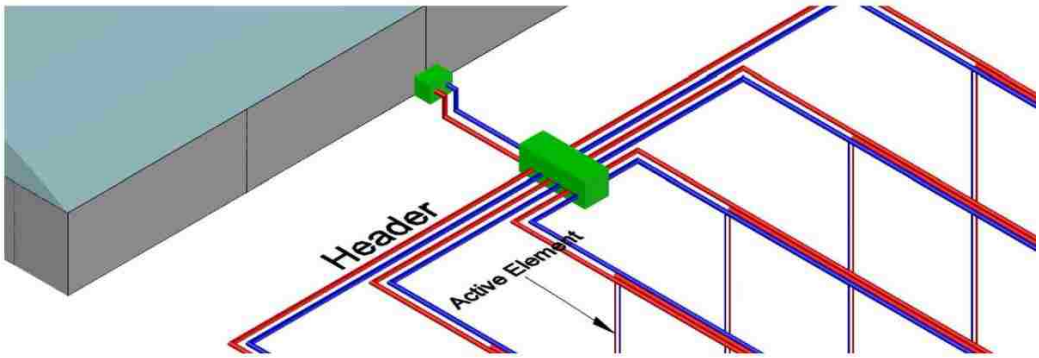

Figure 2.2: Borefield configuration showing U-tube pipes connected in parallel

To minimize the risk of incorrect sizing, a thermal response test (TRT) can be performed on-site to better estimate the thermal properties of the subsurface (Gehlin, 2002). TRTs are typically performed using an above ground heater which delivers a constant rate of heat input to a working-fluid being circulated through a fully operational borehole for typically a minimum duration of 48 hours (Beier and Smith, 2003) (see Figure 2.3 for diagram). By monitoring the inlet and outlet temperatures experienced by the working fluid in the BHE, a mean fluid temperature can be deduced. The mean of the measured fluid temperature can then be fit to an analytical model in order to estimate the *effective* thermal conductivity of the ground and borehole thermal resistance (Philippe et al., 2009).

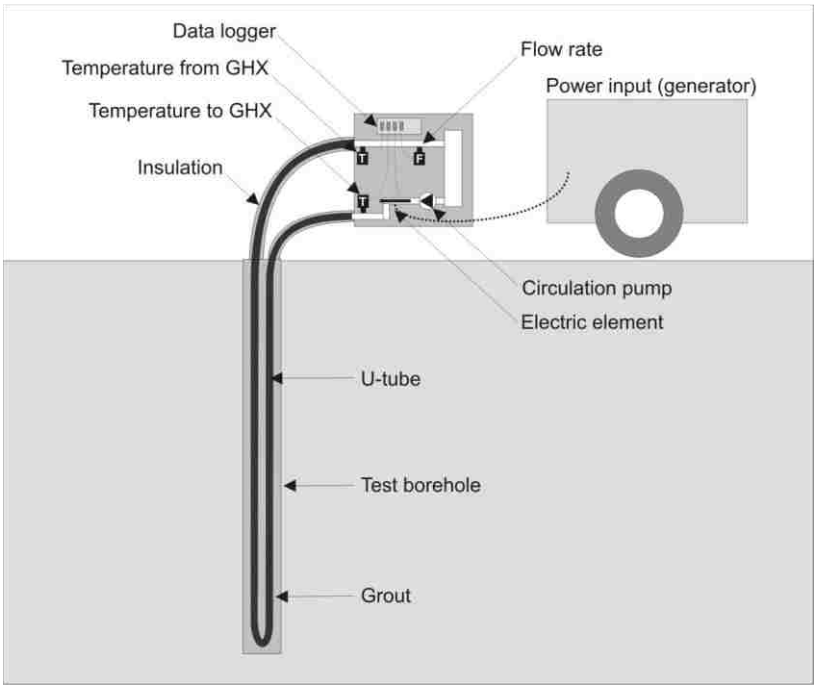

Figure 2.3: Typical thermal response test arrangement (image provided by GeoSource Energy Inc.)

Although U-tube BHEs are the more common piping configuration, coaxial BHEs have more recently become a popular topic in the literature (Acuña, 2013) and remain the focus of this thesis. However, as a starting point, this chapter begins its investigation on U-tube BHEs since there exists a more extensive library of verified data and valid analytical models for them. This thesis chapter provides a summary of the *infinite cylindrical source* (ICS) model which is recommended by ASHRAE in their 2011 HVAC Applications Handbook (ASHRAE, 2011).

It is noted, and can be clearly seen in Equation 2.1, that the actual COP of a heat pump is largely dependent on the entering fluid temperature (T_{EFT} of EFT) (RETScreen International. and Clean Energy Decision Support Centre., 2001):

$$COP_{actual} = COP_{baseline}(k_0 + kT_{EFT} + k_2 T_{EFT}^2) \quad (2.1)$$

where k_0, k_1, and k_2, are correlation coefficients listed below in Table 2.1:

Table 2.1: Correlation coefficients for estimation of coefficient of performance based on entering fluid temperature

CORRELATION COEFFICIENTS		VALUE
$\boldsymbol{COP_{cooling\ mode}}$	k_0	1.53105836
	k_1	-2.29609600x10^{-2}
	k_2	6.87440000x10^{-5}

Equation 2.1 considers a correction to the rated *baseline COP* of a heat pump based on the entering fluid (in this case limited to water) temperature only, related to the amount of primary energy input required to raise or lower the fluid temperature to achieve the desired output of the system. Additionally, the COP may be corrected based on the primary input needed for the ground-side circulation pump and the fan used in the distribution system.

This chapter investigates the performance of a typical residential application considering a single active element (U-tube or coaxial) to meet a 10 kW cooling demand. This can be done approximately by simulating the outlet fluid temperature of the BHE, negating horizontal header losses.

2.3 Analytical models for heat transfer

When considering the entering fluid temperature of a GSHP, it is often appropriate to size a borehole system based on the average fluid temperature experienced within the heat exchanger rather than the outlet. Analytical models exist such as the ICS model which may be coupled with an effective borehole thermal resistance (R_b) and ground thermal conductivity (k_s) to simulate a mean fluid temperature (T_m) within a single borehole.

2.3.1 Heat transfer in surrounding ground

The heat transfer around a BHE of sufficient length may be modelled considering an infinite cylinder emitting a constant and uniform heat flux (q) within an infinite surrounding of homogenous media. The following differential equation would apply where the first line considers

the temperature rise at radial distances extending to infinite around the hollow cylinder, and the second line considers a steady heat flux q being emitted at the borehole radius, that is $r = r_b$ (Carslaw and Jaeger, 1959):

$$\begin{cases} \frac{\partial^2 T}{\partial r^2} + \frac{1}{r}\frac{\partial T}{\partial r} = \frac{1}{\alpha_s}\frac{\partial T}{\partial \tau}, & r_b < r < \infty \\ -2\pi r_b k_s \, \partial T/\partial \tau = q, & r = r_b, \tau > 0 \\ T - T_0 = 0, & \tau = 0, r > r_b \end{cases} \tag{2.3}$$

where T is the surrounding temperature at time τ and radius r from the borehole wall and is equal to the undisturbed ground temperature, T_0, when the time of operation is zero. $\alpha_s = k_s/c_{p_s}\rho_s$ is the thermal diffusivity of the subsurface considering its effective volumetric heat capacity ($c_{p_s}\rho_s$) and effective thermal conductivity of the subsurface.

These solutions were adapted by *Ingersoll et al., 1954* for their use in GCHP system applications as dimensionless response functions where they are first referred to as g-functions. The temperature at the borehole wall considering an infinite hollow cylindrical heat source is given by Equations 2.4 and 2.5, where $Fo_1 = \alpha_s \tau / r_b^2$ is the dimensionless Fourier number related to the transient heat conduction in the surrounding ground at the borehole wall:

$$T(r,p) = T_o + \frac{q}{k_s} g(Fo,p) \tag{2.4}$$

$$g(Fo,p) = \frac{1}{\pi^2}\int_0^\infty \frac{\frac{e^{-(\beta^2 Fo)}-1}{J_1^2(\beta)+Y_1^2(\beta)}[J_0(p\beta)Y_1(\beta)-J_1(\beta)Y_0(p\beta)]}{\beta^2} d\beta \tag{2.5}$$

By setting p equal to 1 (where $p = r/r_b$ with r being the radius of interest) and combining the solution with an analytical model for the heat transfer within the borehole itself, the average fluid temperature may be simulated by the following equation (where T_f corresponds to the *simulated* mean temperature):

$$T_f(\tau) = T_o + \frac{q}{k_s} g(Fo_1, 1) + qR_b \tag{2.6}$$

where R_b is an effective borehole thermal resistance that will be discussed in the following sections for either a U-tube or a coaxial BHE.

2.3.2 U-tube BHEs

To estimate R_b based solely on bore geometry and material properties, superposition is used here to represent the two legs of a U-tube BHE (Claesson and Hellström, 2011; Li and Lai, 2013):

$$R_b = \frac{1}{2}\left[\frac{1}{2\pi k_g}\left(\ln\left(\frac{r_b}{r_o}\right) + \ln\left(\frac{r_b}{D}\right) + \sigma \ln\left(\frac{(r_b)^4}{(r_b)^4 - (D/2)^4}\right)\right) + R_p\right] \quad (2.7)$$

where the thermal resistance of the pipes (R_p) is given by:

$$R_p = \frac{1}{2\pi k_p}\ln\left(\frac{r_o}{r_i}\right) + \frac{1}{\pi d_i h} \quad (2.8)$$

and a dimensionless ratio of thermal conductivities (σ) is given by:

$$\sigma = \left(\frac{k_g - k_s}{k_g + k_s}\right) \quad (2.9)$$

where k_g and k_p are the grout and pipe thermal conductivities, r_o and r_i are the outer and inner pipe radii, D is the distance between the legs of the U-tube, and h is the convective heat transfer coefficient. For simplicity, this thesis chapter does not expand upon the theory behind the above equations, where readers are directed to the stated references and the second chapter of this thesis for more information.

2.3.3 Coaxial BHEs

For a coaxial BHE, an effective borehole thermal resistance can be considered by Equation 2.10, where it is assumed that the fluid temperature within the inner pipe has no effect on the fluid temperature at the outer wall of the annulus. Such a condition would be expected for cases where the flow in the annulus is fully turbulent and a relatively flat temperature profile could be expected (Acuña et al., 2009). The following equation is also limited to a heat flux and borehole wall temperature which are uniform with depth (Hellström, 1991):

$$R_b = R_o\left(1 + \frac{L^2}{3\left(Q_f \rho_f c_f\right)^2 R_i R_o}\right) \quad (2.10)$$

where R_i and R_o are the inner shunt and outer borehole thermal resistances; L is the length of the heat exchanger; Q_f, ρ_f, and c_f are the volumetric flow rate, density, and specific heat capacity of the working fluid. The inner and outer resistances may be calculated as follows, where the outer resistance can be made to include a concentric layer of grout (Beier et al., 2013, 2014):

$$R_i = \frac{1}{2\pi h_{oi} r_{oi}} + \frac{1}{2\pi k_{p_i}} * \log\left(\frac{r_{oi}}{r_{ii}}\right) + \frac{1}{2\pi h_{ii} r_{ii}} \quad (2.11)$$

$$R_o = \frac{1}{2\pi k_{p_o}} * \log\left(\frac{r_{oo}}{r_{io}}\right) + \frac{1}{2\pi h_{io} r_{io}} \quad (2.12)$$

where h_{yx} is the convective heat transfer coefficient at the inner or outer surface (subscript y) of the pipes (subscript x) at radial distances from the center of r_{yx}, and $k_{p_x} is$ the thermal conductivity of the inner or outer pipe.

2.3.4 Fluid flow

The convective heat transfer coefficients may be estimated using the Gnielinski correlation:

$$\begin{cases} Nu = \frac{(f/2)(Re-1000)Pr}{1+12.7(f/2)^{1/2}(Pr^{2/3}-1)}, & 2300 < Re < 5x10^6 \\ Nu = 4.364, & 0 < Re < 2300 \end{cases} \quad (2.13)$$

where the Reynolds number is given by:

$$Re = \frac{\rho_f v_f D_h}{\mu_f} \quad (2.14)$$

where f is the friction factor corresponding to the pipe wall, ρ_f, k_f, μ_f, and v_f are the density, thermal conductivity, dynamic viscosity, and velocity of the working fluid, respectively; and D_h is the hydraulic diameter of the flow path. The convective heat transfer coefficients may be represented by:

$$h_{yx} = \frac{Nu\, k_f}{2r_{yx}} \quad (2.15)$$

where k_f, is the thermal conductivity of the working fluid.

2.4 Design length comparison

A modified version of the recommended ASHRAE borehole length calculation is used in this chapter to demonstrate the importance of the borehole thermal resistance as a semi-controlled design parameter. The following equation was customized by Bernier in order to simplify the required length calculation without having to sacrifice accuracy (Philippe et al., 2010)

$$L = \frac{q_h R_b + q_y R_{10y} + q_m R_{1m} + q_h R_{6h}}{T_m - (T_0 + T_p)} \quad (2.16)$$

where T_p is the temperature penalty due to thermal interference between boreholes; in the present study, since only a single borehole is considered, the temperature penalty is set to zero. q_y, q_m, and q_h are the yearly average ground heat load, highest monthly ground load, and peak hourly ground load, respectively; these are estimated based on a typical residential cooling demand of 10 kW and full-, half-, and quarter-load operating times. R_{10y}, R_{1m}, and R_{6h} are effective ground thermal resistances corresponding to 10 years, one month, and six hour ground loads. It is noted here that the mean fluid temperature considered in Equation 2.16 (T_m) is based on manufacturer data for the chosen heat pump for the purpose of design. The value of T_m is estimated to be the average of the maximum entering fluid temperature rated for the heat pump and the leaving water temperature based on the flow rate and peak heat load rejected to the working-fluid.

Equation 2.16 assumes that heat transfer in the ground occurs only by conduction while moisture evaporation and underground water movement are considered negligible. This equation is also based on a worst case scenario by using thermal pulses corresponding to 10 years, one month and six hours in duration; the following section will explain how these quantities can be calculated.

The effective ground thermal resistances account for transient heat transfer from the borehole to the undisturbed ground. The approach used to calculate these variables is expressed as follows (ASHRAE, 2011; Bernier, 2006; Philippe et al., 2010):

$$R_{6h} = \frac{1}{k_s} g\left(\frac{\alpha_s \tau_{6h}}{r_b^2}\right) \tag{2.17}$$

$$R_{1m} = \frac{1}{k_s}\left[g\left(\frac{\alpha_s \tau_{1m+6h}}{r_b^2}\right) - g\left(\frac{\alpha_s \tau_{6h}}{r_b^2}\right)\right] \tag{2.18}$$

$$R_{10y} = \frac{1}{k_s}\left[g\left(\frac{\alpha_s \tau_{10y+1m+6h}}{r_b^2}\right) - g\left(\frac{\alpha_s \tau_{1m+6h}}{r_b^2}\right)\right] \tag{2.19}$$

where g is evaluated at the time steps considered and the procedure is limited by:

$$0.05\ m \leq r_{bore} \leq 0.1\ m$$

$$0.025\ m^2/day \leq \alpha_s \leq 0.2\ m^2/day$$

An example of the above design procedure is given in Table 2.2, where the ground pulses (q_y, q_m, q_h) are assumed based off the heat extracted or rejected from the ground at six-hour

peak conditions, average peak monthly conditions, and average yearly conditions. They are further based on the rated baseline coefficient of performance (COP typically rated at 0°C for heating and 25°C for cooling) for the heat pump in either its heating or cooling mode of operation, depending on whichever is greater. It is noted that a 10 kW peak hourly cooling demand considering a heat pump with a COP of 5.0 would correspond to 12 kW of heat rejected to the ground loop.

It is clearly indicated in the above design considerations the importance of reducing the overall borehole thermal resistance as this is the parameter over which there is most control. As subsurface properties vary greatly, and can often be largely effected by groundwater flow, the above design equation is not recommended for all site conditions.

Table 2.2 summarizes the input parameters and calculation results used to compare the required design length of a U-tube and a coaxial BHE. The parameters for the coaxial BHE are largely based on the design of an enhanced coaxial BHE presented by *Acuña and Palm, (2010)* and later studied by *Beier et al., (2013, 2014)*; where the U-tube BHE is made to have the same borehole diameter with all but a differing borehole resistance. In Figure 2.4, R_b is found to have a linear effect on L while k_s is set equal to 3.0 W/m-K. On the other hand, if k_s is low enough, it could make the system entirely impractical when considering a typical U-tube arrangement with an R_b of 0.118 m-K/W.

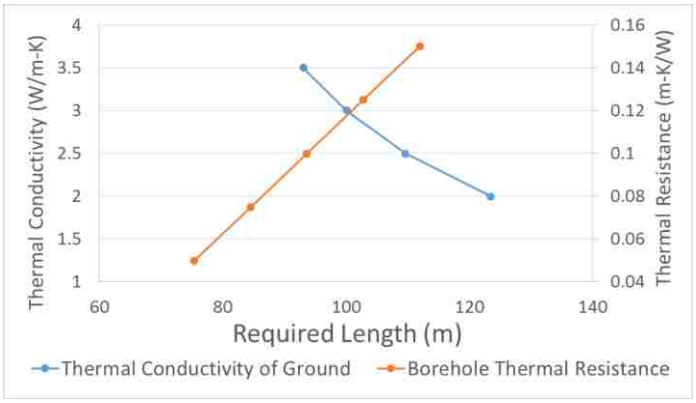

Figure 2.4: Sensitivity of the required length considering the effective thermal conductivity of the ground and the borehole thermal resistance

In order to compare the short-term performance, which in the calculation of Equation 2.16 is considered to be 6 hours of operation from undisturbed conditions, the average fluid temperature is simulated for each case using the ICS model and corresponding borehole thermal

resistances when experiencing an on-going peak hourly heat flux of 12 kW over this duration. These fluid temperatures are used to correct the rated baseline COP of the 10 kW heat pump (COP_{rated} = 5.0) where the results of the corrected COP are shown in Figure 2.5. It is noted that the short-term performance of the coaxial BHE remains higher than that of the U-tube BHE over the six hour duration, even though the lengths of the heat exchangers have been compensated to accommodate the demand of the system. This is largely due to the independent contribution of the effective borehole thermal resistance to the overall length requirement found in Equation 2.16.

Table 2.2: Input parameters for design length calculation and results comparing U-tube and coaxial BHEs

Input Parameters		Units	Single borehole	
			U-tube	Coaxial
Ground loads				
peak hourly ground load	q_h	W	12000	
monthly ground load	q_m	W	6000	
yearly average ground load	q_y	W	1500	
Ground properties				
thermal conductivity	k_s	W/m-K	3.0	
thermal heat capacity	c_{ps}	J/kg-K	2800	
thermal diffusivity	α_s	$m^{2/}$day	0.093	
Undisturbed ground temperature	T_0	°C	10.0	
Fluid properties				
thermal heat capacity	c_{pf}	J/kg-K	4200	
total mass flow rate per kW of peak hourly ground load	m_f	kg/s-kW	0.042	
max/min heat pump inlet temperature	T_i	°C	40.0	
Borehole characteristics				
borehole radius	r_b	m	0.058	
effective borehole thermal resistance	R_b	m-K/W	0.118	0.035
Effective ground thermal resistances				
short term (6 hours pulse)	R_{6h}	m-K/W	0.080	
medium term (1 month pulse)	R_{1m}	m-K/W	0.121	
long term (10 years pulse)	R_{10y}	m-K/W	0.127	
Total length calculation				
heat pump outlet temperature	T_o	°C	45.0	
average fluid temperature in the borehole	T_m	°C	42.5	
total length	L	m	101.3	70.6

The results presented in Table 2.2 show a reduction in the required length of heat exchanger for a thermally improved coaxial BHE of around 30% over a standard U-tube BHE.

Further investigation is required to analyze the effect of insulating the inner pipe of a coaxial BHE. Based on the short-term performance comparison made in Figure 2.5, an insulated inner pipe would further reduce the short-term entering fluid temperature of the heat pump, and in-turn increase the corrected short-term COP, by eliminating any immediate heat transfer from the inner pipe to the outer returning flow passage.

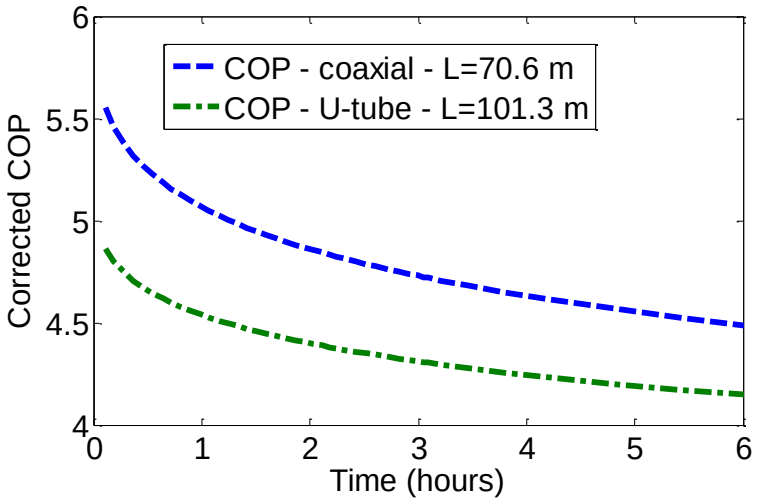

Figure 2.5: Performance comparison between the considered U-tube and coaxial BHEs, where the COP is corrected based on the entering fluid temperature of the heat pump

2.5 Conclusions

This chapter has provided a brief overview of vertical borehole heat exchangers considering U-tube and coaxial BHEs from a design perspective. Following the continuous interest in geothermal technology, this chapter offers insight into the important design parameters and considerations for vertical borehole heat exchangers. Thermal models can be used to estimate design parameters based on thermal response test results. In this chapter, a single BHE was modelled as an existing design for an enhanced coaxial BHE, and compared to a comparably sized U-tube BHE. The U-tube and coaxial BHEs are compared analytically using the common ICS model and the corresponding effective borehole resistances. It is found that an enhanced coaxial BHE can allows for a reduced design length requirement by up to 30% compared to a standard U-tube BHE of comparable size, while maintaining an increased short-term coefficient of performance. It is concluded that further research is necessary on how to improve the design of coaxial BHEs while maintaining economic feasibility and compliance with North American regulations.

Acknowledgments

This work is made possible by an OCE (Ontario Centres of Excellence) VIP project with GeoSource Energy Inc.

References

Acuña, J., 2013. Distributed thermal response tests-New insights on U-pipe and Coaxial heat exchangers in groundwater-filled boreholes.pdf (Doctoral). Royal Institute of Technology KTH, Stockholm, Sweden.

Acuña, J., Mogensen, P., Palm, B., 2009. Distributed Thermal Response Test on a U-pipe Borehole Heat Exchanger, in: The 11th International Conference on Energy Storage. Presented at the Effstock, Stockholm, Sweden.

Acuña, J., Palm, B., 2010. A Novel Coaxial Borehole Heat Exchanger: Description and First Distributed Thermal Response Test Measurements, in: Proceedings of the World Geothermal Congress. p. 7.

ASHRAE, 2011. 2011 Ashrae Handbook: HVAC Applications. ASHRAE, Atlanta, GA.

Beier, R.A., Acuña, J., Mogensen, P., Palm, B., 2014. Transient heat transfer in a coaxial borehole heat exchanger. Geothermics 51, 470–482. doi:10.1016/j.geothermics.2014.02.006

Beier, R.A., Acuña, J., Mogensen, P., Palm, B., 2013. Borehole resistance and vertical temperature profiles in coaxial borehole heat exchangers. Appl. Energy 102, 665–675. doi:10.1016/j.apenergy.2012.08.007

Beier, R.A., Smith, M.D., 2003. Minimum duration of in-situ tests on vertical boreholes. ASHRAE Trans. 109, 475–486.

Beier, R.A., Smith, M.D., Spitler, J.D., 2011. Reference data sets for vertical borehole ground heat exchanger models and thermal response test analysis. Geothermics 40, 79–85. doi:10.1016/j.geothermics.2010.12.007

Benli, H., 2013. A performance comparison between a horizontal source and a vertical source heat pump systems for a greenhouse heating in the mild climate Elaziğ, Turkey. Appl. Therm. Eng. 50, 197–206. doi:10.1016/j.applthermaleng.2012.06.005

Bernier, M.A., 2006. Closed-loop ground-coupled heat pump systems. Ashrae J. 48, 12–25.

Brenn, J., Soltic, P., Bach, C., 2010. Comparison of natural gas driven heat pumps and electrically driven heat pumps with conventional systems for building heating purposes. Energy Build. 42, 904–908. doi:10.1016/j.enbuild.2009.12.012

Carslaw, H.S., Jaeger, J.C., 1959. Conduction of Heat in Solids, Second. ed. Oxford University Press.

Claesson, J., Hellström, G., 2011. Multipole method to calculate borehole thermal resistances in a borehole heat exchanger. HVACR Res. 17, 895–911.

Gehlin, S., 2002. Thermal Response Test: Method Development and Evaluation.pdf (Doctoral). Lulea University of Technology, Lulea, Sweden.

Hellström, G., 1991. Thesis_Goran_Hellstrom.pdf. University of Lund, Sweden.

Ingersoll, L.R., Zobel, O.J., Ingersoll, A.C., 1954. Heat conduction: With engineering, geological applications, 2nd ed. McGraw-Hill.

IRENA, 2015. Renewable Energy Prospects: United States of America, REmap 2030 analysis. IRENA, Abu Dhabi.

Li, M., Lai, A.C.K., 2013. Analytical model for short-time responses of ground heat exchangers with U-shaped tubes: Model development and validation. Appl. Energy 104, 510–516. doi:10.1016/j.apenergy.2012.10.057

Lind, L., 2011. Swedish Ground Source Heat Pump Case Study (2010 Revision), GNS Science Report 2010/54. 30p.

Lund, J.W., Boyd, T.L., 2016. Direct utilization of geothermal energy 2015 worldwide review. Geothermics 60, 66–93. doi:10.1016/j.geothermics.2015.11.004

Philippe, M., Bernier, M., Marchio, D., 2010. Vertical Geothermal Borefields - Sizing Calculation Spreadsheet. ASHRAE J.

Philippe, M., Bernier, M., Marchio, D., 2009. Validity ranges of three analytical solutions to heat transfer in the vicinity of single boreholes. Geothermics 38, 407–413. doi:10.1016/j.geothermics.2009.07.002

Raymond, J., 2015. Direct Utilization of Geothermal Energy from Goast to Coast: a Review of Current Applications and Research in Canada.

RETScreen International., Clean Energy Decision Support Centre., 2001. Clean energy project analysis RETScreen engineering & cases textbook. Minister of Natural Resources Canada, [Varennes, Que.].

Sanner, B., 2009. Geothermal Heat Pumps - Ground source heat pumps (Brochure). EGEC.

Chapter 3 – Short-term Fluid Temperature Variations in either a Coaxial or U-tube Borehole Heat Exchanger

3.1 Introduction

Short-term analysis of borehole heat exchangers (BHE) is important when considering systems that often undergo transient ground-loop operation; this will occur when the ground-loop is re-engaged after allowing the fluid temperatures to recover during cyclic operation (Luo et al., 2015). Short-term fluid temperature responses are needed for such a system since the coefficient of performance for a geothermal heat pump is largely based on its entering fluid temperature (Xu, 2007). In order to more accurately size ground-coupled heat pump (GCHP) systems, in the case of bore field design, a thermal response test (TRT) can be performed on-site to estimate the ground's thermal properties and an effective borehole thermal resistance (Gehlin, 2002).

The borehole resistance is typically found for quasi steady-state conditions and is effectively the thermal resistance between the working fluid of a BHE and the surrounding ground. For transient conditions where short-term operation is experienced, it is desirable to size a bore field based not only on a steady-state borehole resistance, but also on the thermal capacity of the heat exchanger material. Analytical models for radial heat conduction are often used to interpret the time-varying temperature response in the working-fluid during a TRT. TRTs are typically performed using an above ground heater which delivers a constant rate of heat input to a working fluid being circulated through a fully operational BHE.

The configuration of these heat exchangers in North America is often of a single U-bend pipe travelling the length of a backfilled borehole (considered here as a U-tube BHE) (Sarbu and Sebarchievici, 2014). However, many different configurations have been investigated worldwide (including concentric pipe-in-pipe heat exchangers considered here as a coaxial BHE) with the aim of lowering the effective borehole thermal resistance, the required length of heat exchanger, and hence the cost.

TRTs reportedly have a typical minimum duration of 10 to 52 hours, which is dependent on the surrounding conditions, and can include an initial pumping phase, a heating phase, and a recovery phase (Liu and Beier, 2009). Prior to the test, it is required to allow the borehole to settle

and approach an undisturbed temperature which usually takes 3 to 7 days. By monitoring the inlet and outlet temperatures experienced by the working fluid during a TRT, a mean fluid temperature can be deduced. The mean fluid temperature (often taken as the arithmetic mean of the inlet and outlet temperatures) from a TRT is often fit with an analytical model in order to estimate the required thermal properties of the ground and borehole (Beier and Ewbank, 2012). A major downfall of previous analytical models is the assumption of a constant heat flux to the surroundings experienced uniformly along the depth of the borehole, where this is not the case during short-term transient operation of a ground-loop.

Traditionally, analytical models have been based off of Lord Kelvin's line source theory (leading to the *infinite line source* or ILS model) or Carslaw and Jaeger's cylindrical-source solutions (leading to the *infinite cylindrical source* or ICS model). The ICS model contains a response function that is commonly expressed in a Fourier-Bessel form and can be thought of as simply multiple line-sources placed around the periphery of a cylinder (Carslaw and Jaeger, 1959). For each analytical model, the solutions have been developed to estimate the temperature response in the ground or, for the case of composite models, in the surrounding composite media. These response functions – referred to in the application of ground heat exchangers as *g-functions* (g) (Ingersoll et al., 1954) – are related to the dimensionless Fourier number (Fo). The Fourier number is a dimensionless time variable that characterizes transient heat conduction by the ratio of conductive heat transport to the quantity of thermal energy storage ($\alpha\tau/L^2$) where; α is the thermal diffusivity of the material, τ is the characteristic time, and L is the length through which heat conduction occurs.

Conventional models for borehole wall temperature variations are often one-dimensional considering only radial heat conduction from a constant heat source in the ground, which is assumed to be a homogenous medium (Philippe et al., 2009). The borehole is typically limited to a small enough diameter to be able to ignore the heat capacities of the material within it; however, in order to effectively interpret short-term temperature responses for a TRT it is necessary to accurately represent the properties of the bore materials (grout, pipes, and working fluid) (Li and Lai, 2013). To do this, g-functions often incorporate two dimensions; this is especially important for conventional U-tube heat exchangers where the heat source does not produce a response that is symmetric in the radial direction (Li and Lai, 2012).

Typically a BHE is sized based on quasi steady-state results where the thermal properties of the borehole material hold less of an effect; however, considering a transient response in the composite media of a BHE is beneficial when considering on/off performance (Pasquier and Marcotte, 2012). Performance during transient operation of a ground loop is important when considering peak loads and the variability of hourly building loads that often result in a transient thermal response. Composite models which consider the thermal capacity effects of bore materials can be used to more accurately simulate the short-term temperature response during a TRT (Yavuzturk and Spitler, 1999).

Furthermore, when considering long-term temperature responses, it is necessary to consider the effects of axial heat conduction by considering a quasi-three-dimensional analytical model to account for fluid advection in the vertical direction (Rees and He, 2013; Pasquier and Marcotte, 2014). A *finite line source* (FLS) model, originally proposed by Eskilson (Eskilson, 1987) and further developed by (Zeng et al., 2002) and (Lamarche and Beauchamp, 2007), considers a finite length of heat exchanger to account for axial effects during long-term analysis (Bandos et al., 2009). The model by Lamarche and Beauchamp solves the pertaining double integrals in a unique manner which is computationally effective; even more recently, research has been conducted towards reducing the computation time of the FLS and similar analytical models (Pasquier, 2015). In the present thesis, models which consider axial effects are outside of the scope of research where focus is kept on developing a simple, one-dimensional composite model for application to coaxial BHE's.

It has been previously shown using a 3D numerical model that the arithmetic mean of the surface inlet/outlet temperatures is not a true representation of the average working fluid temperature as it creates an overestimation in the borehole thermal resistance which can lead to over design (Marcotte and Pasquier, 2008). This overestimation creates error that can be attributed largely to the fact that the fluid temperature response does not vary linearly with depth. It is also noted during short-term operation of a BHE that the heated working fluid does not immediately produce a constant heat flux to its surroundings uniformly along the depth of the borehole, but instead approaches this constant value based on the transient fluid residence time within the BHE. Taking the "p-linear" average has been suggested to improve the approximation of a mean fluid temperature deduced from surface temperature responses; this method makes the assumption that the fluid temperature response raised to the exponent, p,

will vary linearly between the temperature response at the inlet and the outlet each at the same power, p. The value of p may vary with time and an algorithm has been previously proposed to estimate the values of p at each sampling interval and the required ground thermal properties during a TRT (Zhang et al., 2014). This $p(t)$-*linear* method requires either a valid theoretical or measured temperature profile along the flow path of the heat exchanger and cannot be used with a simple one-dimensional model without such data.

Another method of performing a TRT is to directly measure the vertical temperature profile of the working fluid rather than only measuring the entering and exiting temperatures. A distributed thermal response test (DTRT) uses fiber optic cables placed along the pipes of the BHE to measure the temperature variation of the working fluid along its flow path (Fujii et al., 2009; Acuña and Palm, 2010). These tests would typically require more computationally extensive and complicated numerical or analytical models for accurate interpretation; however, they may be applied to either a coaxial or U-tube BHE. From this, a need can be identified for a simple analytical model for the interpretation of short-term fluid temperature variations during a typical TRT utilizing a coaxial BHE since many already exist for U-tube BHEs.

A composite cylindrical source (CCS) model presented by *Hu et al., 2014* is investigated in Section 3.3.3 of this thesis for the simulation of short-term fluid temperature variations during a TRT when considering a single, small-diameter U-tube BHE. Considering transient radial heat conduction within and around the borehole is important when designing systems for peak loads or cyclic operation of the ground-loop or heat pump. In order to model the transient response within a borehole the thermal storage rate of the individual materials should be considered. The model incorporates the thermal storage of the grouting material and has been previously validated for short-term simulation of ground heat exchangers having large diameters, referred to as energy piles, where the thermal interference between the pipes can be greatly reduced by increasing the distance between them.

In the case of deep small-diameter U-tube BHE`s, the ILS model can be used to accurately determine ground thermal properties; this may then be coupled with an analytical solution for steady-state heat transfer within the borehole. In Section 3.4 of this thesis, the CCS model is compared to a simplified ILS model which is coupled with the *multipole method* and a time-varying heat-flux term using principles of temporal superposition. A time-varying heat-flux term is used as a simplification to represent the average distribution of the short-term heat-flux to the ground.

A full-scale TRT is analyzed for a grouted (thermally enhanced grout or TE grout) U-tube BHE having known properties in order to test the CCS model for smaller diameter boreholes against the p-linear average, yielding a root mean square error (RMSE) of 0.37°C; this is compared in contrast to a RMSE of 0.05 °C when using the simplified ILS model discussed.

A composite model is then developed for the case of a coaxial BHE using consistent logic as found in the previous CCS model. For the coaxial case, the simulation of surface fluid temperatures during a TRT may be performed while discarding the equivalent diameter approach. The previous mentioned approach assumes a single cylinder centered along the heat exchanger as the contact between the working fluid and the surrounding grout in the case of a U-tube BHE, an assumption which has been known to degrade the accuracy of similar one-dimensional analytical models. In addition, for the coaxial case the proposed model accounts for the thermal storage rate of piping materials as well as short-circuiting effects. A full-scale TRT is performed with the same diameter of borehole, using a coaxial BHE with no grout, where the proposed model is validated for the coaxial case in comparison to the p-linear average. An RMSE of less than 0.1 °C could be found after an independent estimation of the effective ground thermal conductivity, which was found to increase from 3.73 W/m-K for the U-tube case to 3.93 W/m-K for the coaxial case.

3.2 Analytical Background

3.2.1 Infinite line source model

The ILS model is one-dimensional and is the simplest of the models presented in the literature, having been developed from Lord Kelvin's widely accepted line source theory (Sarbu and Sebarchievici, 2014). A BHE simulated with the ILS model is an infinitely long line acting as a heat source along the center of a borehole. The medium through which the heat source passes is assumed to be homogeneous with constant thermal properties and a uniform initial (undisturbed) ground temperature (T_o) (Zeng et al., 2002); this temperature remains the far-field temperature in the analysis of a BHE. For the purpose of a typical TRT, the temperature at the borehole wall (at the radius of the borehole, r_b) after a given time of operation (τ) can be estimated by the following equation (Monzo et al., 2011):

$$T(r_b,\tau) = T_o + \frac{q}{4\pi k_s}\int_{r_b^2/4\alpha_s\tau}^{\infty} \frac{e^{-u}}{u}du$$

$$\approx T_o + \frac{q}{4\pi k_s}\left(-\ln\left(\frac{r_b^2}{4\alpha_s \tau}\right) - \gamma\right); \qquad \frac{5r_b^2}{\alpha_s} \leq \tau < \frac{H^2}{9\alpha_s} \tag{3.1}$$

In Equation 3.1, the value γ is equal to 0.5772 and is referred to as Euler's constant, q is the heat flux per unit length of the borehole, α_s is the thermal diffusivity of the subsurface, and k_s is the ground thermal conductivity. The validity range of Equation 3.1 has previously been stated to restrict its application to small enough diameter boreholes where the heat capacity of the materials within may be ignored, as well as to operating times less than those resulting in steady-state operation where axial effects along the active depth of the borehole (H) becomes important (Eskilson, 1987).

The following expression has been used for approximating the mean fluid temperature (T_f) and considers the borehole to be a homogeneous medium which adds resistance between the fluid and the surrounding soil; this is a steady-state effective borehole thermal resistance, R_b (Kavanaugh, 2010):

$$T_f(\tau) \approx T_o + \frac{q}{4\pi k_s}(\ln(4Fo) - \gamma) + qR_b \tag{3.2}$$

Equation 3.2 can be used to analyze the results of a TRT to estimate R_b and k_s, where the average fluid temperature T_f may be plotted against the natural logarithm of time. The resulting temperature curve forms a linear trend for operating times typically greater than 10 hours. The slope (m) during the late time is assumed to be inversely proportional to the effective ground thermal conductivity (Mattsson et al., 2008):

$$m = \frac{q}{4\pi k_s} \tag{3.3}$$

where k_s can then be estimated from TRT data results; R_b may be estimated using a valid analytical model for steady-state heat transfer within a U-tube BHE and α_s is typically estimated from the drilling profile. A dimensionless g-function can be interpreted for the ILS model to be the following (Pasquier and Marcotte, 2013):

$$g(Fo) = \frac{1}{4\pi}(\ln(4Fo) - \gamma) \tag{3.4}$$

It is noted that the ILS model presented above is given where a first order approximation of the g-function is used.

3.2.2 Infinite cylindrical source model

Originally developed by *Carslaw and Jaeger* in their work on heat conduction in solids (Carslaw and Jaeger, 1959) are solutions to instantaneous functions of cylindrical heat sources expressed in Fourier-Bessel form with a governing differential equation for heat transfer as follows (Sarbu and Sebarchievici, 2014):

$$\frac{\partial^2 T}{\partial r^2}+\frac{1}{r}\frac{\partial T}{\partial r}=\frac{1}{\alpha_s}\frac{\partial T}{\partial \tau} \qquad r_b < r < \infty$$

$$-2\pi r_b k_s \frac{\partial T}{\partial \tau}=q \qquad r=r_b, \tau>0 \tag{3.5}$$

$$T-T_0=0 \qquad \tau=0, r>r_b$$

These solutions were then adapted by *Ingersoll et al., 1954* for their use in GCHP system applications as dimensionless response functions where they are first referred to as g-functions. The temperature at the borehole wall considering an infinite hollow cylindrical heat source is given by Equations 3.6 and 3.7, where Fo_1 is related to the transient heat conduction in the surrounding ground at the borehole wall:

$$T(r_b,\tau)=T_o+\frac{q}{k_s}g(Fo_1,1) \qquad ,\tau>0 \tag{3.6}$$

$$g(Fo,p)=\frac{1}{\pi^2}\int_0^\infty \frac{\frac{e^{-(\beta^2 Fo)}-1}{J_1^2(\beta)+Y_1^2(\beta)}[J_0(p\beta)Y_1(\beta)-J_1(\beta)Y_0(p\beta)]}{\beta^2}d\beta \tag{3.7}$$

It is known that cylindrical-source models are unstable especially over long-term analysis; this is because they tend to exhibit oscillatory behavior inherent to Bessel functions (Li and Lai, 2013). To avoid the use of complicated Bessel functions in this discussion, tabulated values and curve-fitting techniques have been used to generate an approximation for Equation 3.7 considering various values of p; where, $p=r/r_b$ is the ratio of the radius of interest to the radius of the borehole wall. Setting $p=1$ (*ie.* the response at the borehole wall) yields the following curve fitted function based on tabulated values for $0.1 < Fo < 10^6$ (Bernier, 2001):

$$g(Fo_1,1)=10^{-0.89129+0.36081\times\log_{10}(Fo_1)-0.05508\times\log_{10}^2(Fo_1)+0.00359617\times\log_{10}^3(Fo_1)} \tag{3.8}$$

It is noted that Equation 3.8 is not intended for use in long-term analysis where the higher order terms would dominate the solution. Finally the average fluid temperature may again be considered by the inclusion of an effective borehole thermal resistance.

$$T_f(\tau) = T_o + \frac{q}{k_s} g(Fo_1, 1) + qR_b \quad (3.9)$$

3.2.3 Composite cylindrical source model

Although many composite, analytical, and semi-analytical models exist (Bandyopadhyay et al., 2008; Beier and Smith, 2003; Javed and Claesson, 2011), a simplified composite model is investigated to provide ease of use and understanding. Equation 3.8 was used by *Hu et al., 2014* in the development of their composite cylindrical source model (referred to as the CCS model) which they validated using a 3D numerical model and field tests utilizing large diameter boreholes also known as energy piles. The CCS model treats the borehole as a composite medium by superimposing a series of hollow cylindrical heat sources. The mean fluid temperature may be estimated by the following equation which incorporates a cylindrical response function placed at each of the correspondingly numbered locations in Figure 3.1:

$$T_f(\tau) = T_o + q\left(\frac{g(Fo_1,1)}{k_s} + \frac{g(Fo_2,1)}{k_g} - \frac{g(Fo_3,1)}{k_g}\right) \quad (3.10)$$

where,

$$Fo_1 = \frac{\alpha_s \tau}{r_b^2}, \qquad Fo_2 = \frac{\alpha_g \tau}{r_w^2}, \qquad Fo_3 = \frac{\alpha_g \tau}{r_b^2}$$

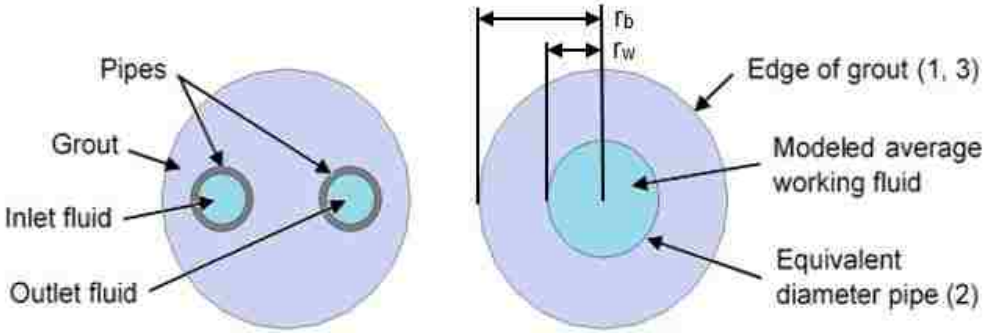

Figure 3.1: U-tube BHE considered (left) using equivalent diameter approximation (right)

Each g-function is related to the Fourier numbers representing (by numbered location): (1) transient radial heat conduction through the surrounding soil outside of the borehole, (2) transient radial heat conduction through the grout, assuming the grout is the infinite surrounding to an equivalent diameter pipe, and (3) transient heat conduction outside of the grout assuming the infinite surrounding is grout. Here, (3) can be seen to correct the assumption in (2) following that the surrounding soil thermal resistance is already accounted for in (1) and the infinite surrounding is soil, not grout.

Here, the equivalent pipe radius is given by the following equation where the effective steady-state borehole resistance (R_b) must be considered (Hu et al., 2014):

$$r_w = \frac{r_b}{e^{(2\pi k_g R_b)}} \tag{3.11}$$

3.2.4 Effective borehole thermal resistance

It is noted that, when either the ILS or the ICS model is fit to TRT results, the accuracy of R_b will depend on the estimated thermal properties of the soil; however, various analytical models have been developed to estimate R_b based solely on bore geometry and material properties. In an attempt to improve upon the classical linear superposition, the multipole method was developed to be able to account for multiple legs of tubes arbitrarily placed in the region of grouting with varying heat flux and can be expressed by the following equation (Claesson and Hellström, 2011):

$$R_b = \frac{1}{2}\left[\frac{1}{2\pi k_g}\left(\ln\left(\frac{r_b}{r_o}\right) + \ln\left(\frac{r_b}{D}\right) + \sigma \ln\left(\frac{(r_b)^4}{(r_b)^4 - (D/2)^4}\right) - \eta\right) + R_p\right] \tag{3.12}$$

where the thermal resistance of the pipes (R_p) is given by:

$$R_p = \frac{1}{2\pi k_p}\ln\left(\frac{r_o}{r_i}\right) + \frac{1}{\pi d_i h} \tag{3.13}$$

and a dimensionless ratio of thermal conductivities (σ) is given by:

$$\sigma = \left(\frac{k_g - k_s}{k_g + k_s}\right) \tag{3.14}$$

In the above equations, k_g and k_p are the grout and pipe thermal conductivities, r_o and r_i are the outer and inner pipe radii, D is the distance between the legs of the U-tube, and h is the convective heat transfer coefficient. It can be seen in Equation 3.12 that this form of the multipole method is an extension of the classical linear superposition where η considers a more thorough thermal network. Following that, if $\eta = 0$, then Equation 3.12 corresponds to linear superposition; for the multipole method, then the following applies (Li and Lai, 2013):

$$\eta = \frac{\left[\frac{r_o}{D}\left(1 - \frac{\sigma D^4}{4(r_b^4 - (D/2)^4}\right)\right]^2}{\frac{1+2\pi k_g R_p}{1-2\pi k_g R_p} + \frac{r_o^2}{D^2}\left[1 + \frac{\sigma D^4 r_b^4}{(r_b^4 - (D/2)^4)^2}\right]} \tag{3.15}$$

It is noted that the thermal conductivity of the piping material and the convective heat transfer coefficient of the working fluid are only indirectly considered here and the thermal

capacity effect of these materials is ignored. The convective heat transfer coefficient (h) in Equation 3.13 has been estimated using the Gnielinski Correlation – an expression relating the Nusselt number (Nu), Reynolds number (Re), and Prandtl number (Pr) for turbulent flow in pipes under forced convection (Beier et al., 2013). It is noted that there often exists a high level of uncertainty in this correlation due in part to the fact that many of the fluid properties used to calculate h should be given as a function of fluid temperature. Curve fitted approximations for these properties as a function of temperature have been developed; the thermal properties are then calculated considering the average of the measured fluid temperatures to provide updated estimations at each time interval.

$$Nu = \frac{(f/2)(Re-1000)Pr}{1+12.7(f/2)^{1/2}(Pr^{2/3}-1)}, \quad 2300 < Re < 5x10^6$$

$$Nu = 4.364, \qquad 0 < Re < 2300 \tag{3.16}$$

$$Re = \frac{\rho v D_h}{\mu} \tag{3.17}$$

$$h = \frac{Nu\, k_f}{D_h} \tag{3.18}$$

where f is the friction factor corresponding to the pipe wall, ρ, k_f, μ, and v are the density, thermal conductivity, dynamic viscosity, and velocity of the working fluid, respectively, and D_h is the hydraulic diameter of the flow path.

In relation to the CCS model discussed in Section 3.2.3 of this thesis, the steady-state R_b used to calculate the equivalent diameter of piping has previously been estimated using methods of linear superposition. In order to provide a consistent comparison with the discussed first order ILS model, the multipole method will instead be considered where the geometry is more accurately represented. *Pasquier and Marcotte (2012)* reference an equivalent borehole resistance found for short-time response using their improved thermal resistance capacity model (TRCM); in this chapter, an equivalent R_b is calculated based on the transient heat conduction occurring through the grout over the timespan of a TRT. A steady-state value for R_b is approached based on the transient thermal properties of the grouting material and may be calculated using the following equation where n_τ is the total number of time steps considered, j:

$$R_{b,CCS} = \frac{\sum\left(\frac{g(Fo_2,1)}{k_g} - \frac{g(Fo_3,1)}{k_g}\right)}{n_\tau} \tag{3.19}$$

3.2.5 Variable heat flux

In order to account for a variable heat flux with respect to time, the principles of temporal superposition are incorporated. Temporal superposition may be applied using the convolution theorem when a heat flux signal is present as a step function along with a selected model-specific integral ($G = g/k$); this may be written as (Pasquier and Marcotte, 2013):

$$\Delta T(r,\tau) = \sum_{j=1}^{n_\tau} f(\tau_j) G(\tau_j - \tau_{j-1}) \tag{3.20}$$

$$f(\tau_j) = q_j - q_{j-1} \tag{3.21}$$

Here, in order to distinguish this response function from the previous g-functions, G represents a chosen dimensionless g-function coupled with the material thermal conductivities considered, resulting in units of thermal resistance. $f(\tau_j)$ is the transfer function for an incremental heat flux per length of borehole (q); a transfer function applicable for a typical TRT having discrete time intervals is proposed here. It is assumed that the heat flux per unit length of a borehole considering an equivalent diameter pipe will approach the constant heat flux experienced by the working fluid at the heater (q_{n_τ}) through an asymptotic relationship based on the residence time (τ_r) along the active depth of the borehole (H):

$$q_j = q_{n_\tau} \tau_j / (\tau_j + \tau_r) \tag{3.22}$$

$$\tau_r = \frac{2H}{v} \tag{3.23}$$

It is noted here that the heat flux emitted from either leg of the U-tube is assumed to be equal to half of the total heat flux emitted to the ground, where this assumption is known to degrade the accuracy of some models. It is then also assumed that the heat flux to the surroundings will likely be delayed by a full fluid residence time within the heat exchanger after the heater is engaged (Zarrella et al., 2011). The latter note would indicate that a response in the surrounding grout and soil would not begin to develop also until a full fluid residence time has passed; this is a reasonable assumption when considering heat exchangers with small residence times. Equation 3.20 may now be applied with chosen functions of f and G. In relation to the composite medium between a working fluid and the surrounding soil, the chosen G is a combination of hollow cylindrical g-functions coupled with their corresponding material thermal conductivities as follows:

$$G_{combined}(\tau_j) = \frac{g(Fo_1,1)}{k_s} + \frac{g(Fo_2,1)}{k_g} - \frac{g(Fo_3,1)}{k_g} = G_{ground}(\tau_j) + G_{grout}(\tau_j) \quad (3.24)$$

3.2.6 U-tube verification

A U-tube BHE is considered to verify the model for radial heat conduction in small diameter boreholes where the parameters used are given in Table 3.1:

Table 3.1: U-tube test parameters

Characteristics	Symbol	Unit	Value
Borehole			
Radius	r_b	cm	4.93
Ground			
Thermal conductivity	k_s	W/m-K	3.68
Thermal diffusivity	α_s	m^2/s	$1.44x10^{-6}$
Pipe			
Equivalent radius	r_w	cm	2.15
Grout			
Thermal conductivity	k_g	W/m-K	1.52
Thermal diffusivity	α_g	m^2/s	$4.73x10^{-7}$

The g-functions corresponding to the simplified ILS model, the ICS model, and the response at the equivalent diameter pipe are plotted against their corresponding Fourier numbers in Figure 3.2. It can be seen for the CCS model that the magnitude of the dimensionless response at each location depends on the Fourier numbers representing transient heat conduction through the individual materials. The cylindrical g-functions are compared to that of the dimensionless response considered for the ILS model at the borehole wall. It can be seen that the first order ILS model does not accurately represent short-term responses since the magnitude of its g-function is negative when considering small Fourier numbers where higher order approximations and the hollow cylindrical g-function aim to correct this. It is noted that the first order ILS model is retained here for simplicity, but would behave similarly to the cylindrical source model if extended to a higher order.

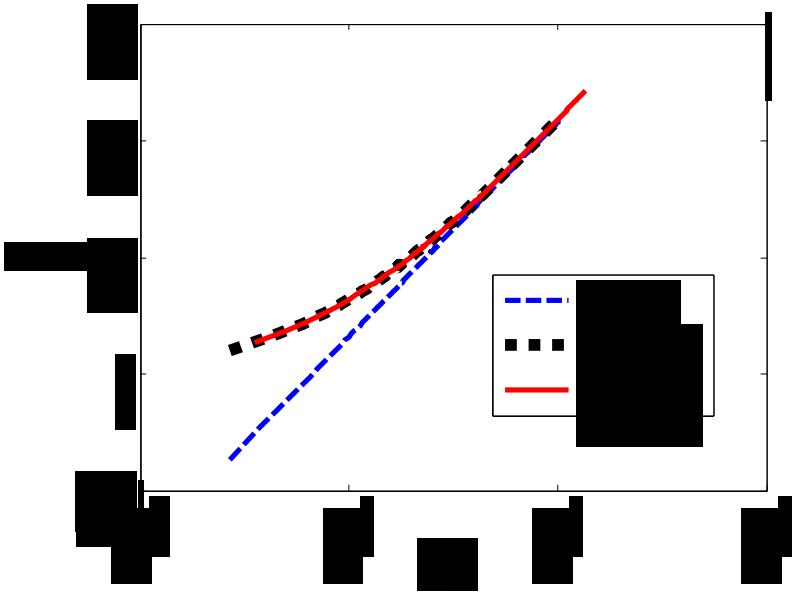

Figure 3.2: Dimensionless g-functions used in the CCS model in comparison to the dimensionless response considered in the ILS model

When considering the cylindrical sources placed at the various locations in the composite model, the ratio of conductive heat transport to the storage rate changes based on the borehole geometry and the thermal properties of the bore material. The results show the greatest response occurring at the inner ring of grout (immediately next to the equivalent diameter) due to it having a smaller diameter considered, and the lowest response occurring at the borehole wall. This is illustrated in Figure 3.3 where the dimensional G-functions are plotted against time in minutes.

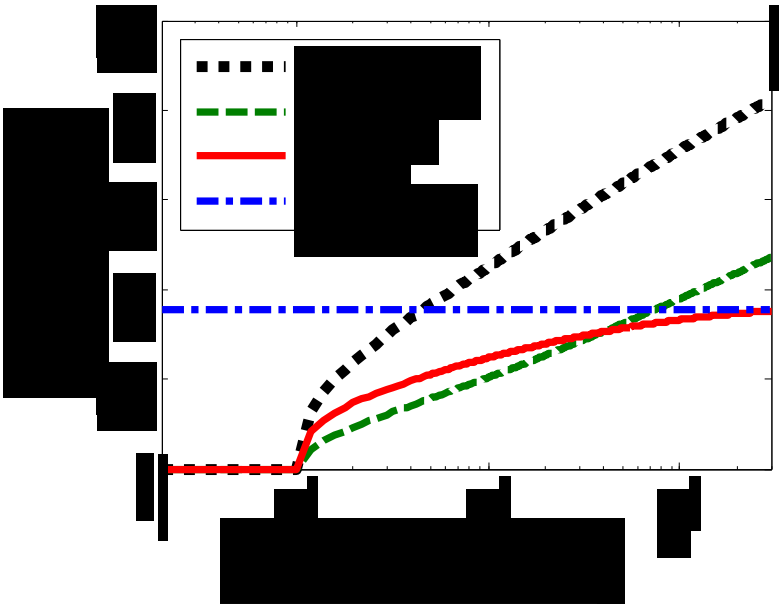

Figure 3.3: U-tube G-functions showing the development of late-time linear trends compared to a steady-state R_b calculated using the multipole method

It is shown in Figure 3.3 that a steady-state R_b will develop over the duration of the test as the change in the response becomes constant with time; this is estimated to be when the thermal energy storage capacity of the grout is reached and is no longer a factor in outward heat transfer. It is noted that the thermal response in the soil becomes the limiting factor for heat transport in the late-time period as the slope diminishes in the combined G-function which represents the equivalent resistance through the grout. This is the basis for the formation of a linear trend during the late-time temperature responses of a TRT which has a slope inversely proportional to the average thermal conductivity of the surrounding ground. It is noted that any heat conduction outside of the equivalent diameter pipe is delayed here by a full fluid residence time after the heater is engaged as this transient residence time is typically found to be similar to the delay realized at the beginning of a TRT in common practice (Zarrella et al., 2011).

3.3 Coaxial heat exchanger

3.3.1 Model development

To extend the use of the CCS model, an application is proposed for the simulation of a single coaxial BHE. In doing this, the equivalent diameter approximation can be discarded while maintaining a one-dimensional analytical model due to the symmetry of a coaxial BHE with cylindrical heat sources; this allows for the thermal heat capacity of the pipes to be included. In the considered case, the fluid will enter through the interior pipe region of the coaxial arrangement and exit through the annulus region. Considering only this case simplifies the problem for conventional TRTs utilizing an above ground heater, as the warmest area will then be located in the center of the arrangement and heat transfer will occur outwards radially. Figure 3.4 shows the considered case for a coaxial BHE (no grout):

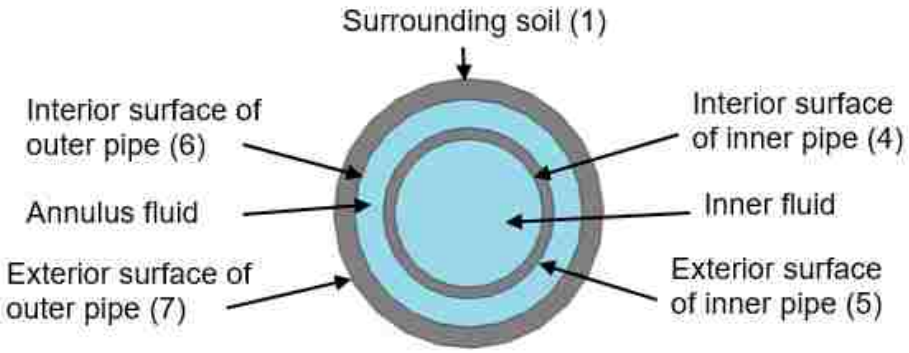

Figure 3.4: Coaxial BHE for the considered case

The following equations represent the dimensional response functions considered through the ground, fluid, piping, and the outer surroundings (grout is omitted in the considered case):

$$G_{ground}(\tau_j) = \frac{g(Fo_1,1)}{k_s} \tag{3.25}$$

$$G_{shunt}(\tau_j) = \frac{1}{2\pi h_{oi} r_{oi}} + \frac{g(Fo_4,1)}{k_{p_i}} - \frac{g(Fo_5,1)}{k_{p_i}} + \frac{1}{2\pi h_{ii} r_{ii}} \tag{3.26}$$

$$G_{outer}(\tau_j) = \frac{g(Fo_6,1)}{k_{p_o}} - \frac{g(Fo_7,1)}{k_{p_o}} + \frac{1}{2\pi h_{io} r_{io}} \tag{3.27}$$

where,

$$Fo_4 = \frac{\alpha_{p_i}\tau}{r_{ii}^2}, \qquad Fo_5 = \frac{\alpha_{p_i}\tau}{r_{io}^2}, \qquad Fo_6 = \frac{\alpha_{p_o}\tau}{r_{io}^2}, \qquad Fo_7 = \frac{\alpha_{p_o}\tau}{r_{oo}^2}$$

Following that k_{p_y}, α_{p_y}, refer to the inner or outer pipe (subscript y) thermal conductivity and diffusivities, h_{xy} is the convective heat transfer coefficient at the inner or outer surface (subscript x at r_{xy}) of the inner or outer pipe respectively. Equation 3.25 is the ground response of the typical ICS model, the response function in relation to the transient heat conduction and constant surface convection between the working fluid within the interior pipe and the fluid within the annulus region may be written as shown in Equation 3.26. Equation 3.27 is the response function in relation to the transient heat conduction and constant surface convection between the fluid within the annulus and the surrounding material layers.

From a simple energy balance performed in relation to Figure 3.4 it can be realized that there is no direct heat transfer between the working fluid within the inner pipe and the infinite

surrounding soil. The following equations are applied in order to calculate the fluid temperature at the inlet and outlet of the heat exchanger using the undisturbed ground temperature as the reference temperature. Temporal superposition is again used to include a similar time-varying heat-flux term as considered in the U-tube case; however, in the coaxial case the heat flux emanating from either pipe may be divided based on the volumetric ratio of fluid in each flow path ($V_{annulus}$,V_{inner}) to the total fluid volume (V_{total}), where:

$$q_{out_j} = \frac{V_{annulus}}{V_{total}} \cdot q_j \tag{3.28}$$

$$q_{in_j} = \frac{V_{inner}}{V_{total}} \cdot q_j \tag{3.29}$$

It should be noted that the above volumetric ratios would only be valid for a coaxial BHE having a similar thermal shunt resistance compared to its outer borehole. In the considered coaxial case, the inner and outer pipes are made of the same material at the same pressure rating, resulting in very similar shunt and outer borehole resistances.

In the following equations, Equation 3.30 represents the fluid temperature rise in the annulus region (a) while omitting the internal pipe. Equation 3.31 represents the fluid temperature rise in the inner pipe (i) while omitting the outer convective resistance, pipe, and surrounding ground (g), where transient heat conduction is considered through the inner pipe with a fluid convective resistance on either side. Equation 3.32 creates an additional temperature rise in the annulus based on the difference between the heat transferred from the inner pipe and the heat lost to the surrounding ground based on the heat flux from the inner pipe.

$$\Delta T_{f,a-g} = \left[\sum_{j=1}^{n_\tau} (q_{out_j} - q_{out_{j-1}}) \left(G_{ground}(\tau_j - \tau_{j-1}) + G_{outer}(\tau_j - \tau_{j-1})\right)\right] \tag{3.30}$$

$$\Delta T_{f,i-a} = \left[\sum_{j=1}^{n_\tau} (q_{in_j} - q_{in_{j-1}}) \left((G_{shunt}(\tau_j - \tau_{j-1})\right)\right] \tag{3.31}$$

$$\Delta T_{f,i-g} = \left[\sum_{j=1}^{n_\tau} (q_{in_j} - q_{in_{j-1}}) \left(G_{shunt}(\tau_j - \tau_{j-1}) - G_{ground}(\tau_j - \tau_{j-1})\right)\right] \tag{3.32}$$

The fluid temperature at the outlet of the annulus may be estimated by the combination of Equations 3.30 to 3.32 in the following equation where the far-field temperature remains that of the undisturbed ground temperature:

$$\Delta T_{f,outlet} = (\Delta T_{f,a-g} + \Delta T_{f,i-a} + \Delta T_{f,i-g}) \tag{3.33}$$

The logic behind Equations 3.28 to 3.33 is that, while holding the total fluid volume constant, as the volume of the annulus increases and the volume of the inner pipe decreases, the solution would approach that of the ICS model with a surrounding outer pipe and possible grout; as the volume of the inner pipe increases, the thermal effect of its presence increases and causes for a decreased slope in the late-time period of a TRT using a coaxial BHE.

The inlet fluid temperature may then be estimated by adding the fluid temperature rise measured across the above-ground heater ($\Delta T_{f,surface}$) based on:

$$T_{f,inlet} = T_{f,outlet} + \Delta T_{f,surface} \tag{3.34}$$

It is noted that it is desirable for the model to express a single average fluid temperature for the basis of ground loop design. A modeled p-linear average fluid temperature may be calculated based on the previous inlet and outlet approximations as they might be with measured inlet and outlet temperatures.

Finally, an effective borehole thermal resistance for a coaxial BHE is related to the resistance between the annulus fluid and the surrounding ground (Beier et al., 2013). This can be calculated using a similar formula as Equation 3.19 in the U-tube case, where there exists a convective resistance at the inner surface of the outer pipe:

$$R_{b,CCS} = \frac{\Sigma\left(\frac{g(Fo_{6},1)}{k_{p_o}} - \frac{g(Fo_{7},1)}{k_{p_o}} + \frac{1}{2\pi h_{io} r_{io}}\right)}{n_\tau} \tag{3.35}$$

The result of this equation taken at the last time step considered for the TRT duration will be later compared with a steady-state solution given by Beier et al., 2013:

$$R_b = \frac{1}{2\pi k_{p_o}} \ln\left(\frac{r_{oo}}{r_{io}}\right) + \frac{1}{2\pi h_{io} r_{io}} \tag{3.36}$$

Equations 3.35 and 3.36 are limited by the fact that they do not account for the effect of an inner pipe, which has potential to greatly influence the behavior of the BHE.

3.3.2 Coaxial verification

In order to verify the proposed model for the coaxial case when considering transient radial heat conduction through the inner pipe and through the outer pipe then ground, the parameters listed in Table 3.2 are used. Equations 3.25, 3.26, and 3.27 for the coaxial case are each plotted against time in minutes in Figure 3.5 to investigate the magnitude of each response

function. It can be deduced from Figure 3.5 that the greatest magnitude of the thermal response will occur through the inner pipe since it is heated first. Likewise, the lowest response will occur in the ground until the surrounding ground becomes the dominant factor. It is noted that the thermal response through the inner pipe begins to decrease in the late times, giving reason for why a coaxial temperature response during a TRT may not end up reaching a quasi-steady state. The effect of short circuiting can be seen in the combination of the ground and shunt G-functions as they are found in Equation 3.32, where this acts as a two-way equivalent thermal resistance to and from the annulus fluid.

Table 3.2: Coaxial test parameters

Characteristics	Symbol	Unit	Value
Borehole			
Radius	r_b	cm	4.93
Depth	H	m	182
Ground			
Thermal conductivity	k_s	W/m-K	3.73
Thermal diffusivity	α_s	m^2/s	$1.44x10^{-6}$
HDPE Pipe			
Thermal conductivity	k_p	W/m-K	0.40
Thermal diffusivity	α_p	m^2/s	$1.84x10^{-6}$
Inner radius of outer pipe	r_{io}	cm	3.59
Outer radius of outer pipe	r_{oo}	cm	4.45
Inner radius of inner pipe	r_{ii}	cm	1.95
Outer radius of inner pipe	r_{oi}	cm	2.41

It is further proposed that heat conduction in the ground and through the outer pipe is delayed by a full fluid residence time after the heater is engaged as done for the U-tube case; however, the heat exchange through the shunt resistance begins immediately. The Fourier time series on which the cylindrical g-functions making up these components are based are therefore padded with zeroes until the initial residence time has passed (note, the convective film resistance is not effected); this time corresponds to when the outlet temperature begins to experience a significant temperature rise.

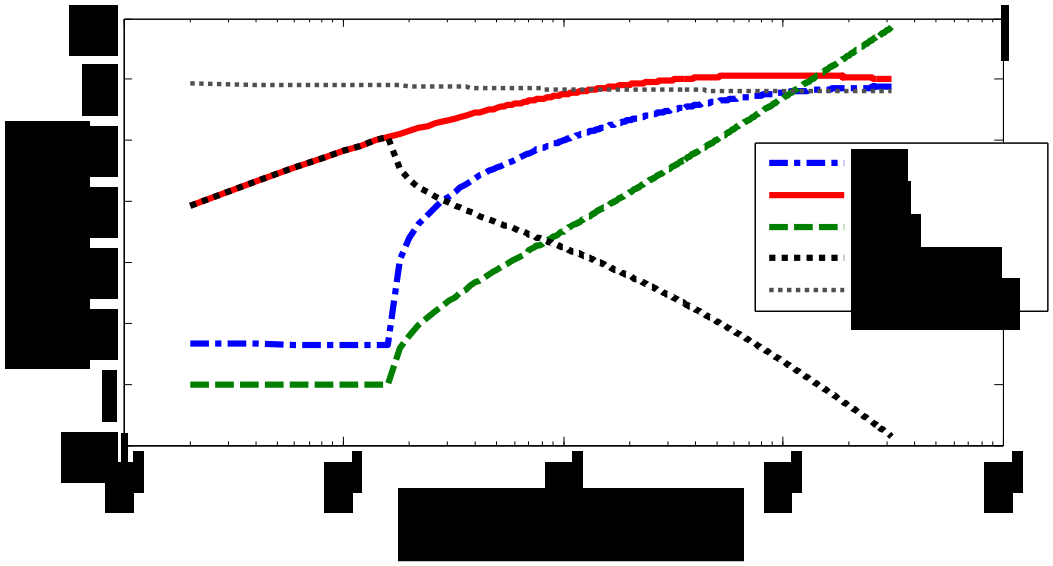

Figure 3.5: Coaxial BHE G-functions for individual areas of heat transfer showing the late-time trends

3.4 Model validation

Two TRTs are analyzed on separate fully operational BHEs having small diameters, one having a grouted U-tube configuration and the other a non-grouted coaxial configuration. Table 3.3 contains a summary of the known input parameters for each test. The experimental results and input parameters for the two tests have been provided by *GeoSource Energy, Inc.* and are used as a comparison between the two configurations. Each borehole was drilled to a depth of 183 m with 9.1 m being sand with a borehole diameter of 140 mm, and the rest being limestone with a borehole diameter of 98 mm; a weighted average value for the diameter is used in the simulation. Independent estimates for the ground thermal conductivity are made by fitting the ILS model to the late-time data of each test; since the two BHEs are within the vicinity of one another, it is found that the ground shares a similar drilling profile an initial estimate for the thermal conductivity is 3.73 W/(m-K) with a borehole resistance of 0.87 (m-K)/W when fit with the ILS without temporal superposition applied. The grout used in the U-tube case is thermally enhanced (TE) consisting of (by volume): 59% water, 32% silica sand ($SG = 2.6$), and 9% bentonite ($SG = 2.2$). The pipes used are high density polyethylene (HDPE) and with specifications provided by *VERSApipe HD.* A *GeoCube™* was used as the above-ground testing unit (connected to a generator) having accuracies presented in Table 3.4:

Table 3.3: Input parameters for full-scale validation

Characteristics	Symbol	Unit	U-Tube	Coaxial
Borehole				
Active length	H	m	182	182
Radius	r_b	cm	4.93	4.93
Test Set-up				
Average rate of heat input	Q	W	11040	11022
Average flow rate	Q_f	l/s	0.560	0.560
Ground (5% sand, 95% limestone)				
Thermal conductivity	k_s	W/m-K	3.73 [a]	3.93[c]
Thermal diffusivity	α_s	m^2/s	$1.44x10^{-6}$ [b]	$1.44x10^{-6}$ [b]
Undisturbed temperature	T_o	°C	10.1	9.8
HDPE Pipe				
Thermal conductivity	k_p	W/m-K	0.40	0.40
Thermal diffusivity	α_p	m^2/s	-	$1.84x10^{-6}$
Distance between U-tube legs	D	cm	4.8	-
Nominal pipe diameters	-	in	1-1/4	3, 1-1/2
TE Grout				
Thermal conductivity	k_g	W/m-K	1.52	-
Thermal diffusivity	α_g	m^2/s	$4.73x10^{-7}$	-

[a.] value estimated using simplified ILS model

[b.] values estimated from geological conditions

[c.] value estimated using proposed coaxial model

Table 3.4: GeoCube components and stated accuracy (Precision Geothermal, 2011)

Component	**Accuracy**	**Operating Range**
AC potential transformer	+/- 1%	10-130% rated voltage
AC current transformer	+/- 1%	10-130% rated current
Flow Meter	+/- 3%	N/A
Temperature Sensor (12 bit smart sensor)	+/- 0.2°C	0-50°C

The undisturbed ground temperature for each case has been estimated by taking the average temperature experienced through the heat exchanger over one residence time before the heater is engaged.

The *p-linear* estimator is used to validate the proposed models (Marcotte and Pasquier, 2008):

$$\left|\Delta T_p\right| = \frac{p\left(|\Delta T_{in}|^{p+1} - |\Delta T_{out}|^{p+1}\right)}{(1+p)\left(|\Delta T_{in}|^{p} - |\Delta T_{out}|^{p}\right)} \tag{3.37}$$

This estimator assumes that the average fluid temperature response will vary linearly between the temperature response at the inlet and outlet each raised to the exponent p. It is noted that when $p = 1$, Equation 3.37 corresponds to the arithmetic mean of the inlet and outlet temperature responses; however, it has previously been shown in comparison to a 3D numerical model that a more accurate estimation of the true mean fluid temperature is when $p \to -1$. The purpose of properly simulating the true mean fluid temperature within the BHE is to improve the estimation of ground thermal properties and an effective borehole thermal resistance during a TRT when the results are interpreted using an appropriate analytical or numerical model. Even more recently there has been an algorithm developed to produce a time-series of p values where p may vary with time (Zhang et al., 2014); however this method, known as the $p(t)$-linear method, requires knowledge of a vertical temperature profile with depth. A comparison between the arithmetic and p-linear averages is shown in Figure 3.6 where the p-linear average ($p \to -1$) more accurately represents the vertical fluid temperature profile within a BHE than the arithmetic mean temperature when a theoretical or measured temperature profile is not available.

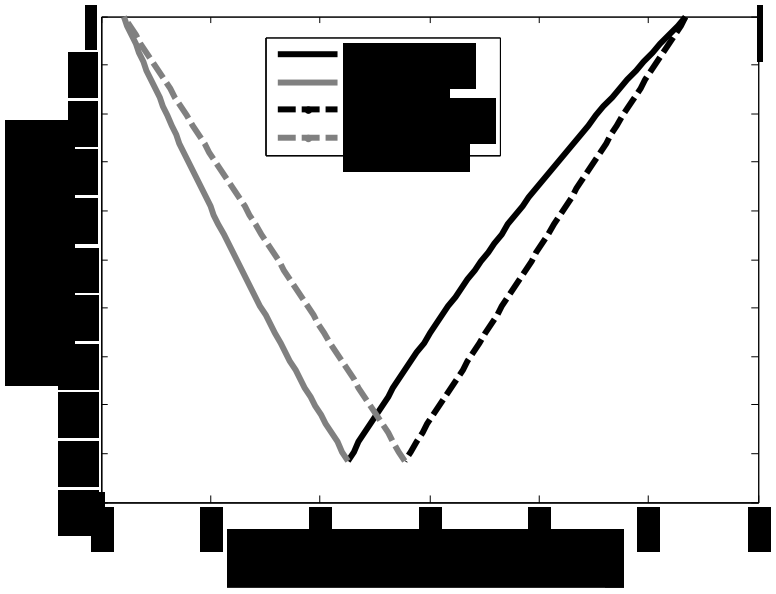

Figure 3.6: Vertical temperature profiles produced for steady-state results comparing p-linear average to the arithmetic mean

Figure 3.7 shows the short-term temperature profiles produced for the p-linear average and the assumed initial undisturbed ground temperature; it can be seen here that taking the arithmetic mean of the inlet and outlet temperatures largely overestimates the true mean fluid temperature during short-term operation.

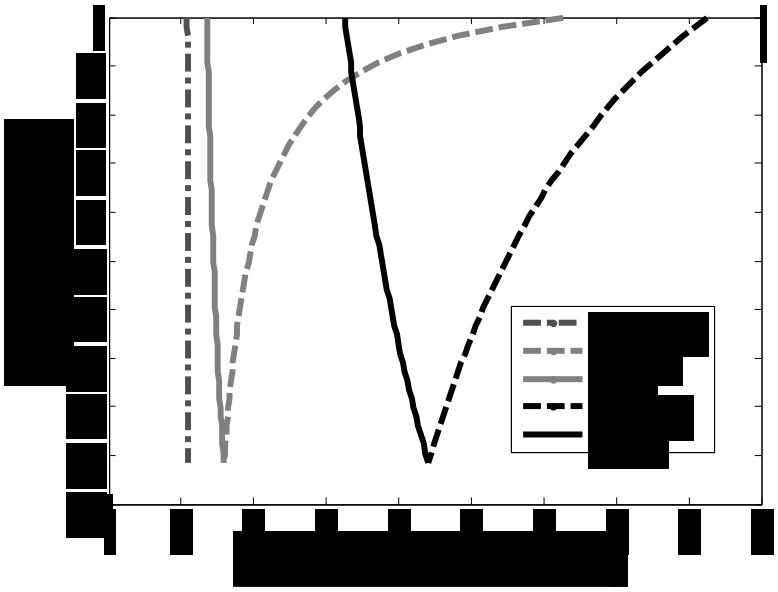

Figure 3.7: p-linear average temperature profiles over the first two residence times

3.4.1 U-tube case results and discussion

Figure 3.8 shows the prescribed heat flux (Equation 3.22) as it approaches the heat flux supplied by the heater for the U-tube case. The flow rate is measured over the duration of the test where poor accuracy is exhibited; an average flow rate has been used to smooth out the model's resulting temperature curve. The simplified ILS model is applied to Case 1 in Figure 3.9 where it is seen to closely follow the measured data from the start to the end of the test having a resulting RMSE of 0.05 °C with a soil thermal conductivity of 3.73 W/(m-K) and a borehole resistance of 0.883 (m-K)/W. The lag noticed during the initial residence time (after the heater is engaged) is due in part to the fluid not yet having travelled the entire length of the heat exchanger and is simulated by delaying the thermal response in the ground and the development of any outward heat flux by a full fluid residence time.

Figure 3.9 includes the base CCS model where the combined G-function is used. It can be seen that the CCS model seems to underestimate the average fluid temperature throughout the majority of a TRT; an RMSE of 0.37 °C is found throughout the test which is greater than the measuring devices' uncertainty. It can be seen that although the CCS model is valid for larger diameter energy piles, as the diameter of a BHE gets smaller; that is, less grout, more error is introduced. The estimation for the ground thermal conductivity while using the discussed ILS model is taken as the average local value and used as the initial estimation for the ground surrounding the coaxial BHE.

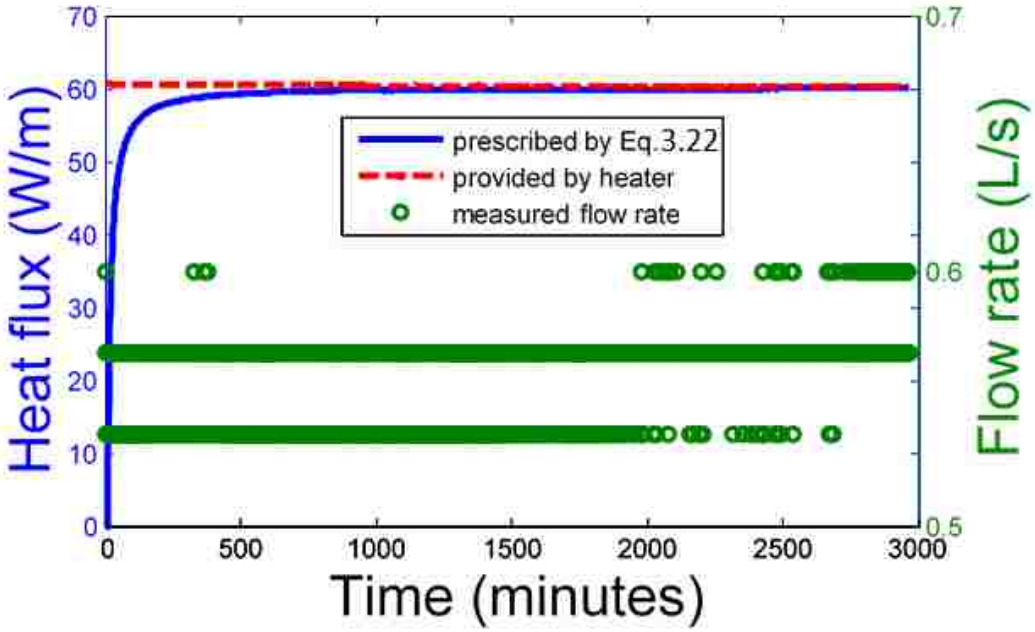

Figure 3.8: Comparison of the heat flux used in the analysis of the U-tube BHE; flow rate was measured over the duration of the test showing high variability

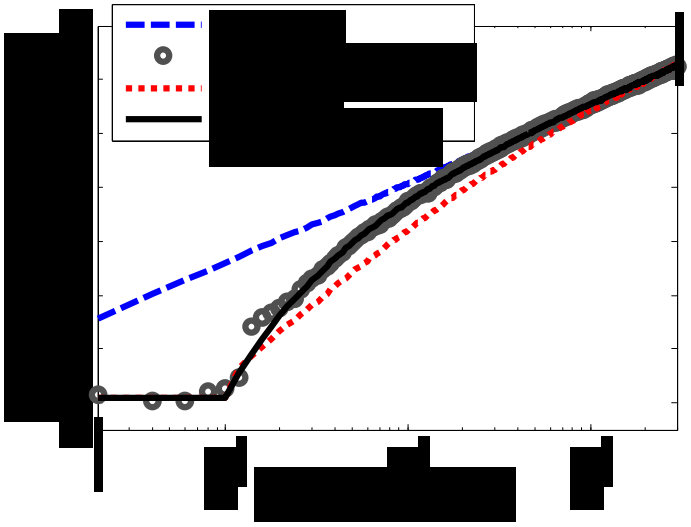

Figure 3.9: Validation of the proposed model for the U-tube BHE

3.4.2 Coaxial case results and discussion

Figure 3.10 shows the prescribed heat flux' for the coaxial model in comparison to the heat supplied by the heater. The composite coaxial model is applied to the coaxial BHE in Figure 3.11. In this figure, each of the inlet, outlet, and the p-linear average fluid temperatures are estimated throughout the duration of a thermal response test; this allows for some flexibility in

the model since the outlet temperature would lead to the direct calculation of a heat pump's coefficient of performance. An RMSE of less than 0.1°C is calculated for the simulated p-linear average fluid temperature over the duration of the test yielding an average soil thermal conductivity of 3.93 W/(m-K). It is shown that the ICS model, when coupled with a steady-state borehole resistance, does not properly capture the temperature curve for a small-diameter coaxial BHE where the inner pipe has a larger effect on heat transfer.

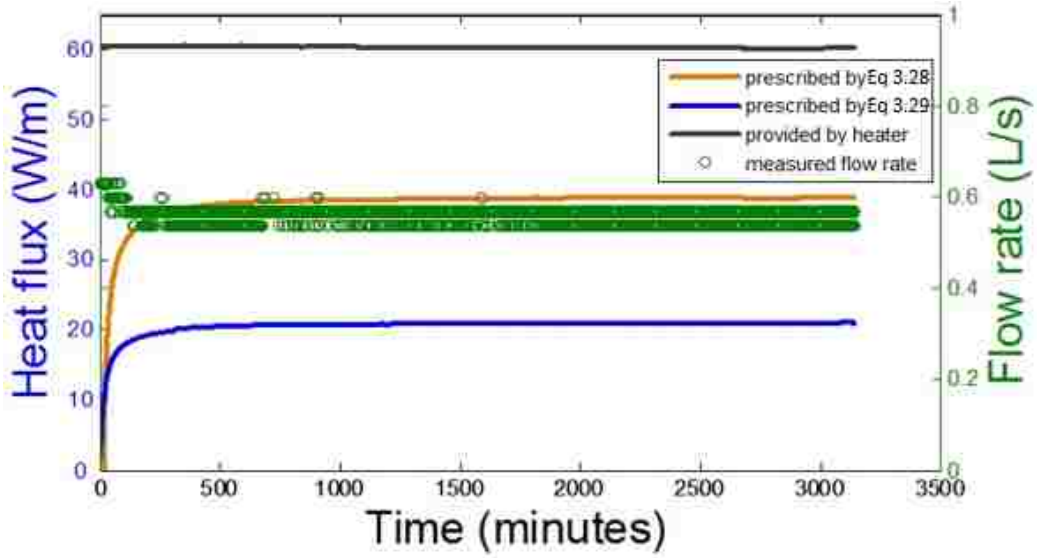

Figure 3.10: Comparison of the heat flux used in the analysis of the coaxial BHE

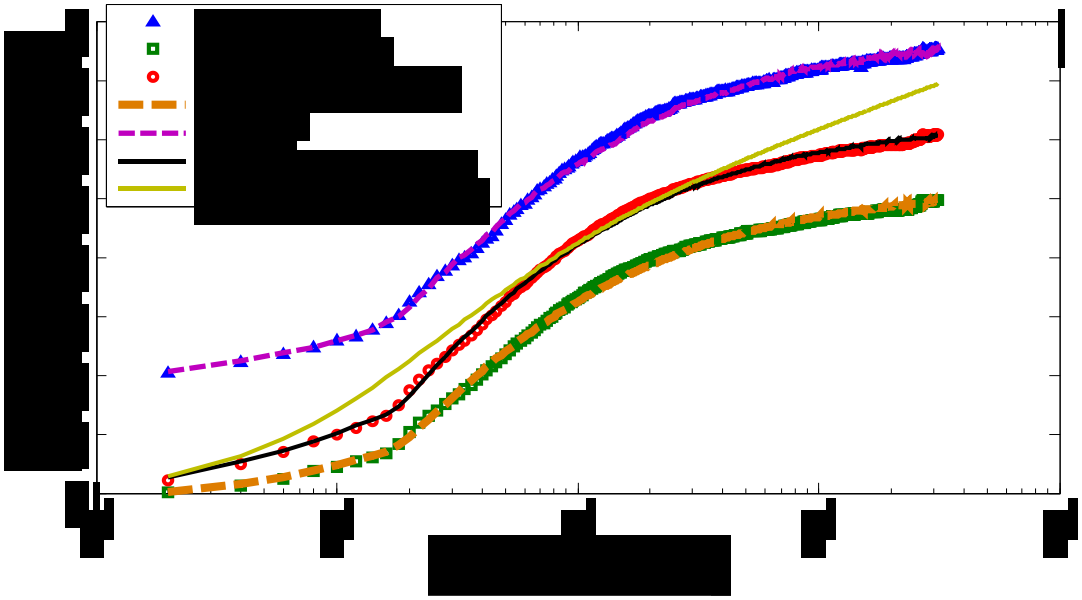

Figure 3.11: Validation of the proposed model for the coaxial case

Borehole thermal resistances for the coaxial case are calculated in the following ways: 1) *Beier et al., 2014, 2013* have developed a vertical temperature profile model using Equation 3.36 (with their inclusion of possible grout) as the borehole resistance; that is, the thermal resistance between the annulus fluid and the surrounding ground. 2) *Raymond et al., 2015* derived the following analytical expression for a three-dimensional borehole resistance:

$$R_b^* = R_{outer}\left(1 + \frac{H^2}{3(\dot{m}_w c_w)^2 R_{shunt} R_{outer}}\right) \tag{3.38}$$

where $\dot{m}_w$ is the mass flow rate within the BHE. Finally, 3) Equation 3.35 and the following equation are used to calculate transient values for each of the outer and shunt resistances:

$$R_{shunt,CCS} = \frac{\Sigma\left(\frac{1}{2\pi h_{oi} r_{oi}} + \frac{g(Fo_4,1)}{k_{p_i}} - \frac{g(Fo_5,1)}{k_{p_i}} + \frac{1}{2\pi h_{ii} r_{ii}}\right)}{n_\tau} \tag{3.39}$$

Equation 3.40 is compared with the following equation from *Beier et al., 2014, 2013* where n_t is equal to the total number of time steps considered (n_t = 1571= 3144 minutes):

$$R_{shunt} = \frac{1}{2\pi h_{ii} r_{ii}} + \frac{1}{2\pi k_{p_i}} \ln\left(\frac{r_{oi}}{r_{ii}}\right) + \frac{1}{2\pi h_{oi} r_{oi}} \tag{3.40}$$

Table 3.5 provides a summary of the borehole thermal resistances calculated for each case. The proposed calculation for a transient resistance is in good agreement with the multipole method for the U-tube case (less than 7% difference) as well as the steady-state approximation made in the coaxial case (less than 3% difference).

Table 3.5: Summary of U-tube borehole thermal resistances

Borehole thermal resistance (W/m-K)		
Method of Calculation	U-tube	Coaxial
ILS (fit to data)	0.087	-
Multipole method	0.088	-
Equation 3.19/3.35 (CCx - outer)	0.082	0.087
Equation 3.40 (CCx - shunt)	-	0.100
Equation 3.36 (steady-state outer)	-	0.096
Equation 3.39 (3D resistance)	-	0.117
Equation 3.41 (steady-state shunt)	-	0.100

Although the borehole resistance seems higher in the coaxial case, benefits can be found in both the short-term and steady-state operation. The increased surface contact between the outer pipe and the surroundings allows for a greater heat-flux to be delivered to the ground; this causes for reduced temperatures in the late-time data for the coaxial case. During transient operation, the short-circuiting effects causing the early increase in average fluid temperature could be seen as beneficial when the ground loop is disengaged as it allows the fluid temperature to recover more efficiently.

3.5 Conclusions

In conclusion, this chapter has validated a composite coaxial model which can accurately simulate short-term fluid temperatures during a TRT for the purpose of ground-loop designs requiring predominately transient ground loads and knowledge of short-term behavior. The short-term behavior of a BHE is important when sizing a system that often undergoes transient ground loads due to high variability in hourly building loads. In order to simulate the transient short-term behavior of a borehole heat exchanger, it is necessary to consider the thermal storage capacity of the borehole materials used. Considering a composite model made up of various cylindrical heat-sources allows for this; such a model is coupled with a time-varying heat flux term for the case of a coaxial BHE. When applied to a coaxial BHE, the composite model is able to discard the equivalent diameter approximation used for U-tube BHEs, an assumption which causes known errors in one-dimensional U-tube models. Since this approximation is discarded, the coaxial model is able to account for the thermal storage capacity of the individual pipes as well as the two-way heat exchange (short-circuiting) occurring between the working fluid within the annulus region, the inner pipe, and the surrounding ground. A simplified ILS model is used to estimate the local ground thermal conductivity from a U-tube thermal response test; a coaxial BHE is then used in a TRT in order to validate the composite coaxial model using known thermal properties. Borehole thermal resistances are calculated a variety of ways for each case in order to verify the results of the proposed coaxial model. The proposed composite coaxial model is found to closely fit the field data over the duration of the test, allowing for heat transfer to be analyzed through each portion of the heat exchanger. Properly interpreting TRT results to determine important thermal design parameters for a coaxial BHE system is imperative for an effective system; the proposed model provides a simple method for such interpretation.

Acknowledgments

This work is made possible by an OCE (Ontario Centres of Excellence) VIP project with GeoSource Energy Inc.

References

Acuña, J., Palm, B., 2010. A Novel Coaxial Borehole Heat Exchanger: Description and First Distributed Thermal Response Test Measurements, in: Proceedings of the World Geothermal Congress. p. 7.

Bandos, T.V., Montero, Á., Fernández, E., Santander, J.L.G., Isidro, J.M., Pérez, J., Córdoba, P.J.F. de, Urchueguía, J.F., 2009. Finite line-source model for borehole heat exchangers: effect of vertical temperature variations. Geothermics 38, 263–270. doi:10.1016/j.geothermics.2009.01.003

Bandyopadhyay, G., Gosnold, W., Mann, M., 2008. Analytical and semi-analytical solutions for short-time transient response of ground heat exchangers. Energy Build. 40, 1816–1824. doi:10.1016/j.enbuild.2008.04.005

Beier, R.A., Acuña, J., Mogensen, P., Palm, B., 2014. Transient heat transfer in a coaxial borehole heat exchanger. Geothermics 51, 470–482. doi:10.1016/j.geothermics.2014.02.006

Beier, R.A., Acuña, J., Mogensen, P., Palm, B., 2013. Borehole resistance and vertical temperature profiles in coaxial borehole heat exchangers. Appl. Energy 102, 665–675. doi:10.1016/j.apenergy.2012.08.007

Beier, R.A., Ewbank, G.N., 2012. In-Situ Test Thermal Response Tests Interpretations, OG&E Ground Source Heat Exchange Study. Oklahoma State Univ., Stillwater, OK (US), Oklahoma City, USA.

Beier, R.A., Smith, M.D., 2003. Minimum duration of in-situ tests on vertical boreholes. ASHRAE Trans. 109, 475–486.

Bernier, M.A., 2001. Ground-coupled heat pump system simulation/Discussion. Ashrae Trans. 107, 605.

Carslaw, H.S., Jaeger, J.C., 1959. Conduction of Heat in Solids, Second. ed. Oxford University Press.

Claesson, J., Hellström, G., 2011. Multipole method to calculate borehole thermal resistances in a borehole heat exchanger. HVACR Res. 17, 895–911.

Eskilson, P., 1987. Thermal Analysis of Heat Extraction Boreholes (Doctoral). University of Lund, Sweden.

Fujii, H., Okubo, H., Nishi, K., Itoi, R., Ohyama, K., Shibata, K., 2009. An improved thermal response test for U-tube ground heat exchanger based on optical fiber thermometers. Geothermics 38, 399–406. doi:10.1016/j.geothermics.2009.06.002

Gehlin, S., 2002. Thermal Response Test: Method Development and Evaluation.pdf (Doctoral). Lulea University of Technology, Lulea, Sweden.

Hu, P., Zha, J., Lei, F., Zhu, N., Wu, T., 2014. A composite cylindrical model and its application in analysis of thermal response and performance for energy pile. Energy Build. 84, 324–332. doi:10.1016/j.enbuild.2014.07.046

Ingersoll, L.R., Zobel, O.J., Ingersoll, A.C., 1954. Heat conduction: With engineering, geological applications, 2nd ed. McGraw-Hill.

Javed, S., Claesson, J., 2011. New analytical and numerical solutions for the short-term analysis of vertical ground heat exchangers. Energy Build. 117, 3–12.

Kavanaugh, S., 2010. Determining Thermal Resistance. ASHRAE J. 72.

Lamarche, L., Beauchamp, B., 2007. A new contribution to the finite line-source model for geothermal boreholes. Energy Build. 39, 188–198. doi:10.1016/j.enbuild.2006.06.003

Li, M., Lai, A.C.K., 2013. Analytical model for short-time responses of ground heat exchangers with U-shaped tubes: Model development and validation. Appl. Energy 104, 510–516. doi:10.1016/j.apenergy.2012.10.057

Li, M., Lai, A.C.K., 2012. New temperature response functions (G functions) for pile and borehole ground heat exchangers based on composite-medium line-source theory. Energy 38, 255–263. doi:10.1016/j.energy.2011.12.004

Liu, Y.D., Beier, R.A., 2009. Required Duration For Borehole Test Validated by Field Data. ASHRAE Trans. 115.

Luo, J., Rohn, J., Bayer, M., Priess, A., Wilkmann, L., Xiang, W., 2015. Heating and cooling performance analysis of a ground source heat pump system in Southern Germany. Geothermics 53, 57–66. doi:10.1016/j.geothermics.2014.04.004

Marcotte, D., Pasquier, P., 2008. On the estimation of thermal resistance in borehole thermal conductivity test. Renew. Energy 33, 2407–2415. doi:10.1016/j.renene.2008.01.021

Mattsson, N., Steinmann, G., Laloui, L., 2008. Advanced compact device for the in situ determination of geothermal characteristics of soils. Energy Build. 40, 1344–1352. doi:10.1016/j.enbuild.2007.12.003

Monzo, P.M., Acuña, J., Palm, B., 2011. Comparison of different Line Source Model approaches for analysis of thermal response Test in a U-pipe Borehole Heat Exchanger. Stockh. Swed.

Pasquier, P., 2015. Stochastic interpretation of thermal response test with TRT-SInterp. Comput. Geosci. 75, 73–87. doi:10.1016/j.cageo.2014.11.001

Pasquier, P., Marcotte, D., 2014. Joint use of quasi-3D response model and spectral method to simulate borehole heat exchanger. Geothermics 51, 281–299. doi:10.1016/j.geothermics.2014.02.001

Pasquier, P., Marcotte, D., 2013. Efficient computation of heat flux signals to ensure the reproduction of prescribed temperatures at several interacting heat sources. Appl. Therm. Eng. 59, 515–526. doi:10.1016/j.applthermaleng.2013.06.018

Pasquier, P., Marcotte, D., 2012. Short-term simulation of ground heat exchanger with an improved TRCM. Renew. Energy 46, 92–99. doi:10.1016/j.renene.2012.03.014

Philippe, M., Bernier, M., Marchio, D., 2009. Validity ranges of three analytical solutions to heat transfer in the vicinity of single boreholes. Geothermics 38, 407–413. doi:10.1016/j.geothermics.2009.07.002

Precision Geothermal, 2011. GeoCubeTM User's Manual.

Raymond, J., Mercier, S., Nguyen, L., 2015. Designing coaxial ground heat exchangers with a thermally enhanced outer pipe. Geotherm. Energy 3. doi:10.1186/s40517-015-0027-3

Rees, S.J., He, M., 2013. A three-dimensional numerical model of borehole heat exchanger heat transfer and fluid flow. Geothermics 46, 1–13. doi:10.1016/j.geothermics.2012.10.004

Sarbu, I., Sebarchievici, C., 2014. General review of ground-source heat pump systems for heating and cooling of buildings. Energy Build. 70, 441–454. doi:10.1016/j.enbuild.2013.11.068

Xu, X., 2007. Simulation and optimal control of hybrid ground source heat pump systems. ProQuest.

Yavuzturk, C., Spitler, J.D., 1999. A short time step response factor model for vertical ground loop heat exchangers. Ashrae Trans. 105, 475–485.

Zarrella, A., Scarpa, M., Carli, M.D., 2011. Short time-step performances of coaxial and double U-tube borehole heat exchangers: modeling and measurements. HVACR Res. 17, 959–976.

Zeng, H.Y., Diao, N.R., Fang, Z.H., 2002. A finite line-source model for boreholes in geothermal heat exchangers. Heat TransferAsian Res. 31, 558–567. doi:10.1002/htj.10057

Zhang, L., Zhang, Q., Huang, G., Du, Y., 2014. A p(t)-linear average method to estimate the thermal parameters of the borehole heat exchangers for in situ theral response test. Appl. Energy 131, 211–221. doi:http://dx.doi.org/10.1016/j.apenergy.2014.06.031

Chapter 4 – A Physical and Semi-Analytical Comparison between Coaxial BHE Designs considering Various Piping Materials

4.1 Introduction

Geothermal heat pump (GHP) systems can be used for a variety of applications; however, they are predominantly used for space heating and cooling. A GHP will transfer thermal energy to and from the conditioned space of a building between the surrounding subsurface of the Earth, providing reversible seasonal operation. Among renewable energy technologies in North America, geothermal resources make up only a small portion of the total installed capacity when compared to options such as biomass or wind (IRENA, 2015). That being said, interest in geothermal direct-use energy applications has continued to grow over the past decade, showing an increase in reported world-wide geothermal energy use of 116.8% since 2005. Under the broad category of direct-use applications, GHP systems have had the greatest economic impact where they were reported to make up 70.9% of total installed capacity for the year 2015, which increased from the 54.4% reported in 2005 (Lund et al., 2005; Lund and Boyd, 2016).

A GHP system can either be a closed- or open-loop system, where a closed-loop system consists of piping buried beneath the subsurface using a circulated working fluid (water, air, anti-freeze solution, etc.) to provide heat exchange with the surrounding ground. Focus is kept here on vertically arranged closed-loop systems which conventionally consist of high-density polyethylene (HDPE) piping placed in a grouted borehole. The pipes are often arranged with a separate supply and return leg where this arrangement is referred to as a U-tube borehole heat exchanger (BHE). In residential applications, usually only one or two boreholes will be sufficient to meet the demands of the project depending on drilling requirements and limitations (Blum et al., 2011). This research focuses on the analysis of specialized vertical coaxial BHE's that could help to increase the overall performance of GHP installations. A coaxial BHE will typically consist of concentric HDPE piping, with one inner and one outer tube. The goal of these heat exchangers is to maximize the area of effective heat transfer with the surrounding ground; where other benefits often include a longer fluid residence time and a reduced overall pressure drop. The reduced pressure drop may be seen as a benefit; however, depending on the geometry of the outer flow path, it may be difficult to achieve turbulent flow within the annulus (Wood et al., 2012). Turbulent flow is desired to promote heat transfer with the surroundings, this is sometimes

achieved in a coaxial BHE by modifying the outer flow path, for example breaking it into multiple smaller flow paths (Hsieh et al., 2014) or considering a helical design (Zarrella et al., 2011). Further improvements can be realized when using a combination of either a steel outer pipe or an insulated inner pipe (Beier et al., 2014; Zanchini et al., 2010a; Zarrella et al., 2011).

This chapter uses a semi-analytical model, referred to as the composite coaxial (CCx) model, to compare various designs of coaxial BHEs. Improvements to the model are presented which make it more capable of considering important design parameters such as pipe sizes and material properties. These systems are usually analyzed using a thermal response test (TRT), the results of which include measurements of the surface fluid temperatures at the inlet and outlet of the heat exchanger during a phase of constant heat injection for a duration of about 48 hours. The model is designed to simulate these operating conditions and is tested against three full-scale thermal response tests where it is found to produce valid results in each case; one of these tests was used in Chapter 3 of this thesis where the model was first validated (Gordon et al., 2017). Further analysis is performed within the tested validity range of the model comparing the required length of a single coaxial BHE having various material properties, and the associated coefficient of performance that would be realized by a typical residential heat pump having a 9 kW cooling capacity with 12 kW of ground-side heat rejection at 6 hour peak conditions.

A simplified design length equation that has been used for typical U-tube BHEs is adapted here for use with the composite coaxial model (ASHRAE, 2011; Bernier, 2006; Philippe et al., 2010). It is found that using a steel outer pipe will have a greater effect on overall length reduction in comparison to only having an insulated inner pipe, where the baseline case is standard HDPE inner and outer pipes. It is noted that if the flow rate (which is typically constant during operation) is decreased while the required length is correspondingly increased, the coefficient of performance will increase due to reduced pumping requirements and a lower pressure drop regardless of the increased length. The previous note is based on a constant heat pump entering water temperature (EWT) of 21.1°C and would indicate that a cost-versus-benefit analysis should be performed on a case-by-case basis considering, but not limited to trade-offs between: material selection, total initial cost, and annual operating costs.

4.2 Literature review

As mentioned, BHEs conventionally consist of U-tube style heat exchangers with a backfilled borehole (often backfilled using a thermally enhanced, or TE grout) (Alrtimi et al., 2013).

Analytical models have been developed for U-tube BHEs such as the line source, cylindrical source, and thermal resistance-capacity models (Bandyopadhyay et al., 2008; Carslaw and Jaeger, 1959; Ingersoll et al., 1954; Lamarche and Beauchamp, 2007; Li and Lai, 2012; Pasquier and Marcotte, 2012); however, they are often based on extreme approximations that may not always be applicable when considering coaxial BHEs. It is noticed that analytical models for coaxial BHEs remain forthcoming, this is likely due to the fact that the *infinite line source* (ILS) model will be in error when used to interpret thermal response test (TRT) data for coaxial arrangements having a significant internal *thermal shunt resistance* (Beier et al., 2013, 2014).

An optimal diameter ratio was investigated by *Mokhtari et al. (2016)* considering the pressure drop within a deep coaxial BHE as well as its thermal efficiency; however, this optimization is done from the perspective of optimizing an Organic Rankine Cycle where the return fluid is through the inner pipe and is steam. *Zanchini et al. (2010a, 2010b)* have presented a comparison between two shallow coaxial ground heat exchangers having slightly different internal geometries and different thermal properties for their inner pipes. Their simulations were limited to operating conditions having a constant inlet temperature rather than typical TRT operating conditions, where a constant heat-flux applied to the working fluid by an above-ground heater. Their investigation is done using COMSOL Multiphysics 3.4 (™*COMSOL*) to study the effects of thermal short-circuiting and flow-direction. Their numerical model does not simulate the internal pipe flow, which is turbulent, and only models the laminar flow through the annular passage where the convective heat transfer coefficient is simpler to compute. They concluded that an inner pipe with a lower thermal conductivity will have a greater benefit at the early time period where this effect will drop off as the outlet temperature begins to approach the inlet temperature.

Raymond et al. (2015) presented a comparison between U-tube heat exchangers and coaxial heat exchangers having a thermally enhanced outer pipe considering design calculations for the required length of heat exchanger. The method they used is based on the original presentation by *Hellström (1991)* for a borehole thermal resistance applied to a counter-flow heat exchanger. In the 1991 model it is assumed that there will be no direct connection between the inner flow channel and the borehole wall, implying that the resistance between the inner flow channel and the surrounding ground tends to infinity. The limitations of this assumption will be investigated further in Section 4.4 of this thesis.

Acuña and Palm (2010) have reported a TRT analysis for a coaxial BHE consisting of an inner pipe having a relatively small diameter compared to the outer pipe diameter, as well as a coaxial BHE having the upper portion of the inner pipe well-insulated. Each of these cases consist of a BHE where the outer pipe is a thin plastic tube, pressed directly to the borehole wall when filled, having a very low thermal resistance. It is noted that the ILS model remains valid in each of these cases as the majority of heat flux to the surrounding ground will come from the annulus region with little to no effect from the inner pipe; that is, the fluid temperature in the annulus at the borehole wall will remain nearly unchanged and will exhibit a relatively flat temperature profile in its cross-section when considering turbulent flow (Acuña and Palm, 2012a).

Beier et al. (2013, 2014) have developed a model for transient heat transfer within a coaxial BHE which can be used in conjunction with a distributed thermal response testing (DTRT) procedure, or a theoretical vertical temperature profile, to produce estimates of the local ground thermal conductivity and the outer borehole thermal resistance with depth. A DTRT is an advanced thermal response test procedure using distributed temperature sensing, or DTS (Bense et al., 2016) technology consisting of fiber optic cables and the interpretation of backscattered laser light to reproduce instantaneous temperatures along the depth of each flow path. Although more advanced, a DTRT may be more expensive to perform; as such, resulting vertical temperature profiles will not be considered in this research where the focus will be kept on simulating surface temperatures.

The purpose of this research is to investigate the effect of material choice and pipe sizing on the performance of a coaxial BHE. The goal of these specially designed heat exchangers is to reduce the effective thermal resistance between the bulk of the working fluid and the surrounding ground (Acuña and Palm, 2011). A BHE having a reduced borehole thermal resistance will allow for more efficient heat exchange with the surrounding ground, resulting in an increased coefficient of performance (COP), reduced design length (L), and, in turn, reduced overall drilling requirements.

It has been previously shown that these designs may be improved by using a steel outer pipe and/or an insulated inner pipe; where a steel outer pipe will greatly reduce the outward thermal resistance from the annulus fluid, and an insulated inner pipe will reduce the shunt heat flow between the inner and outer flow paths (Acuña, 2013; Zanchini et al., 2010b; Zarrella et al., 2011). As having either a steel outer pipe or an insulated inner pipe would drastically increase the

initial cost of the system, an optimal trade-off should be found on a case-by-case basis between the cost of steel per length and the reduction in overall required length while maintaining a desired performance.

4.3 Model development

As mentioned, analytical models for heat transfer are commonly used in the analysis of TRT results by simulating the heat transfer in the surrounding subsurface. When considering long-term operation, heat transfer in the surrounding ground dominates and controls the design; this is a common logical constraint to almost all thermal models for heat transfer around a BHE. Considering the CCx model, much of its related developmental constraints came from one-dimensional radial models such as the infinite cylindrical-source (ICS) model. Many of the equations presented in this chapter of the thesis are repeated to emphasize relevant information.

4.3.1 Infinite cylindrical-source model

First developed by *Carslaw and Jaeger (1959)* in their work on heat conduction in solids, the ICS model is governed by the following differential equations for heat transfer (Sarbu and Sebarchievici, 2014):

$$\begin{cases} \frac{\partial^2 T}{\partial r^2} + \frac{1}{r}\frac{\partial T}{\partial r} = \frac{1}{\alpha_s}\frac{\partial T}{\partial \tau}, & r_b < r < \infty \\ -2\pi r_b k_s \frac{\partial T}{\partial \tau} = q, & r = r_b, \tau > 0 \\ T - T_0 = 0, & \tau = 0, r > r_b \end{cases} \tag{4.1}$$

where T is the temperature and the radius of interest, r, is greater than the radius of the borehole, r_b; k_s and α_s are the effective thermal conductivity and diffusivity of the subsurface, where T_0 is its reference *undisturbed* temperature. It is assumed in this model that a constant heat flux, q, will be delivered between the borehole and the ground; however, this constant heat flux may be replaced by a discretized heat flux applied using temporal superposition with the operating time, τ, as briefly discussed later in this section. A solution adapted by *Ingersoll et al. (1954)* in their study of GHP system applications considers a dimensionless response function referred to as a *g-function*. Considering a hollow cylindrical heat source of infinite length, Equations 4.2 and 4.3 express an analytical solution for the ICS model in Fourier-Bessel form (Ingersoll et al., 1954):

$$T(r_b, \tau) = T_o + \frac{q}{k_s} g(Fo_1, 1), \qquad \tau > 0 \tag{4.2}$$

$$g(Fo,p)=\frac{1}{\pi^2}\int_0^{\infty}\frac{\frac{e^{-(\beta^2 Fo)}-1}{J_1^2(\beta)+Y_1^2(\beta)}[J_0(p\beta)Y_1(\beta)-J_1(\beta)Y_0(p\beta)]}{\beta^2}d\beta \tag{4.3}$$

where $Fo_1=\alpha_s\tau/r_b^2$ is related to the transient heat conduction in the surrounding ground outside of the borehole wall; the remaining terms will not be detailed in this chapter and readers are directed to the related publications for more information on the Bessel functions (J, Y) and storage ratio (β) (Bandyopadhyay et al., 2008; Bernier, 2001). Setting $p=1$ (*ie.* the response at the borehole wall) the following curve-fitted function can be applied for $0.1<Fo<10^6$ (Bernier, 2001):

$$g(Fo_1,1)=10^{-0.89129+0.36081\times\log_{10}(Fo_1)-0.05508\times\log_{10}^2(Fo_1)+0.00359617\times\log_{10}^3(Fo_1)} \tag{4.4}$$

Equation 4.2 may be modified to simulate the average fluid temperature (T_f) within the borehole by including an effective borehole thermal resistance (R_b):

$$T_f(\tau)=T_o+\frac{q}{k_s}g(Fo_1,1)+qR_b \tag{4.5}$$

To model the borehole resistance separately, there exists analytical models for heat transfer *within* the borehole itself, such as the thermal resistance-capacitance model or TRCM; however, to simplify the comparison, the original derivation by *Hellström (1991)* is considered here. For cases where the inner pipe has negligible effect on the annulus fluid temperature at the outer wall during steady-flux conditions, one may write (Hellström, 1991; Raymond et al., 2015):

$$R_b=R_o\left(1+\frac{L^2}{3\left(Q_f\rho_f c_f\right)^2R_iR_o}\right) \tag{4.6}$$

where the steady-state thermal resistance for the inner shunt and outer borehole sections may be represented by Equations 4.7 and 4.8, respectively (Beier et al., 2013, 2014):

$$R_i=\frac{1}{2\pi h_{oi}r_{oi}}+\frac{1}{2\pi k_{p_i}}\log\left(\frac{r_{oi}}{r_{ii}}\right)+\frac{1}{2\pi h_{ii}r_{ii}} \tag{4.7}$$

$$R_o=\frac{1}{2\pi k_{p_o}}\log\left(\frac{r_{oo}}{r_{io}}\right)+\frac{1}{2\pi h_{io}r_{io}} \tag{4.8}$$

where k_{p_x} is the pipe thermal conductivity and h_{yx} is the convective heat transfer coefficient where the subscript x denotes the inner (i) and outer (o) pipes, and y denotes the inner or outer surface of the corresponding pipe. It is noted that care should be taken when selecting an acceptable flow correlation for estimating the convective heat transfer coefficients,

where most are only valid over a specific range of the dimensionless Reynolds number and inner to outer diameter ratios of an annulus (Dirker and Meyer, 2005). In the CCx model, a version of the Gnielinski correlation modified specifically for annular flow is used to model the annulus fluid (Gnielinski, 2009; Ntuli et al., 2010), where h is evaluated at the diameter of the surface considered.

During the analysis given by *Acuña (2013)* on their enhanced coaxial heat exchanger, they note that the temperature in the inner pipe should not be considered in the calculation of local borehole resistances, being that the temperature in the annulus does not change with changing inner pipe temperature. In a case where the temperature in the inner pipe significantly affects the temperature in the annulus, a temperature profile in the annulus region may result in an indirect effect on outward heat transfer.

An effective borehole thermal resistance is steady-state, and does not account for the thermal capacity of the piping material; however, in the published literature there has been discussed an *equivalent* thermal resistance that would account for the thermal capacity of the borehole material and allow for short-term fluid temperature simulations of a U-tube BHE (Li and Lai, 2013; Pasquier and Marcotte, 2012). A schematic of the ICS model for a coaxial BHE is shown in Figure 4.1 where there is a need for the proper consideration of an inner pipe. This schematic shows a representation of a constant heat flux being emitted by the heat exchanger, where the effect of the inner pipe would be lumped into the effective borehole resistance described by Equation 4.6. In cases where heat transfer through the inner pipe strongly influences the fluid temperature in the annular flow path, it is suggested to use the composite coaxial model presented in the following section.

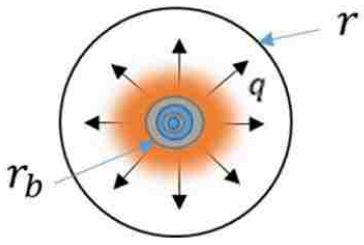

Figure 4.1: Schematic for the ICS model representing a constant heat flux emitted from the borehole; the dimensionless g-function represented in Equation 4.3 may be simulated between the radius of the borehole, r_b, and the radius of interest, r.

4.3.2 Composite coaxial model

The model of primary focus was first developed in Chapter 3 of this thesis, where the original TRT results were used to validate its results (Gordon et al., 2017). Considering the mode of operation where the inlet fluid flow is through the inner pipe, and the outlet through the annulus, it was assumed in the model that the inner shunt and outer borehole resistances were equal, meaning that there would be a *thermal resistance ratio* between them of 1.0. This assumption was based on the borehole configuration used to validate its results where, in the physical test, the borehole consisted of HDPE having a standard dimension ratio (that is, the ratio of the outer diameter to the pipe thickness) of 11 used for both the inner and outer pipes, resulting in nearly equal steady-state thermal resistances.

In this chapter, the original model is improved through better consideration of piping materials and their thermal properties. A thermal resistance ratio between the inner and outer pipes is now considered for values between 0.0 and 1.0 such that the outer resistance is always less than the inner pipe resistance. Logical limits are used to further develop the model to accurately simulate a coaxial BHE having either an insulated inner pipe or a steel outer pipe. When a configuration has a thermal resistance ratio approaching 1.0, the CCx model in this chapter resembles that of the original form presented in Chapter 3 with any modifications clearly noted. Furthermore, the model will approach the curve-fitted ICS model as the thermal presence of the inner pipe diminishes, where the slope of the late-time fluid temperature will become approximately proportional to the ground thermal conductivity. This is for cases where the fluid temperature of the inner pipe has no effect on the fluid temperature at the outer wall of the annulus region.

For transient operation it is important to consider the thermal storage capacity of the borehole itself. The effects of the borehole storage capacities would remain noticeable over the duration of a 6 hour design peak load period of operation. Considering short-term transient behavior, where G is the hollow cylindrical g-function when coupled with the corresponding surrounding material thermal properties. A numbering scheme for the CCx model is given in Figure 4.2 for the following g-functions, where the numbers represent the location and outward material properties considered. Equations 4.9 to 4.11 refer to the instantaneous equivalent thermal resistances (m-K/W) at time-step j in the surrounding ground (G_s), through the inner pipe (G_i), and through the outer borehole (G_o).

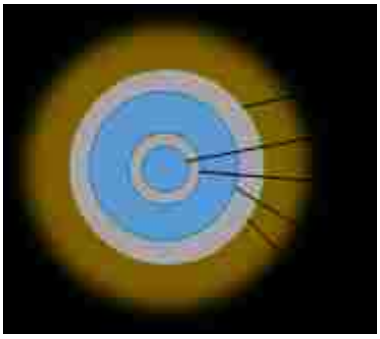

Figure 4.2: Schematic of CCx model showing numbered locations corresponding to the Fourier numbers considered in Equations 4.9 to 4.11 for the various layers of material properties found in a coaxial BHE

$$G_{s\,j} = \frac{g(Fo_1,1)_j}{k_s} \tag{4.9}$$

$$G_{i\,j} = \frac{1}{2\pi h_{oi} r_{oi}} + \frac{g(Fo_2,1)_j}{k_{p_i}} - \frac{g(Fo_3,1)_j}{k_{p_i}} + \frac{1}{2\pi h_{ii} r_{ii}} \tag{4.10}$$

$$G_{o\,j} = \frac{g(Fo_4,1)_j}{k_{p_o}} - \frac{g(Fo_5,1)_j}{k_{p_o}} + \frac{1}{2\pi h_{io} r_{io}} \tag{4.11}$$

The Fourier numbers are labeled Fo_y where the subscript y pertains to the labeled location in Figure 4.2 considering the radial dimension (r_y) and material thermal diffusivity (α_x) used in the following equation:

$$Fo_y = \frac{\alpha_x \tau}{r_y^2} \tag{4.12}$$

The above g-functions utilize the curve-fitted solution to the ICS model given in Equation 4.4 considering the response at the surface of each cylinder. As noted for the ICS model, the equivalent resistance given in Equation 4.9 for the surrounding ground can be combined with a steady-state effective borehole resistance and the total heat flux rejected into the BHE. This combination would result in the ICS model for the borehole outlet fluid temperature in cases where the fluid temperature within the inner pipe has negligible effect on the fluid temperature at the annulus wall. The calculation of G_s may be delayed by up to a full fluid residence time where $G_s = 0$ for $\tau < \tau_r$.

Avoiding the use of the *mean temperature approximation*, the total heat flux rejected to the system can be divided based on the portion of volume of fluid contained in each pipe region; the following equations represent the percent of total volume for the inner pipe and annulus region respectively, and the volumetric ratio (V_r) of the coaxial heat exchanger:

$$p_i = \frac{V_{inner}}{V_{total}} \tag{4.13}$$

$$p_o = \frac{V_{annulus}}{V_{total}} \tag{4.14}$$

$$V_r = V_{inner}/V_{annulus} \tag{4.15}$$

Considering a total volume of the working fluid, the heat flux experienced by the borehole can be assumed to approach the constant value provided at the heater (q_h) based on the fluid residence time (Gordon et al., 2017). This variable heat flux estimation may be modified to be partially delayed, where the heat flux to the inner volume of fluid would be felt immediately (having the time of operation related to time-step $\tau = \tau_j$) and the outer heat flux would be delayed by a duration equal to the fluid residence time (that is, in the second term of Equation 4.16, τ_j is replaced by $\tau_j - \tau_r$ where if $\tau_j - \tau_r < 0$ then $\tau_j - \tau_r = 0$).

$$q_{g_j} = \frac{p_i q_h \tau_j}{\tau_j + \tau_r} + \frac{p_o q_h (\tau_j - \tau_r)}{\tau_j} \tag{4.16}$$

$$\tau_r = \frac{V_t}{Q_f} \tag{4.17}$$

Each heat flux can be further modified based on the ratio of outer and shunt equivalent thermal resistances assuming that the ratio is to always remain between zero and one, since it would be impractical to have an outer pipe with a larger thermal resistance than the inner pipe. The following equation is referred to herein as the thermal resistance ratio:

$$G_{r_j} = \frac{G_{o_j}}{G_{i_j}} \tag{4.18}$$

An additional parameter is defined here for the ratio of the dimensionless response in the outer pipe to that in the inner pipe, where this indicates how much heat may be stored within the inner pipe compared to the outer pipe. The following ratio is referred to herein as the thermal storage ratio.

$$g_{r_j} = \frac{g(Fo_4,1)_j - g(Fo_5,1)_j}{g(Fo_2,1)_j - g(Fo_3,1)_j} \tag{4.19}$$

The three heat flux terms considered in the composite coaxial model are given in Equations 4.20 to 4.22. The inner and outer flux (based on the percent of total volume contained

in each region) convolves the total transient heat flux given in Equation 4.16 with the thermal resistance ratio given in Equation 4.18:

$$q_i = \left[\sum_{j=1}^{n_\tau}(q_{g_j} - q_{g_{j-1}})\left(p_i G_r(\tau_j - \tau_{j-1})\right)\right] \quad (4.20)$$

$$q_o = \left[\sum_{j=1}^{n_\tau}(q_{g_j} - q_{g_{j-1}})\left(p_o G_r(\tau_j - \tau_{j-1})\right)\right] \quad (4.21)$$

The final heat flux is considered based on the reduction in outward heat flow due to the storage capacity of the inner pipe:

$$q_{i-o} = \left[\sum_{j=1}^{n_\tau}(q_{g_j} - q_{g_{j-1}})\left(1 - 2p_i g_r(\tau_j - \tau_{j-1})\right)\right] \quad (4.22)$$

A temperature rise will be experienced at the outlet based on the outward heat transfer, after reduction by the capacity ratio as per Equation 4.22 (q_{i-o}). This remaining heat transfer is applied to the steady-state outer borehole resistance and the equivalent thermal resistance in the surrounding ground while omitting the inner pipe.

$$\Delta T_{f,a-g} = \left[\sum_{j=1}^{n_\tau}(q_{i-o\,j} - q_{i-o\,j-1})\left(R_o + G_s(\tau_j - \tau_{j-1})\right)\right] \quad (4.23)$$

The working fluid at the outlet will experience an average temperature rise based on the inner heat flux (q_i) as it is applied to the steady-state inner shunt resistance, omitting the outer pipe and ground.

$$\Delta T_{f,i-g} = \left[\sum_{j=1}^{n_\tau}(q_{i\,j} - q_{i\,j-1})\,(R_i)\right] \quad (4.24)$$

Since both the equivalent and steady-state shunt resistances are inversely proportional in Equation 4.24, this allows for the effect of shunt resistance to diminish as the equivalent resistance approaches the steady-state value. To make up for the remainder of the heat flux through the inner pipe, an additional temperature rise is considered where the outer heat flux is applied to the equivalent shunt resistance:

$$\Delta T_{f,i-a} = \left[\sum_{j=1}^{n_\tau}(q_{o\,j} - q_{o\,j-1})\left(G_i(\tau_j - \tau_{j-1})\right)\right] \quad (4.25)$$

Equations 4.23 to 4.25 can be superimposed to estimate the fluid temperature rise at the outlet of the heat exchanger:

$$\Delta T_{f,outlet} = \Delta T_{f,a-g} + \Delta T_{f,i-a} + \Delta T_{f,a-g} \quad (4.26)$$

In order to present this equation in a form that might be used for design purposes, the following equation attempts to separate the outer ground resistance from the overall borehole resistance considering the total heat flux rejected (or extracted) to (or from) the heat exchanger:

$$\Delta T_{f,outlet} = \sum_{j=1}^{n_\tau} (q_{g_j} - q_{g_{j-1}}) \left[G_s(\tau_j - \tau_{j-1}) \left(1 - 2p_i g_r(\tau_j - \tau_{j-1})\right) + R_o \left(1 - 2p_i g_r(\tau_j - \tau_{j-1})\right) + Gr(\tau_j - \tau_{j-1}) \left(p_i R_i + p_o G_i(\tau_j - \tau_{j-1})\right)\right] \quad (4.27)$$

where an equivalent borehole thermal resistance can be interpreted from Equation 4.27 to be written as in Equation 4.28; for a singular value it would be useful to take an average value of the following equation over the time of operation considered:

$$G_{b_j} = R_o \left(1 - 2p_i g_{r_j}\right) + G_{r_j} \left(p_i R_i + p_o G_{i_j}\right) \quad (4.28)$$

Following this, an adjusted equivalent ground thermal resistance can be written as:

$$G_{s_j}^* = G_{s_j} \left(1 - 2p_i g_{r_j}\right) \quad (4.29)$$

Equations 4.28 and 4.29 can be compared to the original publication, where the following relationships were modified from *Gordon et al. (2017)* to more effectively consider the thermal resistance and storage ratios:

$$G_{b_{0_j}} = 2p_i G_{i_j} + p_o G_{o_j} \quad (4.30)$$

$$G_{s_{0_j}}^* = G_{s_j}(p_o - p_i) \quad (4.31)$$

The adjusted model should be limited to its tested validity in order to ensure that acceptable results will be produced; the term P_r is referred to as the thermal presence ratio of the inner pipe at each instance and should be limited to approach a maximum value of 0.65 based on the experimental findings of this thesis:

$$2p_i g_{r_j} = P_{r_j} < 0.65 \quad (4.32)$$

The purpose of the proposed ratio is to account for coaxial BHEs where different pipe materials and geometries are used between the inner and outer pipes; for example, a coaxial BHE with an insulated inner pipe will limit the heat flux affecting the annulus fluid and its indirect influence on the ground response, similar to if the inner pipe had a very small volume compared to the annulus region. Further study is needed with greater resolution of physical test results over

a variety of pipe diameter ratios and material properties in order to extend the validity range of the model. In overview of the CCx model, what will be referred to as *design ratios* includes V_r, G_r, g_r, and P_r.

4.4 Comparison with other models and physical data

In order to investigate the effect of geometry and material selection on the performance of coaxial BHEs, three different TRTs are analyzed to extend the validity range of the composite coaxial model (the three different coaxial BHEs will be referred to as CB1, CB2, and CB3). In each physical test, the results of the CCx model are compared to those given by the curve-fitted ICS model both fit to the data, and assuming a borehole thermal resistance corresponding to Equation 4.6. Table 4.1 summarizes the input parameters that have been used in both the ICS and CCx models where applicable. An additional case is considered to compare results of the CCx model with those produced by a three dimensional analytical model for coaxial BHEs when considering the effect of an insulated inner pipe.

Table 4.1: Input parameters used in the CCx and ICS fluid temperature simulations for comparison with physical results

Characteristics	Symbol	Unit	CB1	CB2	CB3
Borehole					
Length	H	m	181	188	60
Diameter	$r_b/2$	mm	88.9	115.0	150
Test Set-up					
Average rate of heat input	Q	W	11020	6000	7590
Average flow rate	Q_f	l/s	0.56	0.58	0.55
Subsurface					
Thermal conductivity	k_s	W/m-K	3.93	3.53	3.80
Thermal heat capacity	C_p	J/m^3-K	2.26x10^6	2.24x10^6	2.40x10^6
Undisturbed temperature	T_o	°C	9.8	8.4	15.1
Inner Pipe			HDPE	HDPE	Insulated
Thermal conductivity	k_p	W/m-K	0.40	0.40	0.10
Thermal heat capacity	C_p	J/m^3-K	2.17x10^6	2.17x10^6	1.36x10^6
Inner diameter	d_{ii}	mm	39.0	35.2	40.8
Outer diameter	d_{oi}	mm	48.3	40.0	50.0
Outer Pipe			HDPE	HDPE	AISI Steel
Thermal conductivity	k_p	W/m-K	0.40	0.40	16.0
Thermal heat capacity	C_p	J/m^3-K	2.17x10^6	2.17x10^6	3.96x10^6
Inner diameter	d_{io}	mm	71.8	113.2	150.0
Outer diameter	d_{oo}	mm	88.9	114.0	140.0
Root-mean squared error	$RMSE$	°C	0.09	0.13	0.41

The model is applied to each case in an identical manner, unless otherwise noted, and a root-mean-squared-error (RMSE) value when compared to the measured TRT profile is provided in Table 4.1. The undisturbed ground temperature for each case has been estimated by taking the average temperature experienced through the heat exchanger over one residence time before the heater is engaged; also similar among the cases, the thermal heat capacity of the subsurface was estimated based on the experienced drilling profile. For each case, independent estimations for the ground thermal conductivity are used to ensure validation of the model, where various borehole thermal resistance estimations are provided to note any comparable variance in result. The resulting temperature curves for each case are presented in the following sections along with each configuration's corresponding volumetric ratio (V_r), thermal resistance ratio (G_r), thermal storage ratio (g_r), and thermal presence ratio (P_r) to provide visual comparison between the functionality of the systems.

4.4.1 Case 1: CB1

The model is developed considering CB1 where the steady-state inner shunt resistance is similar to the outer borehole resistance since the system utilizes standard 3 inch (outer) and 1.5 inch (inner) SDR11 HDPE piping with specifications provided by *VERSApipe HD*. This test was performed at the shop facilities of *GeoSource Energy, Inc.* where an 11 kW *GeoCube™* was used as the above-ground testing unit (connected to a generator) having +/- 0.2°C temperature sensing accuracy per its corresponding user's manual (Precision Geothermal, 2011). The measured outlet fluid temperature over the duration of the TRT is compared to the outlet temperature simulated by the CCx model in Figure 4.3 (left). In this simulation, the response in the ground (G_s) and the heat flux experienced by the borehole (q_g) are each delayed with respect to a full-fluid residence time, as discussed in Section 4.3.2 of this thesis. It is found that applying these delays drastically improves the fit of the model during short-term operation. The mean of the inlet and outlet fluid temperatures is compared to the mean fluid temperature simulated by the ICS model in Figure 4.3 (right). In this simulation there is no delay applied to either the heat flux or the ground response, and it is seen, that the previous borehole resistance model (Hellström, 1991) overestimates the fluid temperature during the late-time period of the TRT.

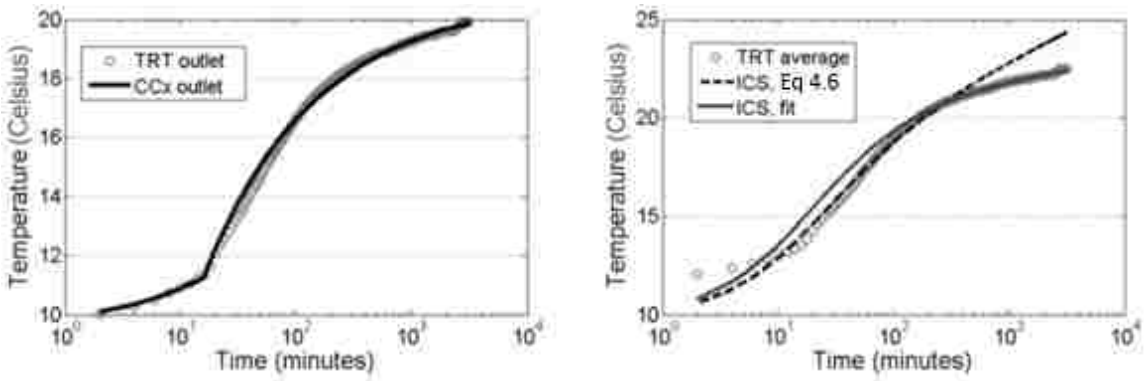

Figure 4.3: Outlet temperature measured during the TRT comparted to the outlet temperature simulated by the CCx model (left). Mean measured TRT surface temperature compared to the ICS model considering both Equation 4.6 for R_b and the reference value for k_s, or values used to fit the model to the experimental results.

The design ratios considered in the model are shown in Figure 4.4, where it is noted that the thermal presence ratio remains below the outer volumetric ratio ($P_r < p_o = 0.65$). This test acted as a control point for further development of the original model; where the effective thermal conductivity of the subsurface was first estimated by a U-tube BHE having a nearly identical drilling profile in a nearby vicinity. This value was estimated to be 3.73 W/m-K considering the slope of the TRT temperature curve (when plotted against the logarithm of time) during the late-time period of the independent U-tube test. A value of 3.93 W/m-K was used in the simulation of the reference coaxial BHE along with the same thermal heat capacity of the subsurface for both the CCx model and the ICS model. The results for this scenario are listed in Table 4.2, where it is noted in comparison to Figure 4.3 that the ICS model (Equations 4.5, 4.6, and 4.16) does not follow the measured temperature curve.

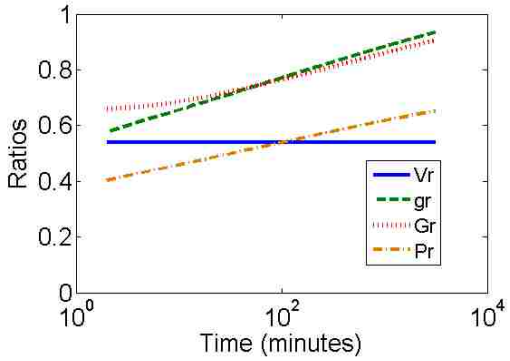

Figure 4.4: Design ratios considered in the CCx model simulation of CB1 showing Pr approach a value of 0.65; this is the currently tested limit of the model.

4.4.2 Case 2: CB2

This case acted as another control point in developing the model as the inner pipe is very small when compared to that of the outer pipe resulting in a thermal presence of the inner pipe that is nearly negligible. The data presented for this case is taken largely from *Acuña (2013)* (BHE9, DTRT2) where the author's estimates for the ground thermal conductivity and borehole thermal resistance are made using the *infinite line source* or ILS model. In this scenario, it would be expected that the CCx model would approach that of the ICS model and that the original estimations provided in *Acuña, (2013)* would remain relatively valid. The results and previously estimated values are given in Table 4.2 and the simulated fluid temperatures and considered design ratios are shown in Figures 4.5 and 4.6, respectively. It is noted that the fluid temperatures were measured at a depth of 17 m into the borehole. It can be seen in Figure 4.5 that the CCx model will overestimate these fluid temperatures since it considers the full depth of the borehole, where the surface temperatures would be slightly higher than those measured at 17 m of depth. The CCx model uses input parameters taken from the original publication (Acuña, 2013) so that a consistent set of data is used. It should be noted that there is no delay applied to either G_s of q_g; this is because there did not seem to exist a sudden rise in temperature near the beginning of the test, which is typically expected during a TRT.

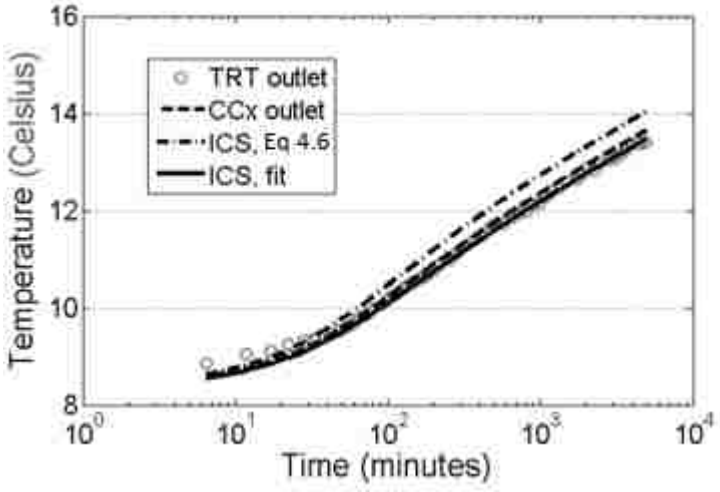

Figure 4.5: Measured and simulated outlet fluid temperatures over the course of the TRT performed on CB2.

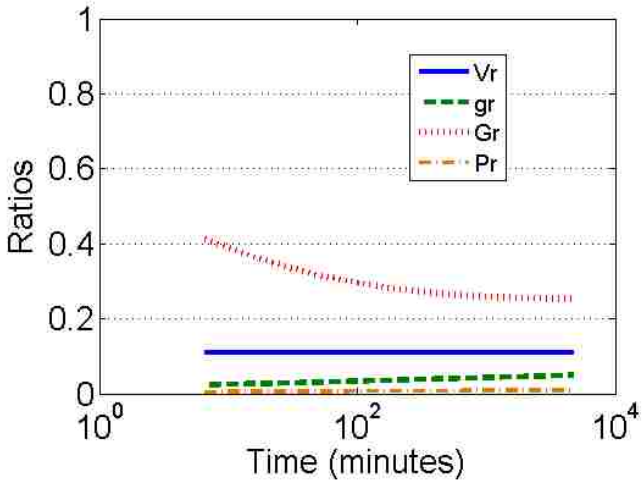

Figure 4.6: Design ratios considered in the CCx model simulation of CB2 showing a low P_r; this simulation helped assure that the CCx model would approach the solution of the ICS model in a situation where the thermal presence of the inner pipe is low.

4.4.3. Case 3: CB3

This scenario is based on a TRT performed for a coaxial BHE having a steel helix as the annular flow path and an insulated inner pipe (Zarrella et al., 2011). This case is meant to further verify the model for its consideration of various piping materials. It is interesting to note, during their analysis on this *enhanced* coaxial heat exchanger, that there was a comparison made with a double U-tube heat exchanger located 7 m away. This comparison showed a large variation in the effective ground thermal conductivity between the two tests, as seen in Table 4.2. It is also noted from Table 4.2 that there is exceptional agreement between the *capacity-resistance model* (CaRM) and the CCx model in each simulations' resulting borehole thermal resistance. For this simulatioin, a value of 0.1 W/m-K is used for the effective thermal conductivity of the inner pipe, accounting for its layers of steel, closed-cell insulation, and HDPE pipe; this value was chosen so that the inner shunt resistance would match that of what was calculated and used in their CaRM simulation. In this scenario, the outlet temperature simulated by the CCx closely matches the temperature simulated by the ICS model considering Equation 4.6 for the evaluation of R_b, as seen in Figure 4.7 (left). The mean surface temperature response is compared to the ICS model in Figure 4.7 (right), where the effective borehole resistance is varied until a reasonable RMSE value is achieved. The individual estimations for the inner shunt and outer borehole resistances are given in Table 4.2.

Table 4.2: Summary of model results

Scenario	k_s (W/m-K)	Effective borehole thermal resistance (m-K/W)	Shunt thermal resistance (m-K/W)	Outer thermal resistance (m-K/W)
CB1				
CCx	3.93	0.096	0.095	0.083
ICS fit	10.5	0.160	n/a	n/a
ICS w/ *Hellström, (1991)* R_b, R_i, R_o	3.73	0.116	0.101	0.097
CB2				
CCx	3.53	0.035	0.061	0.017
ICS fit	3.53	0.029	n/a	n/a
Beier et al., (2014) estimation	3.25	0.013[1]	0.07	0.013
ICS w/ *Hellström, (1991)* R_b, R_i, R_o	3.53	0.047	0.07	0.018
CB3				
CCx	3.80	0.0054	0.47	0.0043
ICS fit	3.80	0.020	n/a	n/a
ICS w/ *Hellström, (1991)* R_b, R_i, R_o	3.80	0.0048	0.87	0.0045
Zarrella et al., (2011) CaRM - Coaxial	3.80	0.005	0.87	n/a
Zarrella et al., (2011) CaRM – Double U-tube	1.75	0.12	n/a	n/a

[1.] Only considers the outer borehole resistance, ignoring the inner pipe

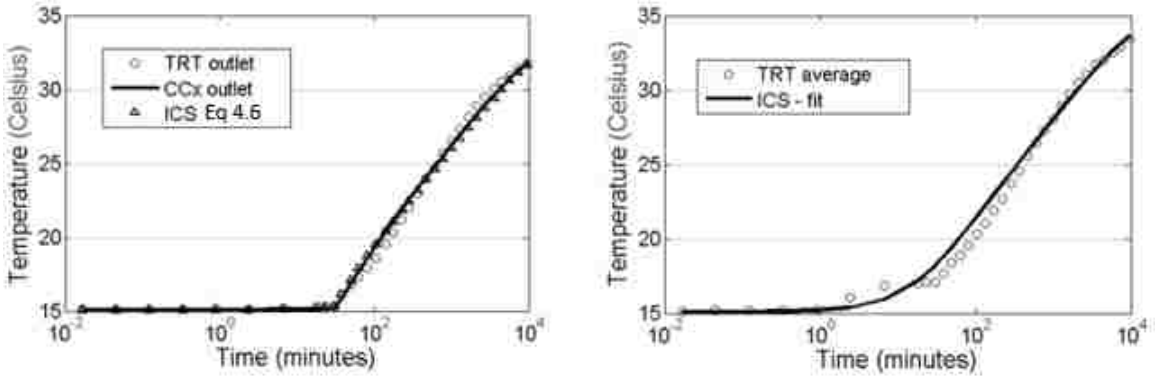

Figure 4.7: Measured and simulated outlet fluid temperatures over the course of the TRT performed on CB3

It is noted that the storage ratio (g_r) goes up in cases where there is a thick, insulated inner pipe, as seen in Figure 4.8. This improves the performance of the system as it allows for heat to be stored within the inner pipe, rather than in the surrounding ground; this would result in a lower amount of heat actually being rejected to the ground. It is important to realize that this would allow for the surrounding ground to recover faster, as it was exposed to a reduced heat flux throughout the early time of operation due to a portion of the heat flux being stored within

the inner pipe. It is also important to note that the thermal presence ratio (P_r) is proportional to g_r, where a higher thermal presence ratio would lead to improved performance.

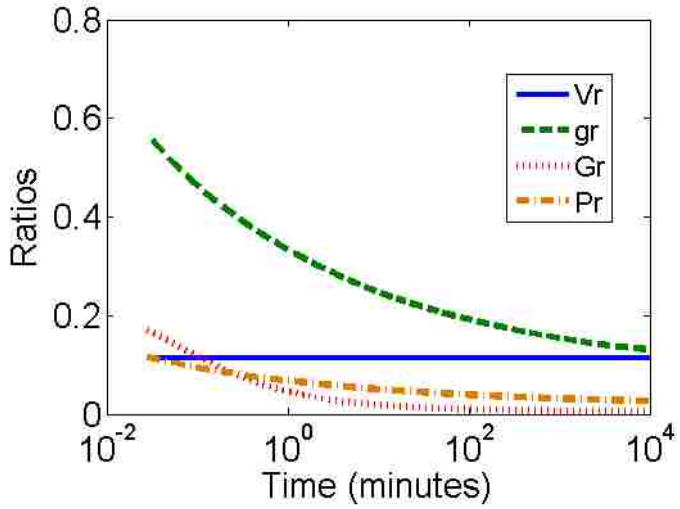

Figure 4.8: Design ratios considered in the CCx model simulation of CB3 showing an increased short-term P_r; it is noted that this would provide a benefit to short-term performance. This simulation helped assure that the CCx model produce acceptable results when considering various pipe material properties such as a steel outer pipe, or an insulated inner pipe.

4.4.4 Comparison to transient model

The CCx model is compared to a *transient* model for the vertical temperature profile of a coaxial BHE developed by *Beier et al. (2013, 2014).* The comparison is made in Figure 4.9 where the input parameters for the CCx model are matched with those for the analytical *grouted* borehole case considered by *Beier et al. (2014);* the input parameters will not be listed here where the reader is directed to the original publication for referenced values. The outlet temperature simulated by the CCx model closely matches the outlet temperature produced by the transient model for the cases of varying inner shunt resistances; this comparison was originally made to study the effect of an insulated inner pipe.

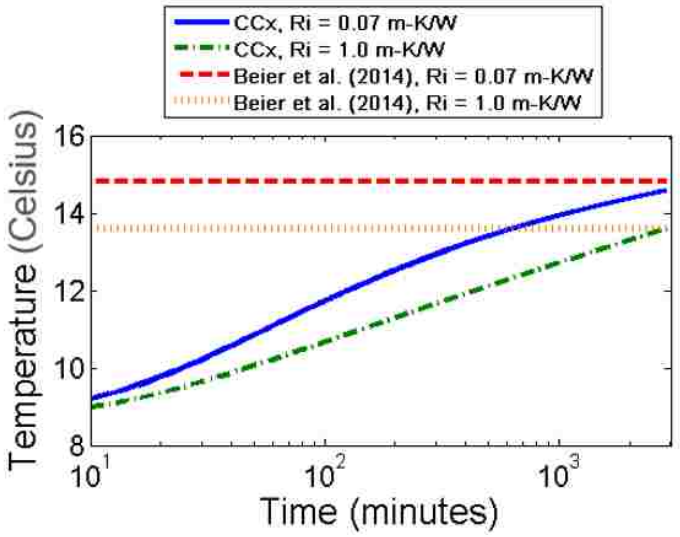

Figure 4.9: Comparison between CCx model and transient model considering two cases of an internal shunt resistance for a grouted coaxial BHE

4.5 Performance analysis

4.5.1 Modified length calculation

A modified version of a borehole length calculation is used in this chapter to demonstrate the effect of material selection on performance and size requirements. The following equation was simplified from a form presented by *Bernier, (2006)* in order to maintain sufficient accuracy of the estimation (Bernier, 2006; Philippe et al., 2010)

$$L = \frac{q_h G_b + q_y G_{10y} + q_m G_{1m} + q_h G_{6h}}{T_m - (T_g + T_p)} \tag{4.33}$$

where L is the total borehole length and T_g is the undisturbed ground temperature. For the purpose of design, T_m is assumed to be the average of the maximum entering water temperature specified for a heat pump and the corresponding leaving water temperature based on the flow rate and the peak heat load rejected to the ground loop. The maximum entering water temperature is set to a value intended to maintain desired performance. T_p is the temperature penalty due to thermal interference between boreholes; in the present study, since only a single borehole is considered, the temperature penalty is set to zero. q_y, q_m, and q_h are the yearly average ground heat load, highest monthly ground load, and peak hourly ground load, respectively; these parameters are estimated in later analysis based on a peak residential cooling demand of about 9 kW. G_{10y}, G_{1m}, and G_{6h} are effective ground thermal pulses corresponding to

ten years (τ_{10y}), one month (τ_{1m}), and six hours (τ_{6h}) ground loads and G_b is the effective borehole thermal resistance of the heat exchanger, averaged over a peak six hour ground load.

The effective ground thermal pulses account for transient heat transfer from the borehole to the undisturbed ground. The approach used to calculate these variables is taken from *ASHRAE, (2011)* and is presented below:

$$G_{6h} = \frac{1}{k_s} g\left(\frac{\alpha_s \tau_{6h}}{r_b^2}\right) \tag{4.34}$$

$$G_{1m} = \frac{1}{k_s}\left[g\left(\frac{\alpha_s \tau_{1m+6h}}{r_b^2}\right) - g\left(\frac{\alpha_s \tau_{6h}}{r_b^2}\right)\right] \tag{4.35}$$

$$G_{10y} = \frac{1}{k_s}\left[g\left(\frac{\alpha_s \tau_{10y+1m+6h}}{r_b^2}\right) - g\left(\frac{\alpha_s \tau_{1m+6h}}{r_b^2}\right)\right] \tag{4.36}$$

This procedure is limited by the following:

$0.05\,m \leq r_b \leq 0.1\,m$

$0.025\,m^2/day \leq \alpha_s \leq 0.2\,m^2/day$

The ground pulses (q_y, q_m, q_{6h}) are assumed based on the heat extracted or rejected from the ground at peak conditions based on the rated baseline coefficient of performance (COP typically rated at 0°C for heating and 25°C for cooling) for the heat pump in either its heating or cooling mode of operation, whichever is greater.

In order to modify this procedure for use with a coaxial BHE, G_b is calculated using Equation 4.28 averaged over 48 hours of consider operating time, and G_{6h} is calculated using Equation 4.29 for the time steps considered. The terms G_{1m} and G_{10y} are calculated using the ICS model assuming that at some point, after sufficient time of operation, the effect of the inner pipe would eventually become negligible.

It is indicated in the above design considerations the importance of reducing the overall borehole thermal resistance as this is the parameter over which there is most control. As subsurface properties vary greatly, and can often be largely effected by groundwater flow, the above design equation is not recommended for all site conditions.

4.5.2 Coefficient of performance

A hypothetical GSHP system is introduced to show how an estimated ground-side pumping requirement will affect the system globally when balanced with the required length of a single borehole. The corresponding borehole and subsurface parameters used in this analysis are listed in Table 4.3. The specified rated heat pump data resembles that of the *Genesis GS Model 030* by *ClimateMaster.* Similar procedures to those used in the reference product manual are used here to correct the rated COP of the heat pump based on the pressure loss through the borehole due to the flow rate and resulting length requirement (ClimateMaster, 2009). The following analysis is carried out at volumetric ratio considering an inner pipe diameter one nominal size smaller than that used for the coaxial BHE tested in Section 4.4.1; this is done to ensure that the model stays within its verified applicable limit. It is noted that this analysis uses the same pipe size for each material where in reality, steel, HDPE, and any form of insulated pipe would all differ in thicknesses; this should be accounted for in practical design.

The referenced heat pump is rated at three different ground-side flow rates over a wide range of temperatures; for the purpose of this comparison, a maximum entering water temperature experienced by the heat pump is assumed to be 26.7°C (80 °F). At this temperature, specified rated values for the heat pump performance are used to calculate the required length of heat exchanger and corresponding pressure drop for each material configuration and flow rate. A summary of the results is presented in Table 4.4 where the pressure drop in the ground-loop only considers the major losses along either flow channel, where the total pressure drop can then be written as:

$$\Delta P_t = \frac{\rho_f f_i L v_{in}^2}{2 d_{ii}} + \frac{\rho_f f_o L v_{out}^2}{2(d_{io} - d_{oi})} \tag{4.37}$$

The friction factors, f_i and f_o, and fluid velocities, v_{in} and v_{out}, are calculated the for the inner and outer flow paths respectively. Once the required length and corresponding pressure drop is calculated at each specified flow rate and material configuration, a correction to the COP based on the required pumping power is performed.

Table 4.3: Input parameters used in the CCx and ICS fluid temperature simulations for analytical performance analysis

Characteristics	Symbol	Unit	Value
Borehole			
Diameter	$r_b/2$	mm	88.9
Inner Pipe			
Inner diameter	d_{ii}	mm	39.0
Outer diameter	d_{oi}	mm	48.3
Outer Pipe			
Inner diameter	d_{io}	mm	71.8
Outer diameter	d_{oo}	mm	88.9
Subsurface			
Thermal conductivity	k_s	W/m-K	3.25
Thermal heat capacity	C_p	J/m^3-K	2.35x10^6
Undisturbed temperature	T_o	°C	10

With decreasing flow rate, and increasing borehole resistance, the required length is increased to maintain a maximum heat pump entering water temperature. After accounting for the reduced pressure drop realized at a lower flow rate, it is found that the heat pump would operate with a higher corrected COP. The required length of heat exchanger is compared to the corrected COP for each scenario in Figure 4.10. This comparison indicates a greater benefit is found when using a steel outer pipe compared to an insulated inner pipe. However, a steel outer pipe may have greater cost implications, and a local and global cost analysis should be performed on a case-by-case basis when designing such systems.

Table 4.4: Summary of required length and corrected coefficient of performance

Borehole properties			Rated values				Calculated values		
Piping Material	R_b (m-K/W)	Flow rate L/s	Cooling capacity (kW)	Heat of Rejection (kW)	Required input (kW)	COP rated	Required length (m)	Pressure drop (Pa)	Power correction (kW)[1]	COP corrected[2]
Steel outer	0.024						74.6	3269	1.55	2.61
HDPE pipes	0.134	0.47	8.97	10.87	1.89	4.74	144.8	6347	3.00	1.83
Insulated	0.123						127.0	5566	2.63	1.98
Steel outer	0.032						74.4	2196	0.76	3.27
HDPE pipe	0.143	0.35	8.97	10.93	1.98	4.53	141.6	4180	1.45	2.61
Insulated	0.131						124.5	3675	1.28	2.75
Steel outer	0.177						140.6	2120	0.49	3.47
HDPE pipe	0.305	0.23	8.94	11.02	2.08	4.30	211.3	3186	0.74	3.17
Insulated	0.285						191.5	2887	0.67	3.25

[1.] Power correction (kW) = Flow rate (m^3/s) x Pressure drop (Pa)

[2.] COP corrected = Cooling capacity (kW) / (Required input (kW) + Power correction (kW))

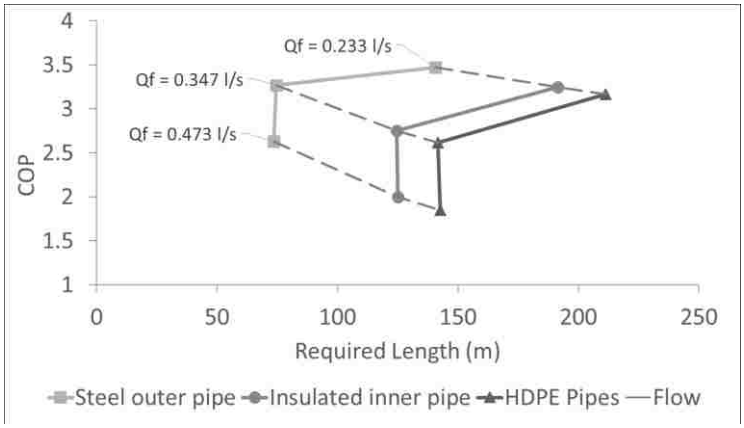

Figure 4.10: Performance analysis considering various material configurations

4.6 Conclusions

This chapter improves upon a semi-analytical model for heat transfer related to a coaxial borehole heat exchanger (BHE); this model is referred to as the composite coaxial model (CCx) and was originally developed in Chapter 3 of this thesis. The system performance of various coaxial BHE configurations is investigated considering both physical testing and analytical results. The CCx model is extended to properly consider the variation of pipe materials, where it had originally only considered a volumetric ratio. Three TRTs are used to validate the presented model, where the model accurately simulates the surface fluid temperatures for each case. The model is verified by comparing its results with the infinite cylindrical-source (ICS) model for situations where the CCx model would logically approach the ICS model; further verification is done by comparing the results of the proposed model with those simulated by a transient vertical temperature profile model for cases where an insulated inner pipe is used. The model is then used to analyze the effect of a coaxial BHE having either an insulated inner pipe, or a steel outer pipe, where standard HDPE pipes are the baseline case for each. A hypothetical ground-source heat pump (GSHP) is introduced, where an analysis is carried out over three different flow rates at which the heat pump is rated by the manufacturer. A length requirement is calculated for each material configuration under each flow rate, where a corrected coefficient of performance (COP) may be calculated to provide the final comparison. The results show a steel outer pipe having a greater impact on reducing the overall length requirement, while maintaining system performance, in comparison to using an insulated inner pipe.

Acknowledgments

This work is made possible by an OCE (Ontario Centres of Excellence) VIP project with GeoSource Energy Inc.

References

Acuña, J., 2013. Distributed thermal response tests-New insights on U-pipe and Coaxial heat exchangers in groundwater-filled boreholes.pdf (Doctoral). Royal Institute of Technology KTH, Stockholm, Sweden.

Acuña, J., Palm, B., 2012. Distributed thermal response tests on pipe-in-pipe borehole heat exchangers.pdf, in: 12th International Conference on Energy Storage. Presented at the Innostock 2012, Stockholm, Sweden.

Acuña, J., Palm, B., 2011. First experiences with coaxial borehole heat exchangers, in: IIR Conference on Sources/Sinks Alternative to the Outside Air for HPs and AC Techniques.

Acuña, J., Palm, B., 2010. A Novel Coaxial Borehole Heat Exchanger: Description and First Distributed Thermal Response Test Measurements, in: Proceedings of the World Geothermal Congress. p. 7.

Alrtimi, A.A., Rouainia, M., Manning, D.A.C., 2013. Thermal enhancement of PFA-based grout for geothermal heat exchangers. Appl. Therm. Eng. 54, 559–564. doi:10.1016/j.applthermaleng.2013.02.011

ASHRAE, 2011. 2011 Ashrae Handbook: HVAC Applications. ASHRAE, Atlanta, GA.

Bandyopadhyay, G., Gosnold, W., Mann, M., 2008. Analytical and semi-analytical solutions for short-time transient response of ground heat exchangers. Energy Build. 40, 1816–1824. doi:10.1016/j.enbuild.2008.04.005

Beier, R.A., Acuña, J., Mogensen, P., Palm, B., 2014. Transient heat transfer in a coaxial borehole heat exchanger. Geothermics 51, 470–482. doi:10.1016/j.geothermics.2014.02.006

Beier, R.A., Acuña, J., Mogensen, P., Palm, B., 2013. Borehole resistance and vertical temperature profiles in coaxial borehole heat exchangers. Appl. Energy 102, 665–675. doi:10.1016/j.apenergy.2012.08.007

Bense, V.F., Read, T., Bour, O., Le Borgne, T., Coleman, T., Krause, S., Chalari, A., Mondanos, M., Ciocca, F., Selker, J.S., 2016. Distributed Temperature Sensing as a downhole tool in hydrogeology: SUBSURFACE DTS. Water Resour. Res. 52, 9259–9273. doi:10.1002/2016WR018869

Bernier, M.A., 2006. Closed-loop ground-coupled heat pump systems. Ashrae J. 48, 12–25.

Bernier, M.A., 2001. Ground-coupled heat pump system simulation/Discussion. Ashrae Trans. 107, 605.

Blum, P., Campillo, G., Kölbel, T., 2011. Techno-economic and spatial analysis of vertical ground source heat pump systems in Germany. Energy 36, 3002–3011. doi:10.1016/j.energy.2011.02.044

Carslaw, H.S., Jaeger, J.C., 1959. Conduction of Heat in Solids, Second. ed. Oxford University Press.

ClimateMaster, 2009. All Products Technical Guide: 2009. ClimateMaster.

Dirker, J., Meyer, J.P., 2005. Convective Heat Transfer Coefficients in Concentric Annuli. Heat Transf. Eng. 26, 38–44. doi:10.1080/01457630590897097

Gnielinski, V., 2009. Heat transfer coefficients for turbulent flow in concentric annular ducts. Heat Transf. Eng. 20, 431–436. doi:10.1080/01457630802528661

Gordon, D., Bolisetti, T., Ting, D.S.-K., Reitsma, S., 2017. Short-term fluid temperature variations in either a coaxial or U-tube borehole heat exchanger. Geothermics 67, 29–39. doi:10.1016/j.geothermics.2016.12.001

Hellström, G., 1991. Thesis_Goran_Hellstrom.pdf. University of Lund, Sweden.

Hsieh, J.C., Lee, Y.R., Guo, T.R., Liu, L.W., Cheng, P.Y., Wang, C.C., 2014. A Co-axial Multi-tube Heat Exchanger Applicable for a Geothermal ORC Power Plant. Energy Procedia 61, 874–877. doi:10.1016/j.egypro.2014.11.985

Hu, P., Zha, J., Lei, F., Zhu, N., Wu, T., 2014. A composite cylindrical model and its application in analysis of thermal response and performance for energy pile. Energy Build. 84, 324–332. doi:10.1016/j.enbuild.2014.07.046

Ingersoll, L.R., Zobel, O.J., Ingersoll, A.C., 1954. Heat conduction: With engineering, geological applications, 2nd ed. McGraw-Hill.

IRENA, 2015. Renewable Energy Prospects: United States of America, REmap 2030 analysis. IRENA, Abu Dhabi.

Lamarche, L., Beauchamp, B., 2007. A new contribution to the finite line-source model for geothermal boreholes. Energy Build. 39, 188–198. doi:10.1016/j.enbuild.2006.06.003

Li, M., Lai, A.C.K., 2013. Analytical model for short-time responses of ground heat exchangers with U-shaped tubes: Model development and validation. Appl. Energy 104, 510–516. doi:10.1016/j.apenergy.2012.10.057

Li, M., Lai, A.C.K., 2012. New temperature response functions (G functions) for pile and borehole ground heat exchangers based on composite-medium line-source theory. Energy 38, 255–263. doi:10.1016/j.energy.2011.12.004

Lund, J.W., Boyd, T.L., 2016. Direct utilization of geothermal energy 2015 worldwide review. Geothermics 60, 66–93. doi:10.1016/j.geothermics.2015.11.004

Lund, J.W., Freeston, D.H., Boyd, T.L., 2005. Direct application of geothermal energy: 2005 Worldwide review. Geothermics 34, 691–727. doi:10.1016/j.geothermics.2005.09.003

Mokhtari, H., Hadiannasab, H., Mostafavi, M., Ahmadibeni, A., Shahriari, B., 2016. Determination of optimum geothermal Rankine cycle parameters utilizing coaxial heat exchanger. Energy 102, 260–275. doi:10.1016/j.energy.2016.02.067

Ntuli, M.P., Dirker, J., Meyer, J.P., 2010. Heat transfer and pressure drop coefficients for turbulent flow in concentric annular ducts, in: Proceedings of the 19th International Congress of Chemical and Process Engineering (CHISA 2010) and the 7th European Congress of Chemical Engineering.

Pasquier, P., Marcotte, D., 2012. Short-term simulation of ground heat exchanger with an improved TRCM. Renew. Energy 46, 92–99. doi:10.1016/j.renene.2012.03.014

Philippe, M., Bernier, M., Marchio, D., 2010. Vertical Geothermal Borefields - Sizing Calculation Spreadsheet. ASHRAE J.

Precision Geothermal, 2011. GeoCubeTM User's Manual.

Raymond, J., Mercier, S., Nguyen, L., 2015. Designing coaxial ground heat exchangers with a thermally enhanced outer pipe. Geotherm. Energy 3. doi:10.1186/s40517-015-0027-3

Sarbu, I., Sebarchievici, C., 2014. General review of ground-source heat pump systems for heating and cooling of buildings. Energy Build. 70, 441–454. doi:10.1016/j.enbuild.2013.11.068

Wood, C.J., Liu, H., Riffat, S.B., 2012. Comparative performance of "U-tube" and "coaxial" loop designs for use with a ground source heat pump. Appl. Therm. Eng. 37, 190–195. doi:10.1016/j.applthermaleng.2011.11.015

Zanchini, E., Lazzari, S., Priarone, A., 2010a. Effects of flow direction and thermal short-circuiting on the performance of small coaxial ground heat exchangers. Renew. Energy 35, 1255–1265. doi:10.1016/j.renene.2009.11.043

Zanchini, E., Lazzari, S., Priarone, A., 2010b. Improving the thermal performance of coaxial borehole heat exchangers. Energy 35, 657–666. doi:10.1016/j.energy.2009.10.038

Zarrella, A., Scarpa, M., Carli, M.D., 2011. Short time-step performances of coaxial and double U-tube borehole heat exchangers: modeling and measurements. HVACR Res. 17, 959–976.

Chapter 5 – Experimental and Analytical Investigation on Pipe Sizes for a Coaxial BHE

5.1 Introduction

Geothermal energy is becoming a popular alternative method for providing everyday heating and cooling demands in today's society (Lund and Boyd, 2016). Although a variety of systems exist, ground-source heat pump systems coupled with vertical borehole heat exchangers (BHE) are the focus of this research. These systems operate using a reversible refrigeration cycle within a geothermal or ground-source heat pump (GSHP) where the ground can act as either a heat source in a heating mode of operation, or a heat sink in a cooling mode of operation. In either case, this heat exchange is accomplished using a closed ground-loop where a borehole system typically consists of buried high-density polyethylene (HDPE) pipes placed within a borehole drilled to depths ranging anywhere between 80 and 200 meters. This configuration, being a closed-loop, circulates a working-fluid between the ground-side heat exchanger and the GSHP. Although U-tube BHEs are the more common piping configuration, coaxial BHEs have more recently seen a rise in interest as a topic in the published literature (Acuña and Palm, 2010; Arias-Penas et al., 2015; Beier and Ewbank, 2012; Focaccia and Tinti, 2013; Gordon et al., 2017; Zhao et al., 2008).

For smaller residential projects, only one to two boreholes may be required, where the required length of the borehole will depend on the dominating demand (heating or cooling) of the project (Blum et al., 2011). In order to maintain performance of a borehole system, it is important to properly size the HDPE pipes so as to minimize the pressure drop while maintaining turbulent flow within the borehole. A *borefield* will contain multiple BHEs that can be connected in parallel to a manifold using connecting *header* pipes, which create an additional loss in efficiency due to their associated pressure drop and heat exchange with the near-surface ground (Luo et al., 2013). Borefields and the effect of header pipe connections are not considered in this thesis in order to isolate the performance of a single *active element*.

This chapter investigates the performance of coaxial heat exchangers both experimentally and analytically. The performance of various borehole designs has often been investigated by the use of thermal response tests (TRT) (Beier and Ewbank, 2012; Choi and Ooka, 2016; Pasquier,

2015; Rainieri et al., 2011; Zhang et al., 2014). These tests are often used to estimate the local subsurface properties for the purpose of accurate borefield sizing and the thermal resistance associated with the borehole design itself (Bernier, 2001).

For clarity, a TRT is performed on a fully-operational borehole to provide knowledge of on-site conditions prior to drilling a borefield. These tests are intended to provide accurate estimations of local subsurface thermal properties such as an effective conductivity and diffusivity; they are also used to verify the performance of a selected borehole configuration. Effective values are used to provide an average value experienced during heat exchange along the depth of a borehole for the purpose of design. The typical process for a TRT is to circulate a working-fluid, heated at a constant rate by an above ground heater, through a fully-operational borehole where the fluid temperatures at the inlet and outlet of the heat exchanger are measured along with the flow rate (Gehlin, 2002).

Analysis of TRT results is done using analytical models for heat transfer in an infinite surrounding media, an example recommended by *ASHRAE (2011)* is the infinite cylindrical source (ICS) model. It can be assumed in the analysis of a TRT that the measured average fluid temperature rise within the heat exchanger will exhibit a linear trend in the late-time period (typically between 10 and 48 hours), and that the slope of this linear trend is inversely proportional to the effective thermal conductivity of the surrounding conditions (Beier and Smith, 2003). An estimation for the volumetric heat capacity of the surrounding ground is often performed based on the drilling profile using a weighted average considering the various depths of each subsurface layer. Once the thermal properties of the surroundings are known, the solution may be applied to the experimental data by means of adjusting the thermal resistance of the borehole.

It has been found that coaxial BHEs will not always show the late-time linear trend during a TRT that is typically exhibited by a U-tube BHE (Beier and Ewbank, 2012). Classical analytical models, such as the ICS model, can greatly overestimate the effective borehole thermal resistance for a coaxial BHE when using either the mean temperature approximation or the *p-linear average* approximation; the error associated with this is largely dependent on the thermal resistance of the inner pipe (Beier et al., 2013); this can additionally be attributed to the ratio of diameters between the inner and outer pipes (Gordon et al., 2017).

Yekoladio et al. (2013) have studied the optimal diameter ratio ($r = r_i/r_o$) for deep coaxial BHEs by minimizing the pressure drop and optimizing the pump performance ($r = 0.653$). They assume an insulated inner pipe with no heat flux from the inner fluid and a highly conductive outer pipe with negligible thermal resistance. It is assumed that the thickness of the pipes is small and that the diameter ratio, r, is equal to the ratio of the inner to outer diameter or the annular passage. However, their analysis on the coaxial geometry is solely based on minimizing the total pressure drop and pumping requirements where thermal properties are not considered. *Mokhtari et al. (2016)* have also studied the optimal diameter ratio for coaxial BHEs, showing a similar result when considering pressure drop ($r = 0.676$). The main difference in their analysis is that they allow for variation in fluid properties with temperature and their considered hydraulic diameter of the annulus. They further included an analysis on optimizing thermal performance ($r = 0.353$) where, although heat transfer through the inner pipe was included, the system configuration was only vaguely similar to a typical coaxial configuration and is not directly applicable here.

In the current research, it is not recommended to relate the slope of the late-time trend realized during a TRT performed on a coaxial BHE to an effective ground thermal conductivity. An exception to this can be made when considering configurations where the inner pipe is either small enough or well insulated enough for the fluid temperature within it to have no effect on the fluid temperature at the outer annulus wall (Hellström, 1991). The assumption that the outer fluid temperature will not change with a changing inner pipe has been considered in many analytical models used in the analysis of coaxial heat exchangers where this is quite nearly the case (Acuña, 2013; Zarrella et al., 2011). In cases where it is necessary to account for the inner pipe having some contribution to outward heat transfer it is recommended to use the composite coaxial model (CCx) for analysis of such systems (Gordon et al., 2017).

A limited amount of lab-scale experimental work has been performed on coaxial systems. However, where available, the results have indicated heat transfer within the surrounding media occurring mainly near the outer wall of the coaxial heat exchanger (Zhao et al., 2008). Many other studies have been performed on different coaxial configurations considering full-scale thermal response tests (Acuña and Palm, 2012b; De Carli et al., 2010; Zarrella et al., 2011); and for this reason, the lab scale work here will be expanded upon considering a semi-analytical analysis of full-scale systems.

Design parameters can be estimated using standard TRT procedures to produce acceptable results when sizing BHEs; however, the properties of the subsurface are largely uncontrollable and can vary greatly based on location. In order to isolate the effects of different borehole configurations, as well as to aid in validation of various thermal modelling techniques, experimental procedures are used to overcome this uncertainty and variability (Beier et al., 2011; Zhao et al., 2008). This chapter presents an experimental procedure used to verify the trends produced by the CCx model for short-term operation, where the fluid flow within the annulus region is laminar and the temperature of the inner pipe holds some effect on outward heat transfer. The results of this experiment are compared with those of the CCx model yielding an RMSE of 0.16 °C, which is well within the accuracy of the measured outlet temperature (0.2 °C). The results of the experiment are then expanded upon using the CCx model by considering various inner pipe sizes in full-depth borehole simulations and comparing the associated required length of heat exchanger and related coefficient of performance. It is found that increasing the diameter of the inner pipe in relation to the outer pipe, the required length of heat exchanger will decrease. Additionally, the overall coefficient of performance realized by a heat pump based on the balancing of pressure drops is increased.

5.2 Experimental setup

The experimental apparatus consists of a horizontally placed commercial water pipe, referred to as a *Big-O* pipe, having an inner diameter of approximately 30.4 cm where the pipe is sealed at both ends and filled with water. This component is referred to as the water jacket. A small coaxial heat exchanger consisting of 5.08 cm and 3.18 cm LLDPE (linear-low density polyethylene) pipe (nominal dimensions) acting as the *outer* and *inner* pipes, respectively, is centered along the water jacket using intermittent spacers. The outer pipe is plugged at one end, and where the other end is sealed to the *top* (that is, where the inlet and outlet of the heat exchanger are located) end cap of the Big-O pipe, penetrating through; a drain/fill hole is located at the opposite end of the water jacket. Intermittent breathing holes were drilled to allow air to escape while the filling took place; these holes served a double purpose allowing easy access for temperature measurements to be taken outside of the outer pipe. A depiction of the sealed arrangement is shown in Figure 5.1.

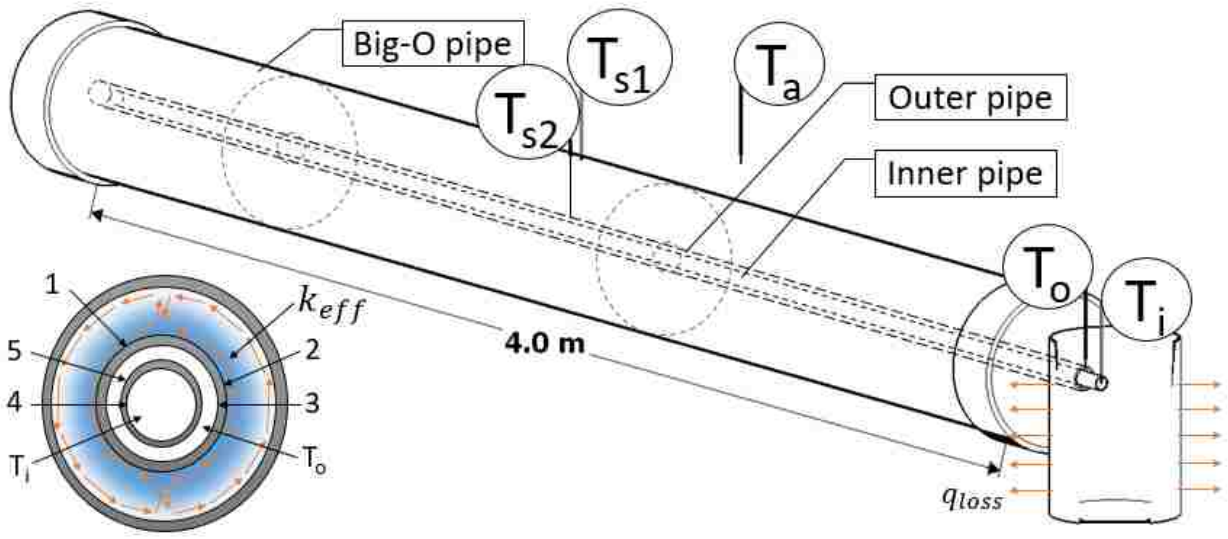

Figure 5.1: Illustration of the experimental apparatus with temperature probe locations shown. The numbering scheme presented in the exaggerated cross section corresponds to the Fourier numbers calculated in the CCx model described in Appendix A.

The end of the outer pipe sealed through the top is attached to a bucket using standard pipe fittings; the layout of the bucket is shown in Figure 5.2. It is expected that the free convection within the horizontal annular cavity where two kidney-shaped flow paths will tend to develop with a temperature difference between T_{s1} and T_{s2} (case shown corresponds to $T_{s2} > T_{s1}$). It is noted that many of these components may easily be swapped out to provide interchangeability of components. The bucket contains a 200 W submerged aquarium water heater and a 45 GPH submersible water pump. The water heater delivers a transient heat flux to the reservoir bucket and has a maximum temperature setting of 30°C. The analysis of the experimental results could then consider the time it takes for the heater to first disengage in order to compare the use of various inner pipe diameters. In this experiment, the pipe fittings are used to attach the inner pipe to the submersible water pump, where the pipe is then fed through the outer pipe until it sits about 2.5 cm from the capped end of the outer pipe; this allows for interchangeability of inner pipe.

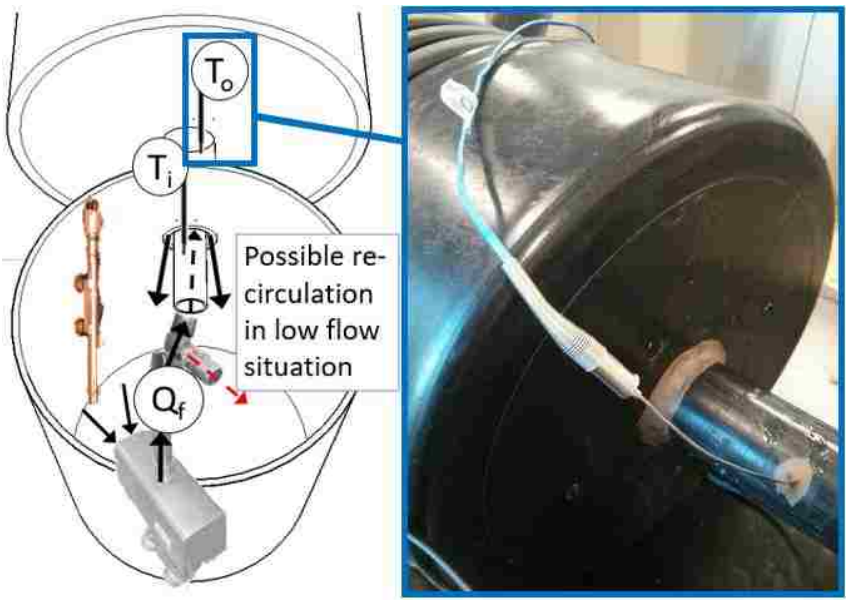

Figure 5.2: View of the bucket configuration and temperature sensor placement for the experimental setup

The bucket and heat exchanger are then filled with water and the bucket is capped. The submersible heater and water pump are used to heat the water within the reservoir (bucket) and circulate the water through the coaxial heat exchanger. The water within the annular space of the water jacket has known parameters and the heat transfer surrounding the heat exchanger can be estimated relatively easily using a correlation for free convective heat transfer within the annular cavity of concentric cylinders (Incropera et al., 2011). Four T-type thermocouples (with +/- 0.2°C rated accuracy) were arranged to measure the temperatures of: the surrounding air, the inner surface of the Big-O pipe, the outer surface of the outer pipe, and the inlet and outlet fluid temperatures just before the water enters or leaves the heat exchanger. The approximate measuring locations are showing in Figures 5.1 and 5.2.

Depending on the model being applied and the chosen configuration of the apparatus, the experiment could be used to verify the behavior of a coaxial BHE as well as to verify the application of certain variable heat flux terms. The heat input (W/m) delivered to the fluid circulating within the heat exchanger itself (q_h) is calculated using the measured inlet and outlet temperatures (T_i and T_o, respectively) using the following expression (Luo et al., 2015):

$$q_h = \frac{(T_i - T_o)\rho c_p Q_f}{L} \tag{5.1}$$

where L is the length of the heat exchanger, ρ and c_p are the density and the specific heat capacity of the working fluid, and Q_f is the volumetric flow rate. The test is run for a minimum of six hours to fully capture the effects of short-term behavior.

The results of the experiment are used in this chapter to verify the trends produced by the composite coaxial (CCx) model (Gordon et al., 2017) for short-term operation where the flow experienced in the annular region is laminar. Under such operating conditions, it is likely that the temperature of the fluid in the inner pipe will have some effect on outward heat transfer to the surroundings. Verifying the ability of the CCx model to simulate short-term behavior of coaxial BHEs under the considered operating conditions allows for confident semi-analytical analysis of these heat exchangers considering design requirements and overall performance.

5.3 Analytical investigation

The CCx model is used to simulate the experimental heat exchanger in order to verify the trends that it produces; this model is based on the infinite cylindrical-source model (ICS) and readers are directed to the initial publication related to these models for more information on their considerations (Carslaw and Jaeger, 1959; Gordon et al., 2017; Ingersoll et al., 1954). Readers are directed to Appendix A for a summary of the model, where the CCx model superimposes hollow cylindrical heat-sources at the interface of each of the materials in the cross section of the experimental coaxial BHE; the outer edge of the outer pipe acting as the borehole radius, and the surrounding still water emulating the infinite surrounding ground. The heat output, rejected from the heat exchanger through the annular space of the water jacket may be estimated by the following correlation (Incropera et al., 2011):

$$q_s = 2\pi k_{eff}(T_{s2} - T_{s1})/\ln(r_{s1}/r_{s2}) \tag{5.2}$$

An independent estimation of an effective thermal conductivity for the water (k_{eff}) in the surrounding annular cavity is used as a transient input for the CCx model. First, the critical Rayleigh Number (Ra_c) is introduced, along with a corresponding characteristic length related to free convection of fluid within a cylindrical annulus (Incropera et al., 2011):

$$Ra_c = (\rho g \beta L_c^3 (T_{s1} - T_{s2}))/\mu\alpha \tag{5.3}$$

where g is the gravity constant and L_c is the characteristic length; β, μ, and α, are the volumetric expansion coefficient, dynamic viscosity, and thermal diffusivity of the surrounding water. The characteristic length may be replaced by:

$$L_c = 2[\ln(r_{s1}/r_{s2})]^{4/3} / \left(r_{s1}^{-3/5} + r_{s2}^{-3/5}\right)^{5/3} \tag{5.4}$$

Using the critical Rayleigh number, an effective thermal conductivity of the surrounding water within the water jacket may be estimated:

$$\begin{cases} k_{eff}/k = 0.386(Pr/(0.861+Pr))^{\frac{1}{4}}(Ra_c)^{\frac{1}{4}} \\ \quad if\ \ k_{eff}/k < 1,\ \ k_{eff}/k = 1 \end{cases} \tag{5.5}$$

Where k is the molecular thermal conductivity and Pr is the Prandtl number of the surrounding water. Equation 5.5 is an acceptable approximation considering the limits of $0.7 \leq Pr \leq 6000$ and $Ra_c \leq 10^7$. Here, the Rayleigh Number, which is related to the instability of the boundary layer, is based on the annular gap between the cylinders and the measured temperatures at the surface of each (T_{s1}, T_{s2}), where if the boundary layer thickness is greater than the annular gap, than the problem of heat transfer approaches pure conduction. It is found that the "still" water will undergo a moderate amount of natural convection, where k_{eff} is calculated based on the measured temperatures at the outer surface of the outlet pipe (T_{s2}) and the inner surface of the Big 'O' pipe (T_{s1}). The thermal properties of the water are set to be calculated at each time-step considering the average of T_{s1} and T_{s2} using correlated quadratic functions developed between temperatures of 15 and 30 degrees Celsius. The results are used as transient input parameters for the composite coaxial model.

A depiction of the cross section for the heat exchanger simulation is found in Figure 5.1 where the inner and annulus fluid temperatures are measured as described in Section 5.2 of this thesis. The heat transfer correlation used to quantify this free convection is based on the inner and outer surface temperatures of the cavity. The results for k_{eff} are plotted against time in Figure 5.3. This figure shows an increase in the surrounding thermal conductivity, where a value of approximately 8 W/m-K is approached representing a moderate amount of natural convection occurring within the outer annular cavity.

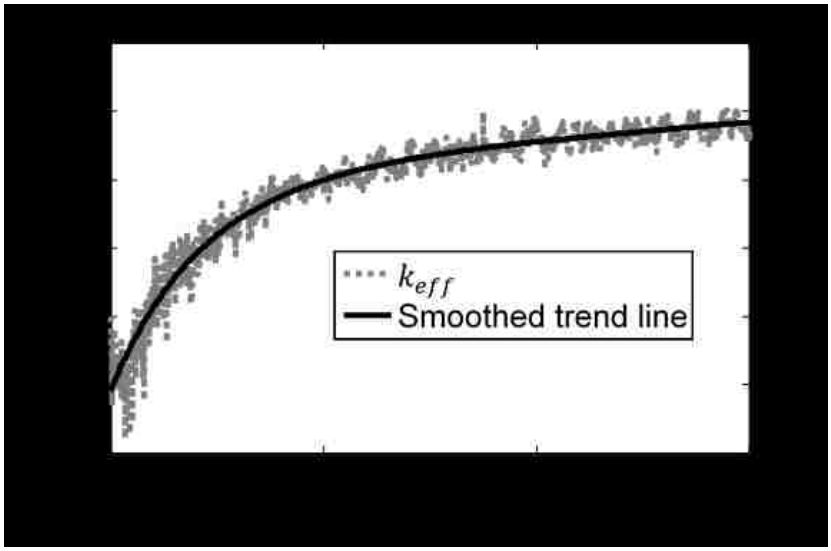

Figure 5.3: Results for k_{eff} calculation using Equation 5.5 at each measured time-step; a value of around 8 W/m-K is approached considering a moderate amount of natural convection occurring within the annular cavity.

The model simulates the outlet fluid temperature of a coaxial heat exchanger, where the following equation may be used which is based on the model provided in the original publication by the author (Gordon et al., 2017).

$$\Delta T_{f,o} = q_g \left[\underbrace{G_s P_r}_{G_s^*} + \underbrace{R_o P_r + Gr(p_i R_i + p_o G_i)}_{G_b} \right] \tag{5.6}$$

Many of the terms above are defined in the previous chapters of this thesis along with their individual relationships; where transient terms are to be superimposed in temporal space as necessary. For the purpose of simplification, notation for temporal superposition has been dropped in this chapter but can be noted by the indication of an equivalent or transient term. An equivalent borehole thermal resistance can be interpreted from Equation 5.6 to be written as:

$$G_b = R_o P_r + G_r(p_i R_i + p_o G_i) \tag{5.7}$$

Following this, an adjusted equivalent ground thermal resistance, affected by the thermal presence of the inner pipe (P_r), can be written as:

$$G_s^* = G_s P_r \tag{5.8}$$

It should be noted that Equation 5.6 may incorporate a variable heat flux term for q_g through temporal superposition with the combination of transient *design ratios* and G-function response terms. Here, the following equation is applied through temporal superposition:

$$q_g = \frac{p_i q_h \tau}{\tau + \tau_r} + \frac{p_o q_h (\tau - \tau_r)}{\tau} \tag{5.9}$$

where the response time, τ_r, will depend on the dominating factor between the fluid residence time and the time it takes for the heater to reach its nominal value. In this case, the fluid residence time within the heat exchanger is small compared to the time it takes for the heater to first shut off; the later value is therefore used as input for the CCx model. It should be noted in Equation 5.9 that if $\tau_j - \tau_r < 0$ then $\tau = 0$. The results of Equations 5.1, 5.2, and 5.9 are compared in Figure 5.4. It is noticed that the heater first shuts off after around 50 minutes of gradual increase in its delivered heat flux. Throughout the entire 6 hours, the average heat flux is found to be approximately 22.5 W/m, where q_h is set equal to this value in Equation 5.9. The value of q_g will approach this average q_h based on the time it takes for the heater to first shut off, that is, approximately 50 minutes. It is noted that the trend produced by Equation 5.9 is similar to that produce by Equation 5.2 where the values are logically larger. Figure 5.4 further illustrates the heat output (q_s as calculated by Equation 5.2) approaching the heat input (q_h as calculated by Equation 5.1), as well as the fluctuating behavior of the water heater.

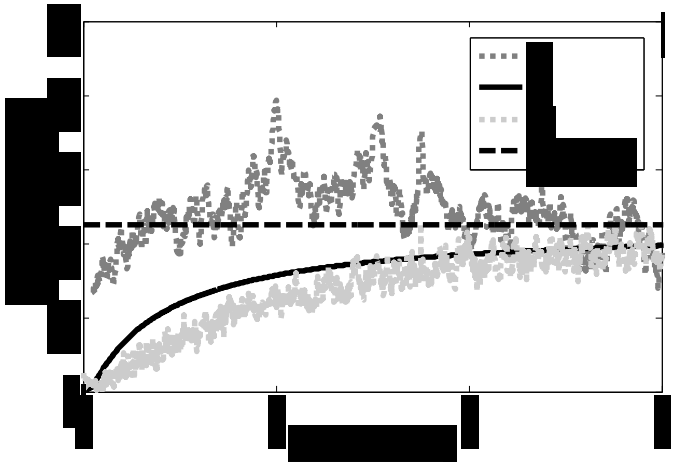

Figure 5.4: Variable heat flux terms calculated by each Equations 5.1, 5.2 and 5.9. Equation 5.9 is set to approach a value of 22.5 W/m based on an approximate value of 50 minutes.

The results of a composite coaxial model when considering the input parameters listed in Table 5.1 are compared to the measured outlet temperature in Figure 5.5. It is noticed that the

model produces comparable results throughout the six hours of operation yielding an RMSE of 0.16 °C. For the purpose of this research, the application of this analytical model to the experimental results is limited to the short-term period of operation due to the nature of the submersible heater where a maximum temperature of 30°C is maintained by its fluctuating on/off behavior. The results of this experiment are used to verify the trends produced by the CCx model for operating times less than six hours and flow rates that result in laminar annular flow. The systematic uncertainty of the experimental analysis is found to be high where the resolution of the temperature sensor has been reached; that is, the variability of the measured temperature exceeds that of the sensors rated accuracy (0.4 °C > 0.2 °C). It is noted that if the typical ICS model were applied using the same input parameters, then the simulated temperatures would be largely overestimated; for this reason, comparison with the ICS model has not been included in this chapter.

Table 5.1: Input parameters for CCx simulation of the experimental coaxial heat exchanger

Characteristics	Symbol	Unit	Value
Heat Exchanger			
Active length	H	m	4.0
Test Set-up			
Average rate of heat input	Q	W	90
Flow rate	Q_f	l/s	0.042
Surrounding conditions (still water)			
Undisturbed temperature	T_o	°C	18.6
Pipes			
Thermal conductivity	k_p	W/m-K	0.33
Volumetric heat capacity	C_{pp}	J-m^3/K	1.90x10^6
Nominal pipe diameters	-	cm	5, 3

The comparison between the experimental results and the semi-analytical model allows for verification that the model is capable of simulating short-term behavior considering laminar flow in the annulus. The results of this experiment allow for confident analytical comparison between coaxial heat exchangers experiencing either laminar or turbulent (or a combination of the two) flow.

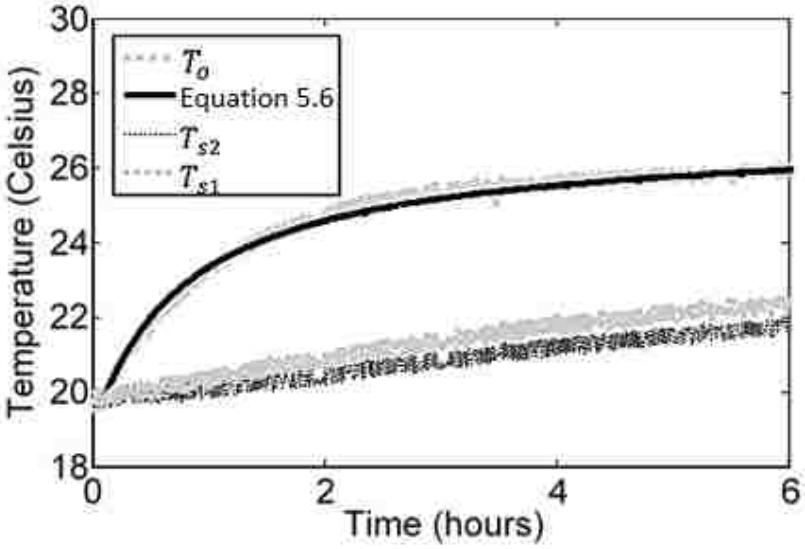

Figure 5.5: Measured temperature results from the experiment in comparison to outlet temperature simulated by the CCx model. An acceptable fit is found between the model output and the experimental data.

5.4 Analytical results and discussion

This chapter investigates the effect that varying the inner pipe has on the overall performance of a heat pump system. During this analysis, a hypothetical geothermal heat pump is introduced; this heat pump uses rated values and considerations published in *ClimateMaster's* "All Products Technical Guide: 2009,". The input parameters found in Table 5.2 are used to simulate a full-scale coaxial BHE having various nominal inner pipe diameters and a fixed 10.2 cm nominal outer pipe diameter. The chosen piping material is HDPE and remains so in each case.

Table 5.2: Input parameters for subsurface considered in the performance comparison

Characteristics	Symbol	Unit	Value
Subsurface			
Thermal conductivity	k_s	W/m-K	3.25
Thermal heat capacity	C_p	J/m^3-K	2.35x10^6
Undisturbed temperature	T_o	°C	10

Three different flow rates are considered for which the chosen heat pump was rated; the rated values for total cooling capacity, heat of rejection, and required input can be used to calculate a COP prior to correction for required pumping power. A required length is calculated

based on results of the CCx model combined with those of the ICS model for a single borehole (Bernier, 2006):

$$L = \frac{q_h G_b + q_y G_{10y} + q_m G_{1m} + q_h G_{6h}}{T_m - (T_g)} \tag{5.10}$$

Equation 5.10 is applied to each case considering the various diameters as input for the model, the resulting required length can then be used to calculate a total pressure drop within the system. A correction many now be applied to the COP based on the required pumping power for each case of varying the inner pipes nominal diameter, and for each of the three rated flow rates. The results of the performance comparison are presented in Table 5.3 and Figure 5.6; where Figure 5.6 plots the COP versus the required length calculated by Equation 5.10 as listed in Table 5.3. It can be seen in Figure 5.6, that increasing the diameter of the inner pipe increases the performance and reduces the overall required length of the system. This analysis only considers cases within the tested validity limit of the CCx model. A simplified pressure drop is used which only accounts for the major losses along the length of the flow path, omitting any end effects:

$$\Delta P_t = \frac{\rho f_i L v_{in}^2}{2 d_{ii}} + \frac{\rho f_o L v_{out}^2}{d_{io} - d_{oi}} \tag{5.11}$$

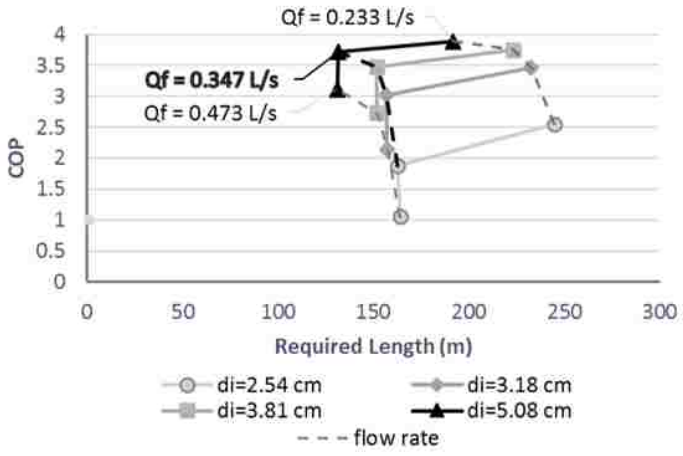

Figure 5.6: Comparison between COP and required length for each case of varying inner pipe diameter with a fixed outer pipe diameter of 10.2 cm (nominal dimensions shown).

Table 5.3: Summary of length calculation and corrected coefficient of performance based on varying inner pipe diameter.

Borehole properties		Rated values					Calculated values			
Inner pipe size (nom.)	R_b (m-K/W)	Flow rate L/s	Cooling capacity (kW)	Heat of Rejection (kW)	Required input (kW)	COP rated	Required length (m)	Pressure drop (Pa)	Power correction (kW)[1]	COP corrected[2]
2.54 cm	0.152	0.35	8.97	10.93	1.98	4.53	164.0	13938	6.60	1.06
3.18 cm	0.147						157.2	4865	2.30	2.14
3.81 cm	0.143						151.8	2955	1.40	2.73
5.08 cm	0.124						131.0	2097	0.99	3.11
2.54 cm	0.164	0.47	8.97	10.87	1.89	4.74	162.6	8054	2.79	1.88
3.18 cm	0.160						156.6	2836	0.98	3.03
3.81 cm	0.157						151.8	1735	0.60	3.47
5.08 cm	0.138						131.6	1250	0.43	3.72
2.54 cm	0.355	0.23	8.94	11.02	2.08	4.30	244.7	6106	1.43	2.55
3.18 cm	0.337						232.6	2135	0.50	3.47
3.81 cm	0.324						223.3	1302	0.30	3,75
5.08 cm	0.278						191.6	939	0.22	3.89

[1] Power correction (kW) = Flow rate (m^3/s) x Pressure drop (Pa)

[2] COP corrected = Cooling capacity (kW) / (Required input (kW) + Power correction (kW)

The plot in Figure 5.6 identifies the improvements desired by maintaining turbulent flow within the BHE while minimizing the pressure drop experienced; that is by maintaining an operating flow rate of at least 0.347 L/s in the present analysis. It can be seen that increasing the diameter of the inner pipe will further increase the performance and reduce the overall required length of heat exchanger. It would be further implied by the results of this comparison that an optimal diameter would exist for the inner pipe beyond the tested limit of the CCx model. In translation to the physical application of coaxial BHEs to a GSHP system, it is important to balance the pressure drops within the system to minimize unwanted pressure drops while maintaining turbulent flow within the active elements of a ground-side heat exchanger. At some point while increasing the inner pipe diameter, when considering like materials, the solution to the CCx model will begin to become unstable when the volume of the inner pipe becomes larger than the volume of the annulus. Further experimental testing would be necessary to truly optimize a coaxial system, including investigations on long-term performance and physical testing of optimal diameter ratios.

5.5 Conclusion

This chapter presents a lab-scale experiment that is used to verify the trends simulated by a semi-analytical model, referred to as the composite coaxial (CCx) model. The experiment maintains turbulent flow within the inner pipe, and laminar flow within the annulus region; the trend of which produces a reasonable comparison with the CCx model (RMSE = 0.16 °C). The results of this experiment are able to provide analysis for short-term behavior of a coaxial BHE where the temperature of the inner pipe fluid will have a noticeable effect on the temperature of the annulus fluid. This chapter further investigates coaxial BHEs from a design perspective using the CCx model to compare systems having different volumetric ratios. It is found that while holding a constant outer pipe diameter that increasing the size of the inner pipe will provide benefits to the overall performance of the system by balancing the pressure drops within each flow channel. It is found to be most important to minimize the system flow rate while maintaining desired turbulence within the annular flow path; the balance of these parameters will in turn lead to reduced overall lengths of heat exchanger along with improved performances that would be realized by a typical residential GSHP system.

Acknowledgments

This work is made possible by an OCE (Ontario Centres of Excellence) VIP project with GeoSource Energy Inc.

References

Acuña, J., 2013. Distributed thermal response tests-New insights on U-pipe and Coaxial heat exchangers in groundwater-filled boreholes.pdf (Doctoral). Royal Institute of Technology KTH, Stockholm, Sweden.

Acuña, J., Palm, B., 2012. Distributed thermal response tests on pipe-in-pipe borehole heat exchangers.pdf, in: 12th International Conference on Energy Storage. Presented at the Innostock 2012, Stockholm, Sweden.

Acuña, J., Palm, B., 2010. A Novel Coaxial Borehole Heat Exchanger: Description and First Distributed Thermal Response Test Measurements, in: Proceedings of the World Geothermal Congress. p. 7.

Arias-Penas, D., Castro-García, M.P., Rey-Ronco, M.A., Alonso-Sánchez, T., 2015. Determining the thermal diffusivity of the ground based on subsoil temperatures. Preliminary results of an experimental geothermal borehole study Q-THERMIE-UNIOVI. Geothermics 54, 35–42. doi:10.1016/j.geothermics.2014.10.006

ASHRAE, 2011. 2011 Ashrae Handbook: HVAC Applications. ASHRAE, Atlanta, GA.

Beier, R.A., Acuña, J., Mogensen, P., Palm, B., 2013. Borehole resistance and vertical temperature profiles in coaxial borehole heat exchangers. Appl. Energy 102, 665–675. doi:10.1016/j.apenergy.2012.08.007

Beier, R.A., Ewbank, G.N., 2012. In-Situ Test Thermal Response Tests Interpretations, OG&E Ground Source Heat Exchange Study. Oklahoma State Univ., Stillwater, OK (US), Oklahoma City, USA.

Beier, R.A., Smith, M.D., 2003. Minimum duration of in-situ tests on vertical boreholes. ASHRAE Trans. 109, 475–486.

Beier, R.A., Smith, M.D., Spitler, J.D., 2011. Reference data sets for vertical borehole ground heat exchanger models and thermal response test analysis. Geothermics 40, 79–85. doi:10.1016/j.geothermics.2010.12.007

Bernier, M.A., 2006. Closed-loop ground-coupled heat pump systems. Ashrae J. 48, 12–25.

Bernier, M.A., 2001. Ground-coupled heat pump system simulation/Discussion. Ashrae Trans. 107, 605.

Blum, P., Campillo, G., Kölbel, T., 2011. Techno-economic and spatial analysis of vertical ground source heat pump systems in Germany. Energy 36, 3002–3011. doi:10.1016/j.energy.2011.02.044

Carslaw, H.S., Jaeger, J.C., 1959. Conduction of Heat in Solids, Second. ed. Oxford University Press.

Choi, W., Ooka, R., 2016. Effect of natural convection on thermal response test conducted in saturated porous formation: Comparison of gravel-backfilled and cement-grouted borehole heat exchangers. Renew. Energy 96, 891–903. doi:10.1016/j.renene.2016.05.040

ClimateMaster, 2009. All Products Technical Guide: 2009. ClimateMaster.

De Carli, M., Tonon, M., Zarrella, A., Zecchin, R., 2010. A computational capacity resistance model (CaRM) for vertical ground-coupled heat exchangers. Renew. Energy 35, 1537–1550. doi:10.1016/j.renene.2009.11.034

Focaccia, S., Tinti, F., 2013. An innovative Borehole Heat Exchanger configuration with improved heat transfer. Geothermics 48, 93–100. doi:10.1016/j.geothermics.2013.06.003

Gehlin, S., 2002. Thermal Response Test: Method Development and Evaluation.pdf (Doctoral). Lulea University of Technology, Lulea, Sweden.

Gordon, D., Bolisetti, T., Ting, D.S.-K., Reitsma, S., 2017. Short-term fluid temperature variations in either a coaxial or U-tube borehole heat exchanger. Geothermics 67, 29–39. doi:10.1016/j.geothermics.2016.12.001

Hellström, G., 1991. Thesis_Goran_Hellstrom.pdf. University of Lund, Sweden.

Incropera, F., DeWitt, D., Bergman, T., Levine, A., 2011. Fundamentals of Heat and Mass Transfer - 6th Edition Incropera, 6th ed. Wiley, Hoboken, NJ.

Ingersoll, L.R., Zobel, O.J., Ingersoll, A.C., 1954. Heat conduction: With engineering, geological applications, 2nd ed. McGraw-Hill.

Lund, J.W., Boyd, T.L., 2016. Direct utilization of geothermal energy 2015 worldwide review. Geothermics 60, 66–93. doi:10.1016/j.geothermics.2015.11.004

Luo, J., Rohn, J., Bayer, M., Priess, A., 2013. Modeling and experiments on energy loss in horizontal connecting pipe of vertical ground source heat pump system. Appl. Therm. Eng. 61, 55–64. doi:10.1016/j.applthermaleng.2013.07.022

Luo, J., Rohn, J., Bayer, M., Priess, A., Wilkmann, L., Xiang, W., 2015. Heating and cooling performance analysis of a ground source heat pump system in Southern Germany. Geothermics 53, 57–66. doi:10.1016/j.geothermics.2014.04.004

Mokhtari, H., Hadiannasab, H., Mostafavi, M., Ahmadibeni, A., Shahriari, B., 2016. Determination of optimum geothermal Rankine cycle parameters utilizing coaxial heat exchanger. Energy 102, 260–275. doi:10.1016/j.energy.2016.02.067

Pasquier, P., 2015. Stochastic interpretation of thermal response test with TRT-SInterp. Comput. Geosci. 75, 73–87. doi:10.1016/j.cageo.2014.11.001

Rainieri, S., Bozzoli, F., Pagliarini, G., 2011. Modeling approaches applied to the thermal response test: a critical review of the literature. HVACR Res. 17, 977–990.

Yekoladio, P.J., Bello-Ochende, T., Meyer, J.P., 2013. Design and optimization of a downhole coaxial heat exchanger for an enhanced geothermal system (EGS). Renew. Energy 55, 128–137. doi:10.1016/j.renene.2012.11.035

Zarrella, A., Scarpa, M., Carli, M.D., 2011. Short time-step performances of coaxial and double U-tube borehole heat exchangers: modeling and measurements. HVACR Res. 17, 959–976.

Zhang, L., Zhang, Q., Huang, G., Du, Y., 2014. A p(t)-linear average method to estimate the thermal parameters of the borehole heat exchangers for in situ theral response test. Appl. Energy 131, 211–221. doi:http://dx.doi.org/10.1016/j.apenergy.2014.06.031

Zhao, J., Wang, H., Li, X., Dai, C., 2008. Experimental investigation and theoretical model of heat transfer of saturated soil around coaxial ground coupled heat exchanger. Appl. Therm. Eng. 28, 116–125. doi:10.1016/j.applthermaleng.2007.03.033

Chapter 6 – Conclusions and Recommendations

6.1 Overview of conclusions

This section provides a summary of the research presented within this thesis, where the main conclusions of each chapter are reviewed in order to provide recommendations for future research. The main scope of this research is related to coaxial borehole heat exchangers (BHE) and their application to ground-source heat pump systems (GSHP). The intention of the research is to first provide a method for fair comparison between a typical U-tube heat exchanger and various configurations of coaxial heat exchangers.

This thesis has provided a simplified comparison between coaxial and U-tube BHEs, specifically considering a residential, single borehole application. Focus has been kept on design approaches presented in published literature to offer a base comparison between the systems and unveil any possible benefits realized by a coaxial configuration. It has been found in a preliminary comparison that an improved coaxial design may have a reduced required length by around 30% when compared to a typical U-tube configuration found in North America, offering motivation for this research.

This thesis has developed an original semi-analytical model to simulate the outlet fluid temperature of a coaxial BHE, where this model is intended to be a tool to compare coaxial BHEs on a case-by-case basis. This model has been developed based on various *design ratios*, where this term accounts for ratios of resistances, capacities, and volumes representative of the chosen pipe configuration. The model, referred to as the composite coaxial (CCx) model, has been first presented only considering the volumetric ratio of the configuration, where the volumetric ratio is defined as the ratio of the volume of working fluid contained in the inner pipe to the volume contained in the annulus. The thermal resistance ratio has been assumed to be equal to unity in the first case of validation. This assumption is then found to be appropriate in the initial validation when considering a coaxial BHE having both the inner and outer pipes made of high-density polyethylene (HDPE) of the same standard dimension ratio. The simulated outlet fluid temperature have been found to accurately simulate the measured temperature during a typical thermal response test (TRT) yielding an RMSE of 0.09 °C, which is well within the uncertainty of the measurement.

The CCx model has been extended later in this thesis to account for variable piping materials. This has been done by considering two additional terms: a thermal resistance ratio – where this term accounts for the varying ratio of the equivalent outer thermal resistance to the inner shunt resistance of a coaxial configuration – and a thermal presence ratio – where this accounts for the thermal energy storage effect of the inner pipe. The extended model utilizes a mixture of transient *equivalent* resistances steady-state *effective* thermal resistances to produce its final result. The model has been assessed by comparing systems based on the inner and outer pipe material selection while holding their diameters constant. This comparison has been made considering the required heat exchanger length and overall performance of a system. It has then been found in this thesis that a steel outer pipe will have a greater effect on reducing the overall required length of heat exchanger than having an insulated inner pipe (by about twice as much); this comparison has been made using each in an isolated case where HDPE is considered as the status quo.

An experimental set-up has been used in this thesis to investigate the short-term behaviour of a coaxial heat exchanger. This experiment has been used to provide further verification of the trends produced by the CCx model; where the CCx model is intended to capture the effect of an inner pipe. In the experimental set-up, laminar flow has been maintained in the annulus to allow for greater influence from the inner pipe fluid temperature. An agreeable comparison is made between the physical and simulated results (RMSE of 0.16 °C). To expand upon the experimental results the CCx model has been used, within its tested validity range, to compare coaxial configurations having typical HDPE pipes and a varying inner pipe diameter. The results of this comparison show that increasing the inner pipe diameter can decrease the required length of the heat exchanger while offering an increase in performance realized by a corresponding heat pump.

In final conclusion, this thesis has accomplished the objectives of the research by developing the CCx model and validating it for future use as a tool to compare coaxial BHE designs on a case-by-case basis.

6.2 Recommendations for future research

In the current state of the present research, the composite coaxial model could be used to estimate the required design length of smaller, residential systems. The model currently allows for quick and versatile comparisons between coaxial arrangements where a trade-off may be

realized between initial costs and long-term performance. To extend the usefulness of the CCx model, it is recommended to incorporate spatial superposition of the proposed corrected ground response to account for multiple heat sources. It is further recommended to keep the application of this model to borefields as simple as possible with the intention to attract designers to a more hand-on and marketable approach. Therefore the chosen approach to sizing borefields should remain analytical in nature; however, benefits could also be realized by verifying the results of the model through a thorough comparison with numerical methods.

It is recommended to further develop the lab-scale experimental set-up presented in Chapter 5 of this thesis by implementing an insulated casing and inserting various inner pipe materials for comparison. This experiment could be used to capture the short-term effects caused by varying the inner pipe diameter and material properties.

Vita Auctoris

Name:	David Gordon
Place of Birth:	Windsor, Ontario
Year of birth:	1992
Education:	Holy Names High School, Windsor 2006-2010
—	University of Windsor 2010-2014 BASc Environmental Engineering